TECHNICAL MEMORANDUM

ANL-CT-78-51
Structural Materials
and Design Engineering
UC-79h

# ON THE UNIQUENESS AND STABILITY OF ENDOCHRONIC PLASTICITY THEORY

by

B. J. Hsieh

Components Technology Division

Argonne National Laboratory

Argonne, Illinois



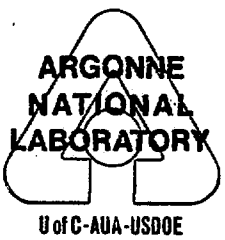


BASE TECHNOLOGY

September, 1978

# ON THE UNIQUENESS AND STABILITY OF ENDOCHRONIC PLASTICITY THEORY

B. J. Hsieh

## Abstract

Several numerical and analytical analyses are described which evaluate the uniqueness and stability of solutions of structural models whose material behavior is governed by the endochronic theory of placticity. The simplest form of this theory is used in both one- and two-dimensional problems. It has been found that this simplest form does show some "material instability" in the sense it does not satisfy Drucker's postulate when subjected co a limited loading cycle. In other words, an endochronic material creeps under the action of applied force. However, this "instability" or "lack of a hysteresis loop" can be circumvented by using more complicated forms of the endochronic theory.

It is also noted that even the simplest endochronic model yields very good results compared to those of an elastoplastic model when the structural model is subjected to conditions wherein loading predominates. Uniqueness and stability of the solution are observed in all such cases studied. The numerical efficiency and the minor effect of unstable material behavior in the simple endochronic theory make it attractive in safety analysis of many structures where peak deformation is of paramount importance.

## INTRODUCTION

The endochronic theory of material behavior was purposed by K. C. Valanis [1], and uses the principle that the history of deformation is defined in terms of a "time scale" which is not the real time, but is in itself a property of the material. No use of the classical yield surface concept is required in this theory. It was used by Valanis [2] to predict the mechanical response of aluminum and copper under conditions of complex strain histories. One constitutive equation described with remarkable accuracy and ease of calculation many phenomena, such as cross-hardening, loading and unloading loops, cyclic hardening as well as the effect of pre-shearing on tension behavior. Z. P. Bazant and his co-workers further developed the theory to describe the liquefaction of sand [3] and the inelastic behavior and failure of concrete [4]. The use of a two-dimensional endochronic constitutive relation in dynamic transient analysis of shells was first considered by H. C. Lin [5].

Basically, the endochronic theory uses an "intrinsic time" in place of real time in the visoelastic constitutive equations. In other words, the time convolution integrals present in viscoelasticity are replaced by the "intrinsic time" convolution integrals. Obviously, the accuracy of an endochronic model in describing the behavior of a real material is dependent on the form of the "relaxation" function, G, and on the definition of intrinsic time. Important material phenomena may be lost when either is not defined properly. In such a case, the applicability of an endochronic model must be limited to a restricted class of problems.

I. S. Sandler [6] recently pointed out that the use of a simple endochronic model causes the material to be unstable and, hence, non-uniqueness of problem solutions can result. In this study, we show that the stability of a

material is a matter of definition, and the stability of an endochronic model can be improved by using a more realistic "relaxation function." Furthermore, in a practical sense, unique and stable numerical solutions can be obtained for a structure whose material may violate Drucker's criterion of stability.

STABILITY OF MATERIALS

Drucker's stability criterion for materials as used in Sandler's paper is simply that no material is allowed to have negative material damping. The simple endochronic models used by Sandler and Valanis, however, show negative damping when subjected to certain strain or stress histories. In order for a material to have positive damping, the constitutive law must be able to form a hysteresis loop upon a complete loading and unloading cycle. To show the inability of some endochronic models to form hysteresis loops, consider the simplest endochronic model used by Valanis [2] which is given by

$$E_o d\varepsilon = d\sigma + \sigma \alpha dz; \quad \alpha dz = \frac{\alpha_1 \beta_1}{1+\beta\xi} |d\varepsilon|; \quad \beta d\xi = \beta_1 d|\varepsilon| \tag{1}$$

where $\sigma$ and $\varepsilon$ are the stress and the strain, $E_o$ is the initial slope of the one-dimensional stress-strain curve, and $\alpha_1$, $\beta_1$ are material properties that are determined from a one-dimensional tension test. If we define loading and unloading as when $d\varepsilon > 0$ and when $d\varepsilon < 0$ respectively, then we have

$$\frac{d\sigma}{d\varepsilon} = \left( E_o \mp \frac{\alpha_1 \beta_1 \sigma}{1+\beta\xi} \right); \quad \begin{matrix} (-) \text{ loading} \\ (+) \text{ unloading} \end{matrix} \tag{2}$$

For a hysteresis loop to be formed as shown in Fig. 1, the unloading and loading paths must intersect each other. Let the two points of extreme stress value on the loop be denoted by A and B, then the slope of the line connecting A and B is simply $(\sigma_A - \sigma_B)/(\varepsilon_A - \varepsilon_B)$. The mean value theorem of calculus then states that there exists two points, x and y, whose coordinates are $(\sigma_x, \varepsilon_x)$ and $(\sigma_y, \varepsilon_y)$ on either side of the line AB, and their slopes are the same as that of line AB. By assuming the positions for x and y and using Eq. (2) with appropriate signs, we find the following condition

$$\frac{-\sigma_x}{1+\beta\xi(x)} = \frac{\sigma_y}{1+\beta\xi(y)} \tag{3}$$

for the formation of a hysteresis loop for the model depicted by Eq. (1). Since $\xi$ is a monotonically increasing positive number, Eq. (3) indicates that $\sigma_x$ and $\sigma_y$ must be opposite in sign for hysteresis loop formation. When the stress or strain history is such that a material always stays in either tension or compression, the endochronic constitutive law given by Eq. (1) may behave in an unstable manner in the sense described by Sandler.

Stress-strain curves for an endochronic model subjected to different strain histories are shown in Figs. 2 and 3 by using Eq. (1). These results are obtained by connecting a mass to a massless endochronic spring. The values for $E_o$, $\alpha_1$, $\beta_1$ are $6.895 \times 10^{10}$ Pa ($1 \times 10^7$ psi), 49, and 8.75; the mass used is $4.378 \times 10^{-2}$ Kg ($3.000 \times 10^{-3}$ slug). The unstable behavior shown in Fig. 2 is obtained by subjecting this spring-mass system to a suddenly applied constant force of magnitude $4.448 \times 10^4$ N ($10^4$ $lb_f$) while the stable hysteresis loops are obtained by subjecting the system to an initial displacement that is equivalent to 1% of straining in the spring. These results confirm

the condition derived in Eq. (3) for the formation of hysteresis loops.

It should be noted that even though the "unstable" constitutive relation shown in Fig. 2 may not be a realistic representation of a real material behavior as we know it, it does not mean that such a material may never exist. However, we'll show that such unstable behavior of an endochronic model can be improved.

The endochronic model represented by Eq. (1) is obtained by assuming the intrinsic relaxation function G to be a single exponential function, i.e.

$$G(z) = E_o e^{-\alpha z} \tag{4}$$

It is, therefore, reasonable to improve the accuracy of the constitutive model by including more terms in the relaxation function, say

$$G(z) = E_o + E_1 e^{-\alpha z} \tag{5}$$

The differential constitutive equation corresponding to the above equation is simply

$$(E_o + E_1)d\varepsilon + E_o\varepsilon\,(\alpha dz) = d\sigma + (\alpha dz)\,\sigma \tag{6}$$

where $E_o$, $E_1$ are material parameters and $\alpha dz$ is defined in Eq. (3). The equation for the slope of the stress-strain curve is, therefore, given by

$$\frac{d\sigma}{d\varepsilon} = (E_o + E_1) \pm (E_o\varepsilon - \sigma) \frac{\alpha_1\beta_1}{1+\beta\xi} \quad ; \quad \begin{matrix}(+) \text{ loading} \\ (-) \text{ unloading}\end{matrix} \tag{7}$$

The necessary condition for a hysteresis loop can now be derived as in the previous case to be

$$\frac{E_o\varepsilon_x - \sigma_x}{1+\beta\xi(x)} = \pm \frac{E_o\varepsilon_y - \sigma_y}{1+\beta\xi(y)} \tag{8}$$

From this, we see that there are possibilities for a hysteresis loop to be formed even for the cases where $\sigma_x$ and $\sigma_y$ have the same sign. A hysteresis loop for a copper specimen subjected to unloading and reloading in tension is excellently reproduced by using Eq. (6) in [2]. It is reasonable to assume that other types of loading-unloading-reloading may be described by using more general forms of the relaxation function.

It should be emphasized that no single constitutive law as yet can describe all the material behavior observed in laboratories. That is, most constitutive laws are accurate in describing certain materials under certain conditions only. It is important to use appropriate constitutive laws for practical problems. However, the inability to represent a material in some situation by a constitutive law should not exclude its usefulness in representing the material in other situations. It will be shown later that the simple one-term relaxation function used in Eq. (1) can predict reasonably good results for many practical problems.

We reiterate that a constitutive law is simply a model used to approximate the behavior of a material. Certain models may represent some materials

better than others in some situations and vice versa. The "unstable" behavior of the one-term endochronic model, hence, should be treated carefully when it occurs. It could be used to compute the upper bounds of solutions for real problems similar to the use of the elastic-perfectly-plastic constitutive model in limit analysis. The cause of this unstable behavior will be discussed later.

## UNIQUENESS OF SOLUTION

The uniqueness of solution to a system of equation is defined as when one, and only one, set of results is obtained when the system is subjected to a set of initial and boundary conditions. Non-uniqueness of solution exists if more than one set of results are possible when the system is subjected to the same conditions. The question of uniqueness of an endochronic model was discussed by Sandler [6] for both a spring-mass system and a continuum system. The spring-mass system in [6] is formed by slowly adding weights to a one-term endochronic spring and then subjecting this system to a small excitation; the continuum system is a prestressed rod subjected to a stress history at one generic point.

The response of such a spring-mass system obviously depends on the magnitude of weight, direction of excitation, etc. The computed response for a system ($\alpha_1 = 49$, $\beta_1 = 8.75$ and $E_o = 6.895 \times 10^{10}$ Pa) that is first extended to a state of 8% strain and then subjected to an initial displacement that is equivalent to 0.1% are shown in Figs. 4-6. The results of the same system subjected to an initial displacement of -0.1% are shown in Figs. 7-9. The unstable response predicted in [6] is clearly observed in these figures. The strain histories are qualitatively represented by the displacement histories since they differ only by multiplicative constants. In both cases, the stresses oscillate about certain values while the strains drift as predicated

in [6]. However, this drifting of displacements (strains) may not go unbounded within a finite time, since the velocity histories shown in Figs. 5 and 8 clearly indicate the vaniching of velocity of the mass.

The weight used in the above example causes the spring to be extended to a strain of 8%. This makes the initial equilibrium position of the mass well into the plastic range. One would hope that the unstable behavior would be less severe if the system is pre-strained to a lesser degree by using a smaller weight. The responses of a system whish is pre-strained to 0.1% and then subjected to initial displacements equivalent to -0.001% and +0.001% are shown in Figs. 10 and 11, respectively. It can be seen that no improvement is observed by setting the initial state in the "elastic range." This surprising result may be caused by the use of a much smaller mass, since the pre-straining is generated by the weight of the mass. It is worth mentioning that the stress-strain curves for these results all have forms similar to that of Fig. 2.

To circumvent the complexity generated by the use of different masses, the mass is now set to a constant value of $4.378 \times 10^{-2}$ Kg, then the system is subjected to various external excitations from its initially undisturbed state. The qualtitative responses are independent of the directions of the external excitations, since no initial strain exists. Figs. 12, 13, and 14 show the displacement histories of the system subjected to suddenly imposed initial displacements equivalent to -1%, -0.5%, and 0.1%, respectively. The stress-strain curves for these cases all have forms similar to that shown in Fig. 3. The dashed lines in these figures are the equilibrium positions of residual vibrations of the associated linearly elastic, perfect plactic systems that have the same

initial Young's moduli and yield strrsses as those of endochronic models. Figure 15 is the response when the system is subjected to a very small initial velocity which is equivalent to 0.2% strain per second. The classical linear elastic solution is identical to the endochronic model in this case and the endochronic stress-strain curve is a straight line.

All these results show that the endochronic theory prodicts results different than those of the classical theories. The final equilibrium positions of this theory are larger than those of the linearly elastic, perfectly plastic theory. However, no instability or non-uniqueness phenomenon is observed in these models. It is important to note that the unstable behavior shown in earlier examples exists only when external forces are present through the use of weights. This unstable behavior is actually the creep phenomenon of the endochronic model with respect to its intrinsic time instead of real time, as can be seen by considering the similarity between endochronic and viscoelastic theories. Whether a creeping material should be termed as unstable is a question of definition; it does not present any difficulty in problem solving.

The possibility of non-uniqueness of solution to the spring-mass system proposed by Sandler [6] does not exist. Sandler presented an interesting and useful model to uncover some "undesired" behavior of a simple endochronic model. However, the small disturbance used in his example and previous studies should not be interpreted as an error which expresses the difference between the numerical and analytical "exact" solutions. A computer does not know the real problem, it sees only a specific model and solves it with certain accuracy. Therefore, the exact solution is meaningless to a computer. A numerical solution is obtained in a computer by applying prescribed methods to the equilibrium equation or equation of motion. Hence, the numerical solution always satisfies the equilibrium equation exactly within the accuracy of the said computer.

We reiterate that though the "erroneous" numerical solution may be different than the "exact" solution to a real problem, it is the "exact" solution that satisfies equilibrium within the accuracy of a computer.

The continuum model used by Sandler to study the non-uniqueness of an endochronic model is a rod initially at rest and at equilibrium under the pressure $\sigma_o$. At $t = 0$, a generic point of the rod is brought to a state of $\sigma = \sigma_2$ and $v = 0$ where $v$ is the velocity. The solution obtained by Sandler is

$$\sigma_2 = \sigma_o \rho (V_{UN} - V_{LD}) v \tag{9}$$

where $\rho$ is the density, $V_{UN}$ and $V_{LD}$ are the unloading and loading wave speeds, and $v$ is the velocity of the rod in the region bounded by the unloading and loading wave fronts.

For a bi-linearly elastoplastic material, the loading and unloading wave speeds are the same, hence $\sigma_2 = \sigma_o$. That is, for an elastoplastic rod at rest, no point can be brought to another stress level and have the point still at rest except when the stress change is trivial. For an endochronic rod, however, this change of stress is possible as indicated by Eq. (9). A unique solution is obtained, since $\sigma_2$ is an initial condition while $v$ is part of a solution set, according to the previous definition of uniqueness. In other words, Eq. (9) states that if a point is brought to another stress state and is again at rest, a definitive wave propagation of disturbance from this point will occur. Another point of view is: an elastoplastic material does not know whether it has been subjected to a complete stress cycle or not at $t = 0$ since the effects cancel each other out because the speeds for loading and unloading are identical; but

an endochronic material knows. It seems that the endochronic solution is "more unique" than the bi-linearly elastoplastic material from this viewpoint.

RANGE OF APPLICATION

No single constitutive law has been found to include all observed material behavior. To see the range of applicability of the one-term endochronic theory, one dimensional spring-mass and two dimensional continuum systems are studied.

The spring-mass system is formed by attaching a concentrated mass m to the spring which is either endochronic or bi-linearly elastoplastic. The system is initially at rest without pre-straining and is suddenly subjected to a step loading or to various initial conditions. The one-term endochronic and bi-linearly elastoplastic constitutive equations are related by the following equations

$$n = E_o/E_p; \quad \beta_1 = E_p/\sigma_o; \quad \alpha_1 = n-1; \quad \sigma_y = \sigma_o/(1-\frac{1}{n}) \tag{10}$$

where $E_o$, $E_p$ are the elastic and plastic moduli of the material and $\sigma_y$ is the initial yield stress. The material parameters used are $\alpha_1 = 49$; $\beta_1 = 8.75$; $E_o = 6.895 \times 10^{10}$ Pa; $\sigma_y = 1.608 \times 10^8$ Pa and $m = 4.378 \times 10^{-2}$ Kg.

Figs. 16 to 33 are the responses of the spring-mass system subjected to step loadings of various magnitudes obtained by using the one-term endochronic theory and the bi-linearly elastoplastic theory. The former responses are represented by solid lines and the latter by chain-dashed lines. The loading magnitudes vary from 4.448 N (1 $lb_f$) in Figs. 16-18 to $4.448 \times 10^5$ N ($10^5$ $lb_f$) in Figs. 31-33. The responses include the displacement (strain) histories,

the velocity histories and the stress-strain curves. For loadings smaller than $4.448 \times 10^{1}$ N (10 $lb_f$), both endochronic and elastoplastic theories reduce to linearly elastic theory and the results are almost identical to each other. For median loading that lies between $4.448 \times 10^{2}$ N (100 $lb_f$) and $4.448 \times 10^{4}$ N (10,000 $lb_f$), the endochronic displacements are consistently higher than those of the elastoplastic model. The amplitudes of the endochronic displacement oscillation, however, are damped out as time increases as indicated by the vanishing amplitudes of the velocity histories. This difference is mainly caused by the fact that endochronic materials have different stiffness properties during unloadings and reloadings as shown in Figs. 27 and 30 The elastoplastic unloading-loading curves form straight lines and the endochronic ones form zigzag patterns. For loadings not less than $4.448 \times 10^{5}$ N ($1 \times 10^{5}$ lb), the responses are very similar. Hence, only the results for loading $4.448 \times 10^{5}$ N are presented in Figs. 31-33.

The free vibrational responses of the spring-mass system subjected to initial displacements equivalent to from 0.1% to 100% strain are shown in Figs. 34-45. The elastoplastic solutions (chain-dashed lines) for displacements and velocities are simple harmonic motions with constant amplitudes, while the endochronic ones are simple harmonic motions with decaying amplitudes. Again, the equilibrium positions of residual vibrations of the endochronic material are larger than those of the elastoplastic ones. Furthermore, the endochronic equilibrium position is never its initial equilibrium position, though this is so for the elastoplastic one if the initial displacement is not greater than half of the initial yield strain (displacement) as shown in Fig. 34. It should be noted that hysteresis loops are observed in all these initial displacement examples.

Figs. 46 to 60 show the responses of the spring-mass system subjected to various initial velocities. For a velocity equivalent to 200% strain per second, almost identical responses are obtained for both the endochronic and elastoplastic solutions as shown in Figs. 46, 47 and 48. For initial velocity not lower than 2,000% strain per second, the solutions are very similar to the solutions obtained for the initial displacement cases. Namely, solutions osciliate about equilibrium positions with constant amplitudes for elastoplastic materials and with decaying amplitudes for endochronic ones. The endochronic equilibrium positions are always higher than those of elastoplastic ones, and hysteresis loops are observed for the endochronic stress-strain curves. Note that excellent comparison between elastoplastic and endochronic theories is obtained for the initial velocity of $2 \times 10^6$% strain per second as shown in Figs. 58-60.

From the above results for a one-dimensional spring-mass system subjected to various initial conditions or constant loadings, we find that all solutions are unique. Hysteresis loops are observed for the spring-mass system except when it is subjected to external loading. In the latter case, the unstable behavior is simply the creeping of an endochronic material with respect to the intrinsic time since it is well known that a viscoelastic material creeps under the action of an external load. The creeping phenomenon of an endochronic model is, therefore, expected to cease when the external load is removed. Figs. 61 to 70 show the displacements, velocities and stress-strain curves of the spring-mass system subjected to a constant force whose magnitude is $4.448 \times 10^4$ N ($10^4$ $lb_f$) and whose durations are 0.5T, 2.3T and 5T where T is the period of the associated linearly elastic system. The value of T used is $\pi \times 10^{-5}$ sec. and the

arrow marks on the time axes in these figures indicate the times the loadings are removed. The solution for the case of 0.5T is very similar to the result obtained when the system is subjected to an initial velocity. This is expected because very short duration loadings can be treated as initial conditions. From the stress-strain curves in Figs. 63, 66 and 69, we see that the strains for the elastoplastic model are smaller than its initial yield strain (0.233%) and the elastoplastic constitutive equations are straight lines. Hence, the residual vibrations after the removing of loads oscillate about their initial equilibrium position for the elastoplastic model. It is known, from the analytical solution [7] of an elastic spring-mass system subjected to rectangular-pulse loading, that the amplitude of residual vibration is zero if the load duration is not small and is an integer multiplier of the half period of the system. The small oscillation after the removing of loading in Fig. 67 is caused by the error in representing the loading duration and the period of the system by the finite accuracy of a computer. It is expected that the residual vibration amplitude will be reduced if the accuracy of the computation is improved. Fig. 70 shows the displacement history of the same problem using double precision (on an IBM machine) and a numerical time integration step that is an integer fraction of the period. Much smaller residual vibration is observed though it still exists. This residual vibration may not be eliminated unless the period of the model seen by the computer is exactly equal to that of the analytical model; otherwise, a small error in the period will grow after many cycles of vibration

This phenomenon of no residual vibration when the load duration is an integer multiplier of the half period is a particular property of a linearly elastic material. It indicates that a system may have residual vibration when subjected

Figs. 46 to 60 show the responses of the spring-mass system subjected to various initial velocities. For a velocity equivalent to 200% strain per second, almost identical responses are obtained for both the endochronic and elastoplastic solutions as shown in Figs. 46, 47 and 48. For initial velocity not lower than 2,000% strain per second, the solutions are very similar to the solutions obtained for the initial displacement cases. Namely, solutions oscillate about equilibrium positions with constant amplitudes for elastoplastic materials and with decaying amplitudes for endochronic ones. The endochronic equilibrium positions are always higher than those of elastoplastic ones, and hysteresis loops are observed for the endochronic stress-strain curves. Note that excellent comparison between elastoplastic and endochronic theories is obtained for the initial velocity of $2 \times 10^6$% strain per second as shown in Figs. 58-60.

From the above results for a one-dimensional spring-mass system subjected to various initial conditions or constant loadings, we find that all solutions are unique. Hysteresis loops are observed for the spring-mass system except when it is subjected to external loading. In the latter case, the unstable behavior is simply the creeping of an endochronic material with respect to the intrinsic time since it is well known that a viscoelastic material creeps under the action of an external load. The creeping phenomenon of an endochronic model is, therefore, expected to cease when the external load is removed. Figs. 61 to 70 show the displacements, velocities and stress-strain curves of the spring-mass system subjected to a constant force whose magnitude is $4.448 \times 10^4$ N ($10^4$ $lb_f$) and whose durations are 0.5T, 2.3T and 5T where T is the period of the associated linearly elastic system. The value of T used is $\pi \times 10^{-5}$ sec. and the

arrow marks on the time axes in these figures indicate the times the loadings are removed. The solution for the case of 0.5T is very similar to the result obtained when the system is subjected to an initial velocity. This is expected because very short duration loadings can be treated as initial conditions. From the stress-strain curves in Figs. 63, 66 and 69, we see that the strains for the elastoplastic model are smaller than its initial yield strain (0.233%) and the elastoplastic constitutive equations are straight lines. Hence, the residual vibrations after the removing of loads oscillate about their initial equilibrium position for the elastoplastic model. It is known, from the analytical solution [7] of an elastic spring-mass system subjected to rectangular-pulse loading, that the amplitude of residual vibration is zero if the load duration is not small and is an integer multiplier of the half period of the system. The small oscillation after the removing of loading in Fig. 67 is caused by the error in representing the loading duration and the period of the system by the finite accuracy of a computer. It is expected that the residual vibration amplitude will be reduced if the accuracy of the computation is improved. Fig. 70 shows the displacement history of the same problem using double precision (on an IBM machine) and a numerical time integration step that is an integer fraction of the period. Much smaller residual vibration is observed though it still exists. This residual vibration may not be eliminated unless the period of the model seen by the computer is exactly equal to that of the analytical model; otherwise, a small error in the period will grow after many cycles of vibration

This phenomenon of no residual vibration when the load duration is an integer multiplier of the half period is a particular property of a linearly elastic material. It indicates that a system may have residual vibration when subjected

to a loading, but it may be at rest after a certain time when subjected to a "longer" loading. Figs. 71, 72 and 73 are the results of the system subjected to a rectangular pulse whose magnitude and duration are $8.896 \times 10^4$ N ($2 \times 10^4$ $lb_f$) and 6T. The times of load removal are indicated by arrow marks on the time axes. As can be seen, this pulse magnitude has clearly caused plastic response of the elastoplastic model.

The termination of creeping phenomena of endochronic models immediately upon removal of loads is observed in all these results. This confirms our previous premonition of creeping of an endochronic material under the action of external force. Hence, the endochronic material is unstable - in the sense that it creeps with respect to the intrinsic time - when subjected to external force just as a viscoelastic material does. The results also show that an endochronic material has permanent plastic strains when subjected to some boundary conditions while the elastoplastic material does not. The plastic strains of an endochronic material are always larger than those of the corresponding bi-linear elastoplastic material subjected to the same conditions. This is not surprising since the relationship as expressed by Eq. (10) shows that the endochronic material is softer than the corresponding elastoplastic material when they are subjected to loading ($d\varepsilon>o$)only. This is confirmed by all the results indicating the stress-strain curves for the examples studied. Better fitting of these curves in some range of strains for specific problems may be obtained by adjusting the endochronic material parameters, $\alpha_1$, $\beta_1$ and $E_o$.

Whether a real material should be represented by an endochronic or elastoplastic model should be decided by its stress-strain curve obtained through laboratory tests. It is noted that some materials may be well represented by the bi-linear elastoplastic model such as mild steel, but some materials cannot, such as lead or copper. It should also be noted that the dividing of

elastic and plastic ranges by the yield stress causes the transition from elastic response to plastic response to occur abruptly while no such transition exists in an endochronic model.

For stable numerical integration of a spring-mass system, the time integration step should be small enough. No criterion exists for defining the smallness of time step for arbitrary material properties. It is customary to use the elastic criterion as a guide in choosing the time step for an elastoplastic material. For an elastic spring-mass system, the stable time integration step should be no more than about one tenth of its period [7]. For a bi-linear elastoplastic material, this criterion still works since the plastic modulus is always smaller than the elastic modulus. For an endochronic material, the elastic criterion should be used with care because the slope of the constitutive equation during the motion of the system may be greater than the initial slope which is normally used in determining the stability criterion. The time step used in obtaining numerical solutions in this study is $T/10\Pi$. This time step yields satisfactory results with the only exception of Fig. 57, where two kinks are noted in the resulting endochronic stress-strain curve. These kinks will disappear when a smaller time step is used.

Before going into two dimensional continuum problems, we will point out that the constitutive relations used in the one dimensional spring-mass system are represented exactly by the numerical model. This is not true for an elastoplastic problem when more than one stress component is involved.

We present the final constitutive equations for general bi-linear elastoplastic and one-term endochronic materials in the following:

For an elastoplastic material, the constitutive equations for obtaining stress increments from strain increments are

$$
\begin{aligned}
d\sigma_{ij} &= 2\mu d\varepsilon^{e}_{ij} + K\,\delta_{ij} d\varepsilon^{e}_{kk}\ ; \\
d\varepsilon^{e}_{ij} &= d\varepsilon_{ij}\ ;\quad \text{if}\quad f(\sigma_{ij}) < \kappa \text{ or if } f(\sigma_{ij}) = \kappa \text{ and } df < 0; \\
d\varepsilon^{e}_{ij} &= d\varepsilon_{ij} - d\lambda\,(\sigma_{ij})\ \frac{\partial f(\sigma_{ij})}{\partial \sigma_{ij}}\ ;\quad \text{if}\quad f(\sigma_{ij}) = \kappa \text{ and } df \geq 0;
\end{aligned}
\tag{11}
$$

where $\sigma_{ij}$, $\varepsilon_{ij}$ are the stress and the strain components, f is the yield function, $\mu$, K and $\kappa$ are material properties, $\delta_{ij}$ is the Kronecker delta and $d\lambda$ is given by

$$
d\lambda = \frac{2\mu g_{ij} d\varepsilon_{ij} + K g_{ii} d\varepsilon_{jj}}{2\mu g_{ij} g_{ij} + K g_{ii} g_{jj} + m[\sigma_{ij} g_{ij} - \sigma_{ii} g_{jj}/3]};\quad g_{ij} = \frac{\partial f(\sigma_{ij})}{\partial \sigma_{ij}}
\tag{12}
$$

and m is a work hardening parameter.

The constitutive equations for a one-term endochronic material are

$$
\begin{aligned}
d\sigma_{ij} &= 2\mu d\varepsilon_{ij} + \frac{1}{3}(K-2\mu)\delta_{ij} d\varepsilon_{kk} - \frac{\alpha_1 \beta d\xi}{1+\beta\xi}\,(\sigma_{ij} - K\delta_{ij}\,\varepsilon_{kk}); \\
\beta d\xi &= \beta_1 \left[(d\varepsilon_{ii} d\varepsilon_{jj}) + \frac{2\mu}{K}\,(d\varepsilon_{ij} d\varepsilon_{ij})\right]
\end{aligned}
\tag{13}
$$

where $\alpha_1, \beta_1$, $\mu$, K are material properties. Index notation is used in writing Eqs. (11) to (13) and repeated indices indicate summation. The constitutive

equations for particular cases such as plane strain or stress can be derived from the above general formulations for both material models.*

Equation (13) shows that the stress increment $d\sigma_{ij}$ is linearly related to the stress $\sigma_{ij}$, which can be written as $\sigma_{ij}^{\circ} + d\sigma_{ij}$, where $\sigma_{ij}^{\circ}$ is the stress at the previous time step. Hence, Eq. (13) can be reformulated such that $d\sigma_{ij}$ is a function of $\sigma_{ij}^{\circ}$ rather than $\sigma_{ij}$ which is unknown. By doing so, the endochronic constitutive relations yield a unique stress increment at any time once the strain history, strain increment and previous stress are given. An examination of Eqs. (11) and (12) indicates that this is not true for an elastoplastic model. Hence, either an iterative technique must be used or the time step must be so small that $d\sigma_{ij}$ can be neglected compared to $\sigma_{ij}^{\circ}$ so that $\sigma_{ij}$ in these equations can be replaced by $\sigma_{ij}^{\circ}$. This implies that a time step much smaller than needed for stability must be used for some problems. Hence, it is important to do a convergence test on the effects of time step when there are no experimental data or other solutions available for comparison.

An existing finite-element code based on the corotational coordinate finite element method was modified to accept a constitutive formulation in terms of endochronic plasticity theory. The accuracy of this code is well studied in [8] for axisymmetric shell problems. The time step is taken as half of what is needed for an elastic system. This time step is stable for an elastoplastic system but is not necessarily stable for an endochronic model as explained before. Since our purpose is to evaluate endochronic theory, the same time step is used for all material models. Von Mises' yield criterion is used in computing the elastoplastic responses for the following continuum problems.

The first example of a two dimensional continuum problem is that of a clamped spherical cap subjected to suddenly applied uniform pressure on its

* Elastoplastic constitutive equations for plane stress and plane strain are available in [8]

* Endochronic constitutive equations for plane stress and plane strain are supplied by H. C. Lin.

convex surface. The geometrical dimensions and material properties of the cap are: radius of curvature, $R = 5.657 \times 10^{-1}$ m (22.27 in); thickness, $h = 1.041 \times 10^{-2}$ m (0.41 in); half angle of cap, $\alpha = 26.67°$; elastic modulus, $E_o = 7.239 \times 10^{10}$ Pa ($10.5 \times 10^6$ psi); plastic modulus, $E_p = 1.448 \times 10^9$ Pa ($2.1 \times 10^5$ psi); yield stress, $\sigma_y = 1.665 \times 10^8$ Pa ($2.4 \times 10^4$ psi); mass density, $\rho_o = 2.618 \times 10^3$ Kg/m$^3$ ($2.45 \times 10^{-4}$ lb$_f$-sec$^2$/in$^4$) and Poisson's ratio, $\nu = 0.3$. The equivalent material parameters in the endochronic formulation are $\alpha_1 = 49$ and $\beta_1 = 8.75$. The magnitude of the step pressure is $4.137 \times 10^6$ Pa (600 psi). The problem is studied by assuming either a plane stress of a plane strain condition exists in the direction normal to the surface of the cap.

The apex displacements of the cap obtained by using the classical elastic, classical elastoplastic, and the endochronic constitutive laws for the plane strain case are shown in Fig. 74. The results obtained for the plane stress case are shown in Fig. 75. For comparison, the results of Nagarajan and Popov [9] were also presented in both Figs. 74 and 75. From these results, we see that noticeable differences are introduced when the endochronic theory is used. The results using an endochronic constitutive law compare favorably with the conventional elastoplastic isotropic work-hardening assumption as far as dynamic response at the apex of the cap is concerned. In the endochronic approach, due to the earlier deviation from the linear elastic line (as can be seen from the uniaxial stress-strain curve), the results show more "plastic" deformation than the classical theory. The mean value of displacement is thus higher in the endochronic theory than in the classical theory. It can also be seen that the amplitude of vibration is somewhat smaller in the endochronic result than in the classical result. This is due to the greater dissipation of energy and the resultant greater damping effect when compared to the elastoplastic and

linear elastic cases. The creep phenomena of the endochronic model under the action of external pressure are again observed in these results. It seems that all the characteristics of one dimensional endochronic models are preserved in this cap problem.

Next, a hardening system was examined - a clamped circular plate laterally loaded over a circular central region with sheet explosive. It is assumed that a plane stress condition will be valid for the plate. Fig. 76 shows the resulting nondimensional apex displacement versus time for 6061-T6 aluminum. The plate geometry is: thickness, $h = 1.588 \times 10^{-3}$ m (1/16 in) and diameter, $D = 1.524 \times 10^{-1}$ m (6 in.). The material properties used for aluminum are : $E_o = 7.098 \times 10^{10}$ Pa ($1.029 \times 10^7$ psi); $E_p = 3.754 \times 10^8$ Pa ($5.444 \times 10^4$ psi); $\sigma_y = 2.923 \times 10^8$ Pa ($4.240 \times 10^4$ psi); ultimate stress, $\sigma_u = 3.096 \times 10^8$ Pa ($4.490 \times 10^4$ psi); mass density, $\rho_o = 2.680 \times 10^3$ Kg/m$^3$ ($2.508 \times 10^{-4}$ lb$_f$-sec$^2$/in$^4$) and $\nu = 0.3$. The applied impulse is $I = 1.67$ N·s; it is assumed to be uniformly distributed over a central circular region of diameter $5.080 \times 10^{-2}$ m (2 in.). The parameters used for the endochronic model are $\alpha_1 = 2.755 \times 10^4$ and $\beta_1 = 0.01252$.*

The experimental result and another finite difference numerical result DEPROSS were taken from [10]. It appears that all numerical results are in good agreement with the experimental result. Fig. 77 shows the results obtained for a similar problem where $h = 3.175 \times 10^{-3}$ m (1/8 in) and $I = 1.96$ N·s. Reasonable agreement is observed between numerical results at least for the peak displacement. Fig. 78 shows the apex response of a 1022 steel plate whose dimensions are exactly those of Fig. 76 ($h = 1.588 \times 10^{-3}$ m) and whose material parameters are: $E_o = 1.960 \times 10^{00}$ Pa ($2.842 \times 10^7$ pse); $E_p = 3.618 \times 10^9$ Pa ($5.248 \times 10^5$ psi); $\sigma_y = 5.585 \times 10^8$ Pa ($8.1 \times 10^4$ psi); $\sigma_u = 6.205 \times 10^8$ Pa ($9 \times 10^4$ psi); $\rho_o = 7.789 \times 10^3$ Kg/m$^3$ ($7.288 \times 10^{-4}$ lb$_f$-sec$^2$/

* Values for ($\alpha_1$) and ($\beta_1$) are supplied by H. C. Lin

$in^4$); $\nu$=0.3; I = 2.20 N·s; $\alpha_1 = 2.222 \times 10^5$ and $\beta_1 = 2.045 \times 10^{-3}$*. Very good agreement is again noted. No creeping from endochronic model is observed in these results since the impulses are treated as initial velocity conditions.

It is noted that the endochronic parameters $\alpha_1$ and $\beta_1$ used in these impulse problems are not obtained by using Eq. (10). This is done in order to get closer resemblance between the constitutive curves near the yield point, since Eq. (10) best fits the bi-linear curve at $\varepsilon \to 0$ and $\varepsilon \to \infty$ and fits worst around the yield point. Better results are obtainable by adjusting $\alpha_1$ and $\beta_1$ to best fit the endochronic constitutive equations to experimental data at the regions of interest.

The last example is the penetration of one short solid nickel cylinder into another short but wider aluminum cylinder. The geometric dimensions of the cylinders and their configuration at the instant of impact is presented in Fig. 79. Since the problem is axisymmetric, only the shaded area needs to be studied. The problem is represented by a finite element model composed of 236 nodes and 400 corotational triangular elements. For this example, the cylinders are assumed to be bonded to each other such that no slippage can occur between the two surfaces and the materials are not allowed to fracture. The material properties for nickel are: $E_o = 1.963 \times 10^{11}$ Pa; $E_p = 2.413 \times 10^9$ Pa; $\sigma_y = 6.200 \times 10^8$; $\nu = 0.3$; and $\rho_o = 8.86 \times 10^3$ Kg/m$^3$. The material properties for aluminum are: $E_o = 7.65 \times 10^{10}$ Pa; $E_p = 8.045 \times 10^8$ Pa; $\sigma_y = 3.1 \times 10^8$ Pa; $\nu = 0.3$; and $\rho_o = 2.785 \times 10^3$ Kg/m$^3$. The velocity of the projectile at the instant of impact is 500 m/s.

Severe distortions are expected for this example. Hence, the nonlinear Mie-Grüneisen equation of state relating the hydrostatic pressure p and density change $\mu$ is used in place of the linear equation used in the previous examples for both the elastoplastic and endochronic models. This equation can be written

* Values for $\alpha_1$ and $\beta_1$ are supplied by H. C. Lin.

as [11]

$$p = (K_1\mu + K_2\mu^2 + K_3\mu^3)(1 - \frac{\Gamma\mu}{2}) + \Gamma(1 + \mu)\rho_o E$$

where

$$\Gamma = \Gamma_o + A\mu + B\mu^2 + C\mu^3$$

and

$$\mu = \frac{\rho}{\rho_o} - 1$$

The specific internal energy, E, is obtained from the work done by various stress. $K_1$, $K_2$ and $K_3$ are material dependant constants; $\Gamma_o$, A, B, and C are Grüneisen coefficients. The initial density and density during motion are $\rho_o$ and $\rho$, respectively. The following values in SI units obtained from [11] are used for this example:

Ni - $K_1 = 1.963 \times 10^{11}$, $K_2 = 3.750 \times 10^{11}$, $K_3 = 0$,

$\Gamma_o = 1.91$, $A = -8.007$, $B = 3.528 \times 10^1$ and $C = -5.982 \times 10^1$

Al - $K_1 = 7.65 \times 10^{11}$, $K_2 = 1.659 \times 10^{11}$, $K_3 = 4.28 \times 10^{10}$,

$\Gamma_o = 2.13$, $A = -7.245$, $B = 2.471 \times 10^1$ and $C = -3.257 \times 10^1$

The final configurations of the cylinders before failure occurs for elasto-

plastic, endochronic and linearly elastic models using various time integration steps are shown in Fig. 80. Failure is defined as when an element is so severely deformed that its area changes sign during a time step. All time steps used in Fig. 80 are much smaller than required for stability for a linear elastic system. It can be seen that a stable time step may not guarantee accurate results in the elastoplastic case. The material behavior is more like plastic flow theory only when the time step is much smaller than the stability requirement. It behaves more like a total-deformation-theory material when the time step is large (but still well below the stability requirement). The cause of this high sensitivity to time step for this problem is the inability to formulate the stress increment in terms of known quantities for an elastoplastic model as previously discussed. Since no criterion exists for determining the time step for accurate solution, it is suggested that a parameter study on the effect of time step size be performed for this type of problem when an elastoplastic model is used.

A severely distorted strip along the 45° direction is lost in the elastoplastic model when the time step is greater than 0.05 μs. This strip is observed in all endochronic solutions; furthermore, no appreciable difference in solution exists over a wide range of time steps. All endochronic solutions show two severely distorted strips - one along 45°, another one along 90°, while the elastoplastic ones show two strips only when time steps are not greater than 0.05 μs. Fig. 81 shows the final configuration of the endochronic model before failure. The circles indicate the position of the interface of the two cylinders. It is interesting to note that the severe distortion does not occur at the interface. The endochronic parameters for this penetration problem are computed from the elastoplastic parameters by using Eq. (10).

## CONCLUSION

Extensive numerical studies have been performed for spring-mass systems and axisymmetric continuum systems using various constitutive models. The following conclusions were made:

(1) Perment plastic strains are larger and occur at lower stress levels in the endochronic model than in the elastoplastic model when they are connected by Eq. (10).

(2) Hysteresis loops occur for an endochronic model when the system is subjected to initial displacement or velocity conditions.

(3) An endochronic model creeps when subjected to an external force. However, hysteresis loops start forming immediately after removal of the external force.

(4) Better agreement with the elastoplastic solution can be obtained for a particular range of interest by adjusting values of $\alpha_1$ and $\beta_1$ rather than using Eq. (10), which gives the best fit to the bi-linear elastoplastic material only as $\varepsilon \to 0$ and $\varepsilon \to \infty$ and which fits worst around the yield point.

(5) The stress increment can not be formulated with reasonable effort in terms of known quantities for a multi-dimensional elastoplastic model. Hence, much smaller time steps are needed for accurate solution of an elastoplastic model. No such difficulty exists for an endochronic model.

(6) Physically reasonable qualitative solutions are obtained for the endochronic model for all the problems studied.

(7) Numerically unique and stable solutions are obtained for all the constitutive models.

(8) An endochronic model may be physically unstable in the sense it may creep with respect to the intrinsic time.

(9) The endochronic model has higher numerical efficiency compared to the elastoplastic model in multi-dimensional problems.

(10) The creep phenomenon of an endochronic model can be used as a safety factor in design problems.

REFERENCES

[1] Valanis, K. C., "A Theory of Viscoplasticity without a Yield Surface," Archives of Mechanics, Archiwum Mechaniki Stosowanej, Vol. 23, No. 4, pp. 517-533, Warszawa, 1971.

[2] Valanis, K. C., "A Theory of Viscoplasticity without a Yield Surface," Archives of Mechanics, Archiwum Mechaniki Stosowanej, Vol. 23, No. 4, pp. 535-551, Warszawa, 1971.

[3] Bazant, Z. P. and Krizek, R. J., "Endochronic Constitutive Law for Liquefaction of Sand," J of Engineering Mechanics Division, ASCE, Vol. 102, No. EM4, pp. 225-238, 1976.

[4] Bazant, Z. P. and Bhat, P., "Endochronic Theory of Inelasticity and Failure of Concrete," J of Engineering Mechanics Division, ASCE, Vol. 102, No. EM4, pp. 701-722, 1976.

[5] Lin, H. C., "Dynamic Plastic Deformation of Axi-symmetric Circular Cylindrical Shells," Nuclear Engineering and Design, Vol. 35, No. 2, pp. 283-293, 1975.

[6] Sandler, I. S., "On the Uniqueness and Stability of Endochronic Theories of Material Behavior," J of Applied Mechanics, Vol. 45, pp. 263-266, June 1978.

[7] Biggs, J. M., "Introduction to Structural Dynamics," McGraw-Hill, Inc., 1964.

[8] Hsieh, B. J., "Nonlinear Dynamic Analysis of Axisymmetric Shells by the Corotational Finite Element Method," ANL-CT-77-36.

[9] Nagarajan, S. and Popov, E. P., "Elastic-Plastic Dynamic Analysis of Axisymmetric Soldis," Computers & Structures, Vol. 4, pp. 1117-1134, 1974.

[10] Duffey, T. A. and Key, S. W., "Experimental-Theoretical Correlations of Impulsively Loaded Clamped Circular Plates," Experimental Mechanics, pp. 1-9, June 1969.

[11] Walsh, J. M., Rice, M. H., McQueen, R. G., and Yarger, F. L., "Shock-Wave Compressions of Twenty-Seven Metals. Equation of State of Metals," Physical Review, Vol. 108, No. 2, pp. 196-216, October 1957.

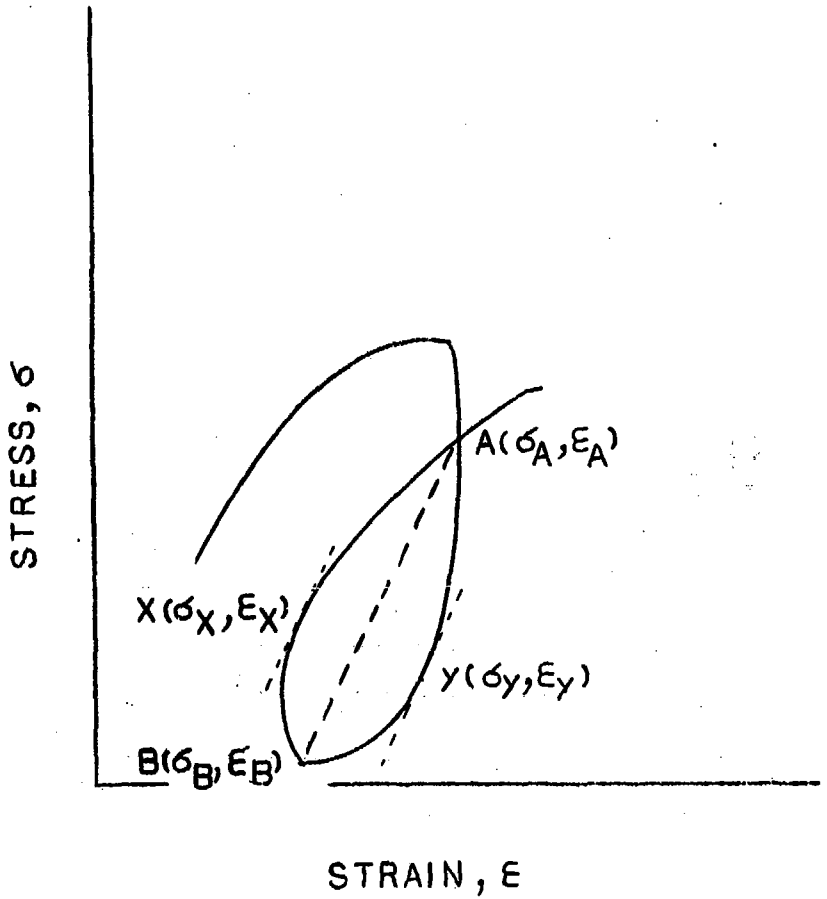


**Figure 1**

**Condition for forming a hysteresis loop**

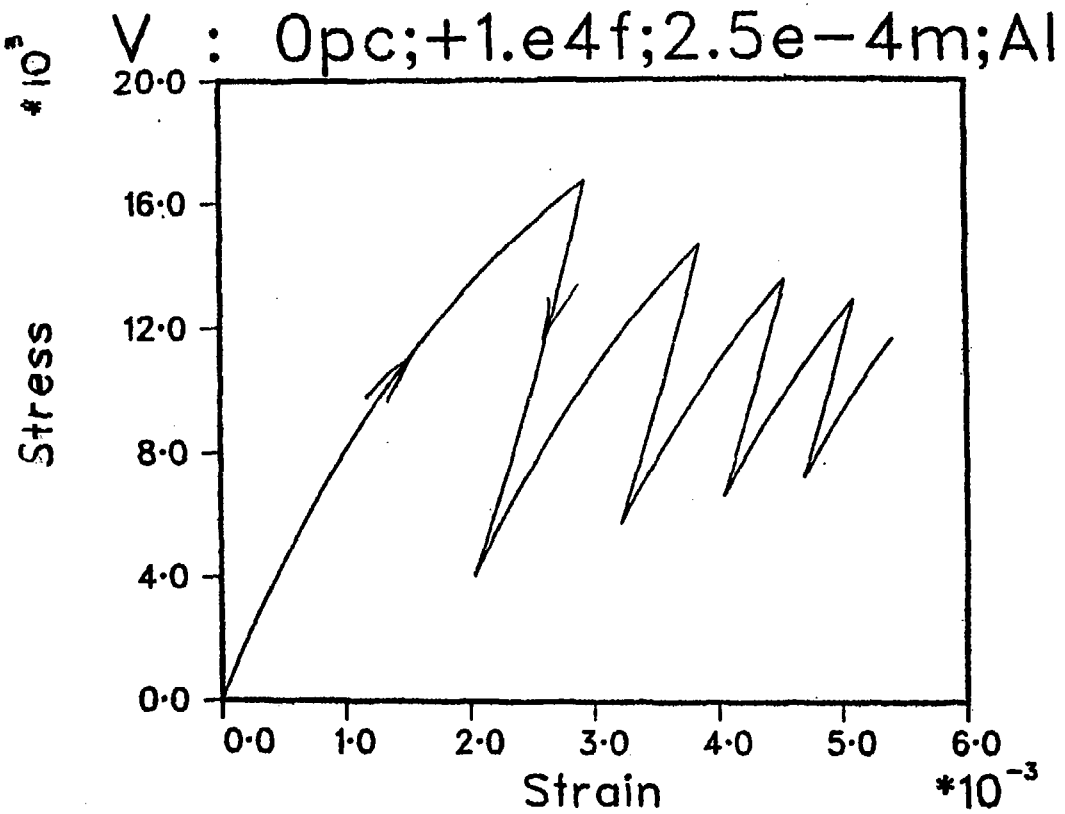


Figure 2

"Unstable" endochronic stress-strain curve

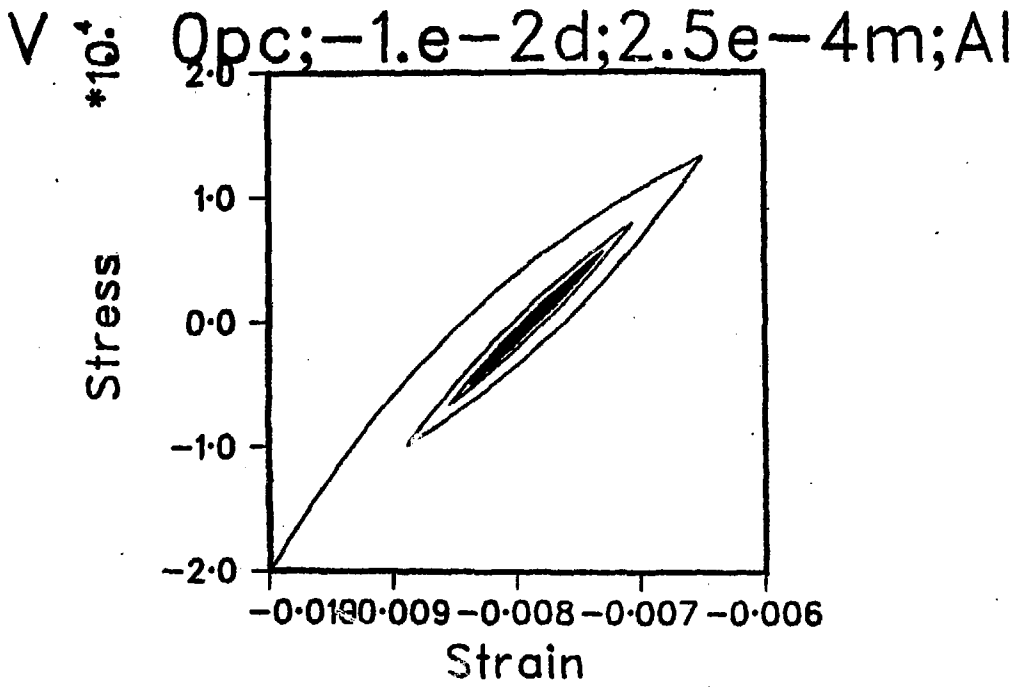


Figure 3

Stable endochronic stress-strain curve with hysteresis loops

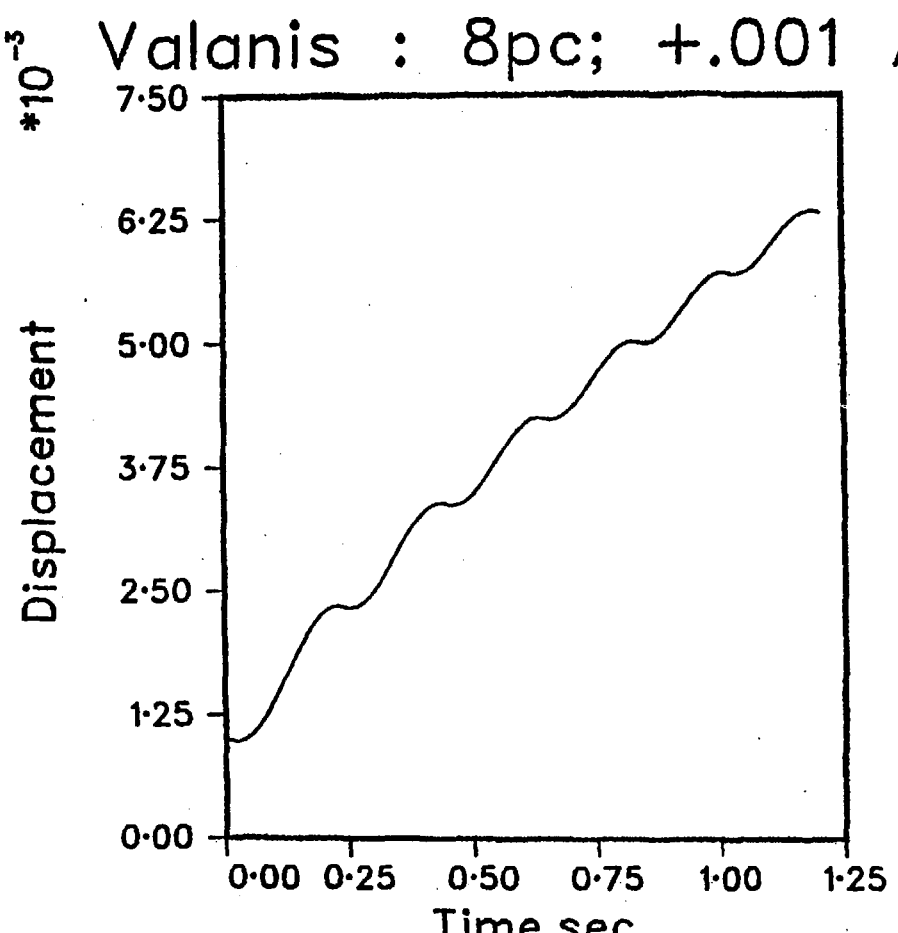


Figure 4

Dynamic response of an endochronic spring-mass system that is pre-strained by adding weight to 8% strain then subjected to an initial displacement equivalent to +0.1% strain

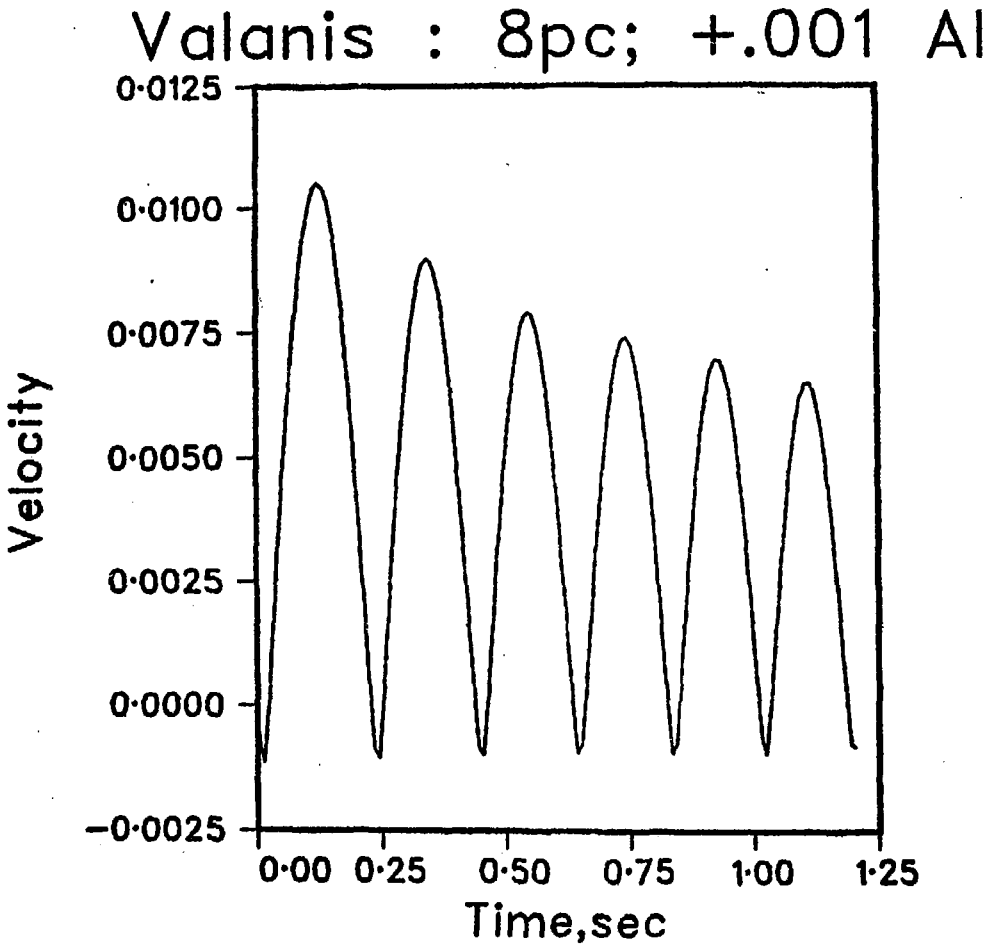


Figure 5

Dynamic response of an endochronic spring-mass system that is pre-strained by adding weight to 8% strain then subjected to an initial displacement equivalent to +0.1% strain

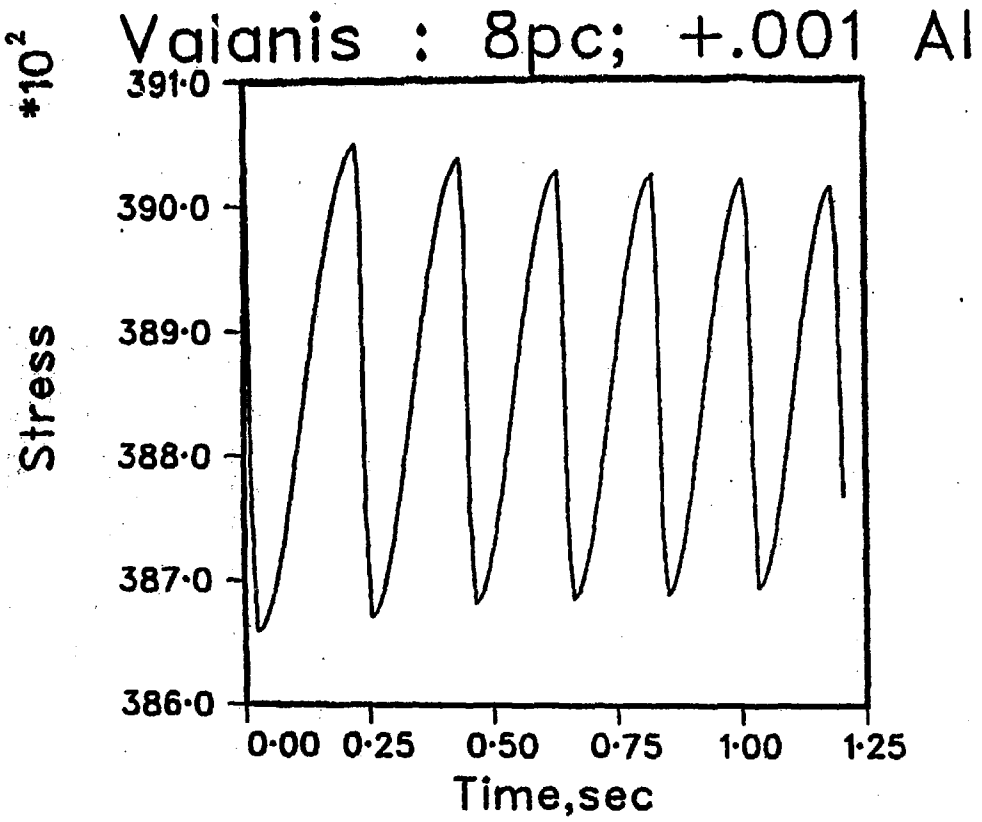


Figure 6

Dynamic response of an endochronic spring-mass system that is pre-strained by adding weight to 8% strain then subjected to an initial displacement equivalent to +0.1% strain

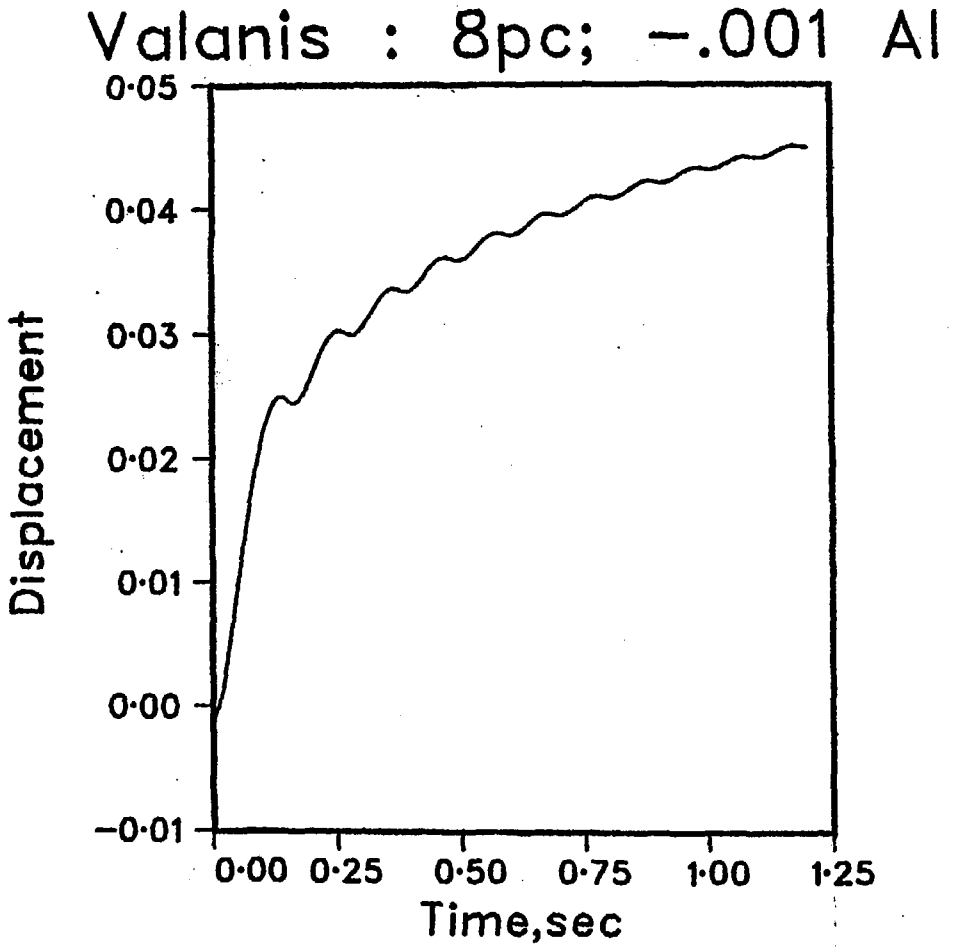


Figure 7

Dynamic response of an endochronic spring-mass system that is pre-strained by adding weight to 8% strain then subjected to an initial displacement equivalent to -0.1% strain

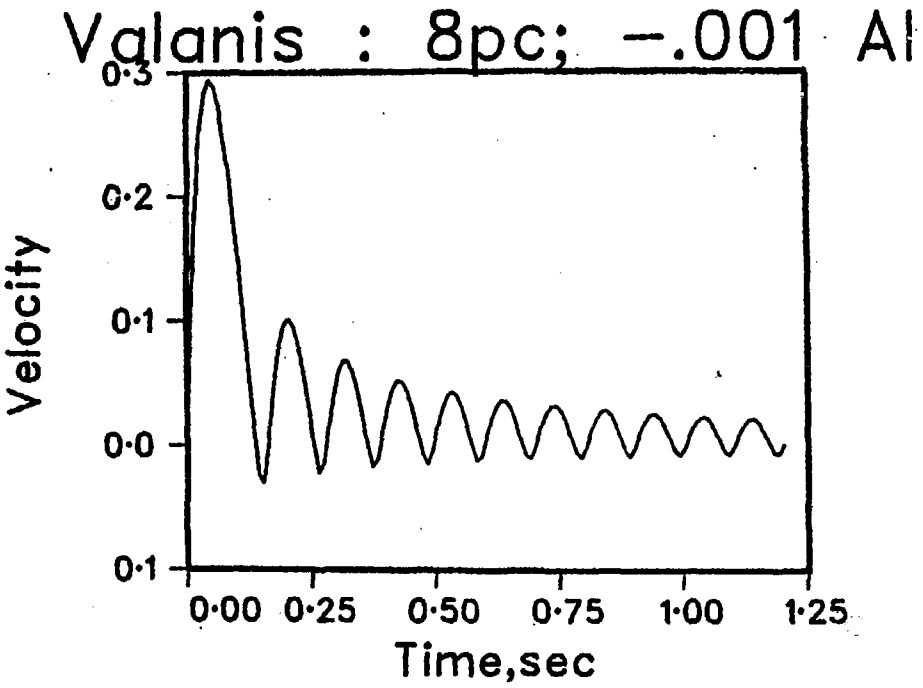


Figure 8

Dynamic response of an endochronic spring-mass system that is pre-strained by adding weight to 8% strain then subjected to an initial displacement equivalent to -0.1% strain

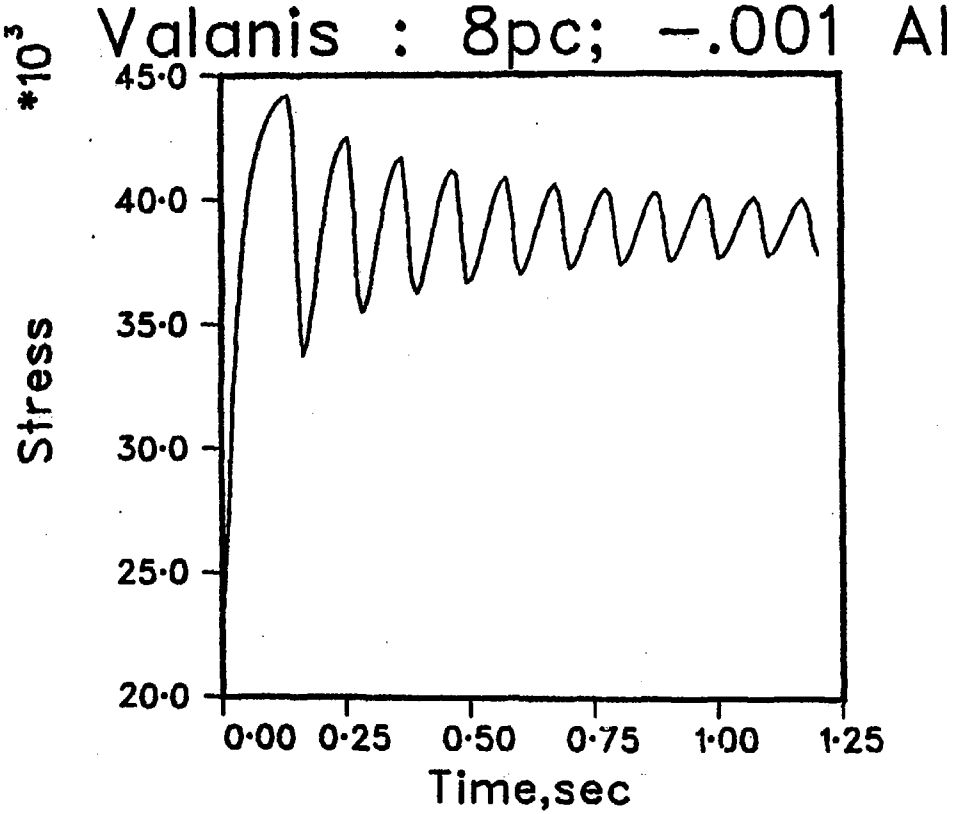


Figure 9

Dynamic response of an endochronic spring-mass system that is pre-strained by adding weight to 8% strain then subjected to an initial displacement equivalent to -0.1% strain

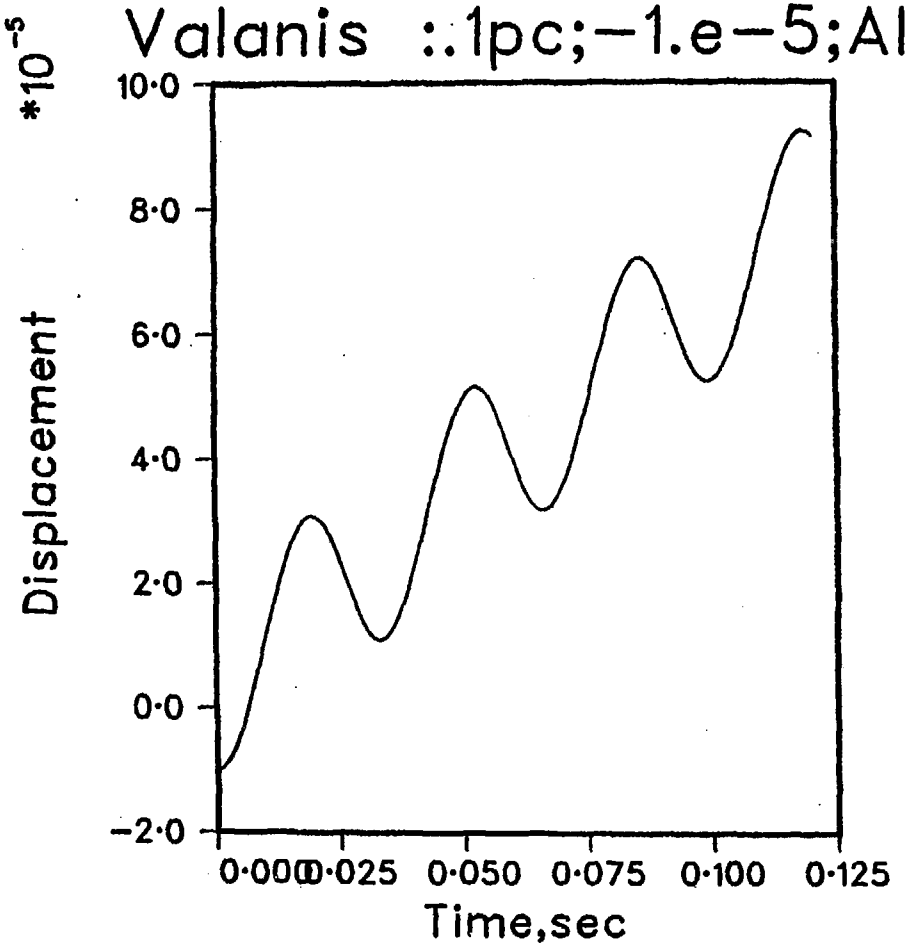


Figure 10

Dynamic response of an endochronic spring-mass system that is pre-strained by adding weight to 0.1% strain then subjected to an initial displacement equivalent to -0.001% strain

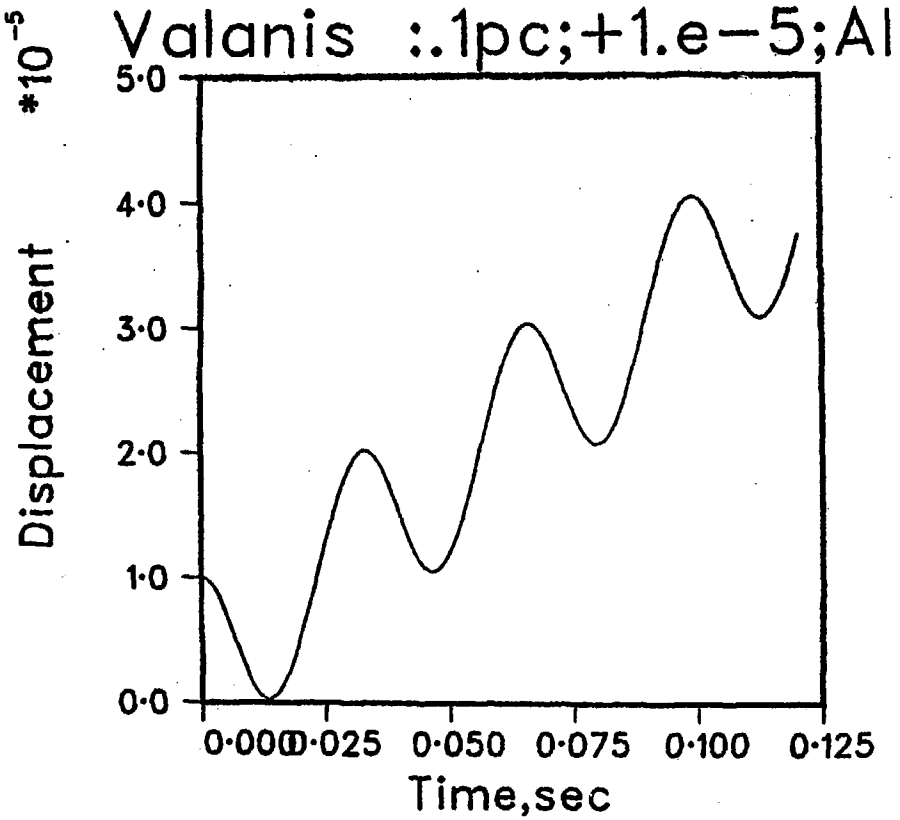


Figure 11

Dynamic response of an endochronic spring-mass system that is pre-strained by adding weight to 0.1% strain then subjected to an initial displacement equivalent to +0.001% strain

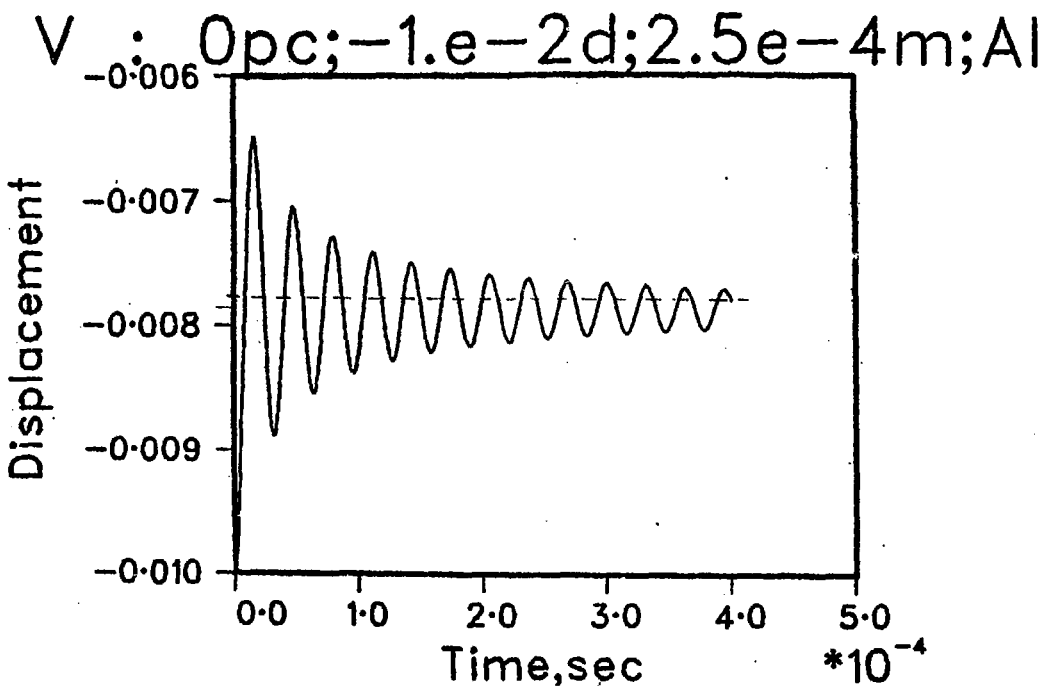


Figure 12

Dynamic response of an endochronic spring-mass system that is subjected to an initial displacement equivalent to -1% strain. Dotted line is the final equilibrium position of the associated linearly elastic, perfectly plastic system.

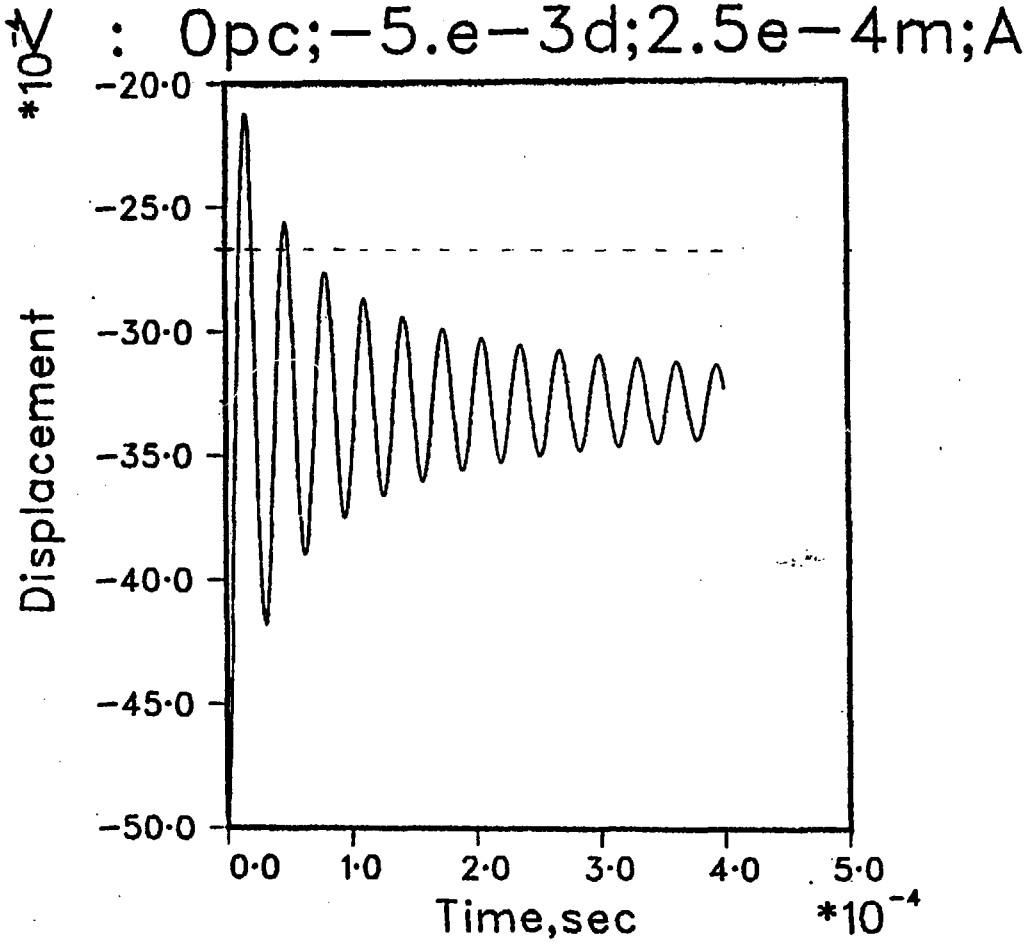


Figure 13

Dynamic response of an endochronic spring-mass system that is subjected to an initial displacement equivalent to -0.5% strain. Dotted line is the final equilibrium position of the associated linearly elastic, perfectly plastic system.

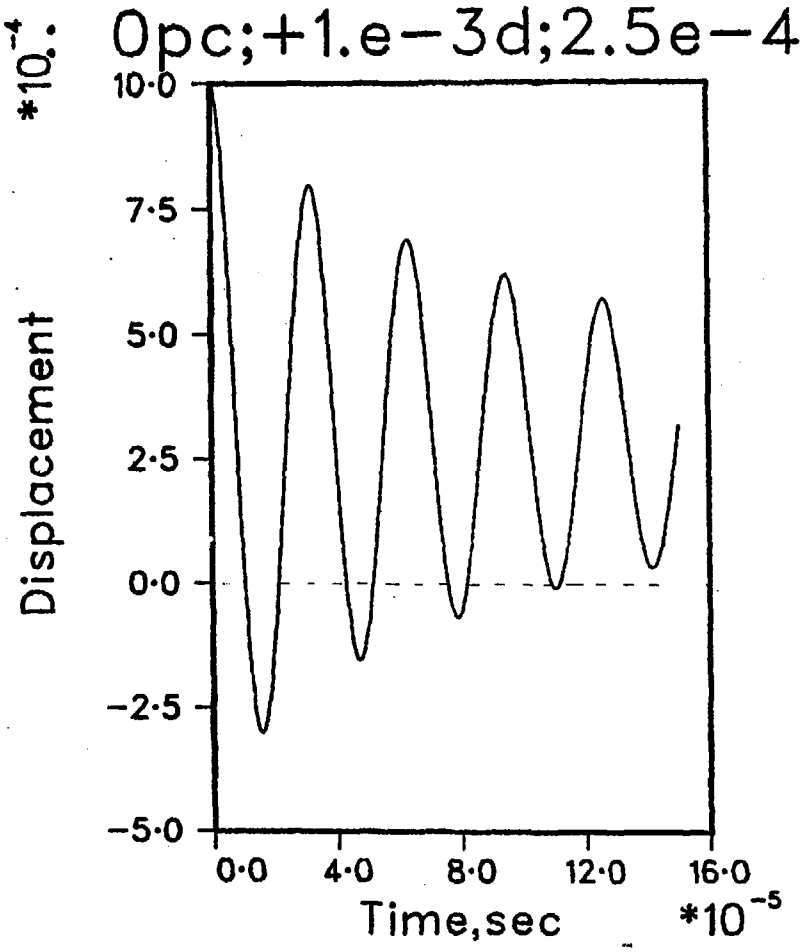


Figure 14

Dynamic response of an endochronic spring-mass system that is subjected to an initial displacement equivalent to 0.1% strain. Dotted line is the final equilibrium position of the associated linearly elastic, perfectly plastic system.

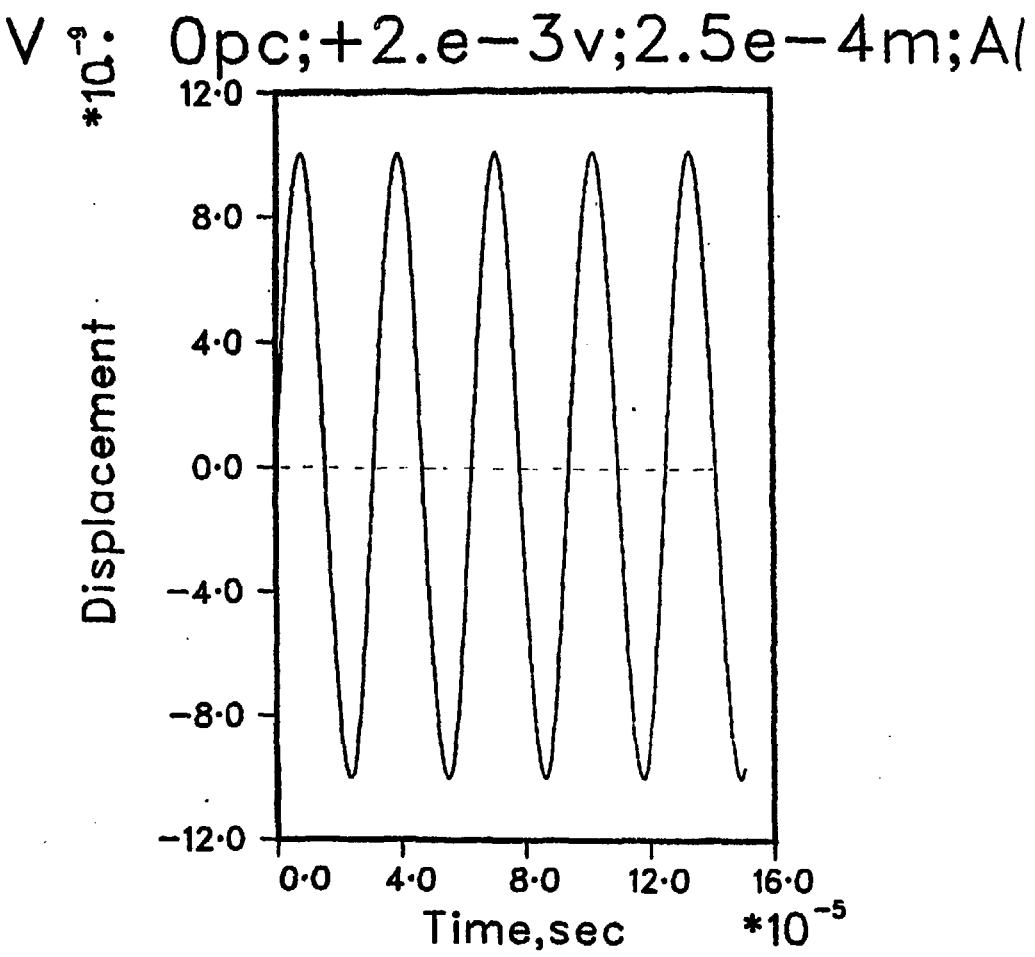


Figure 15

Dynamic response of an endochronic spring-mass system that is subjected to an initial velocity equivalent to 0.2% strain/sec.

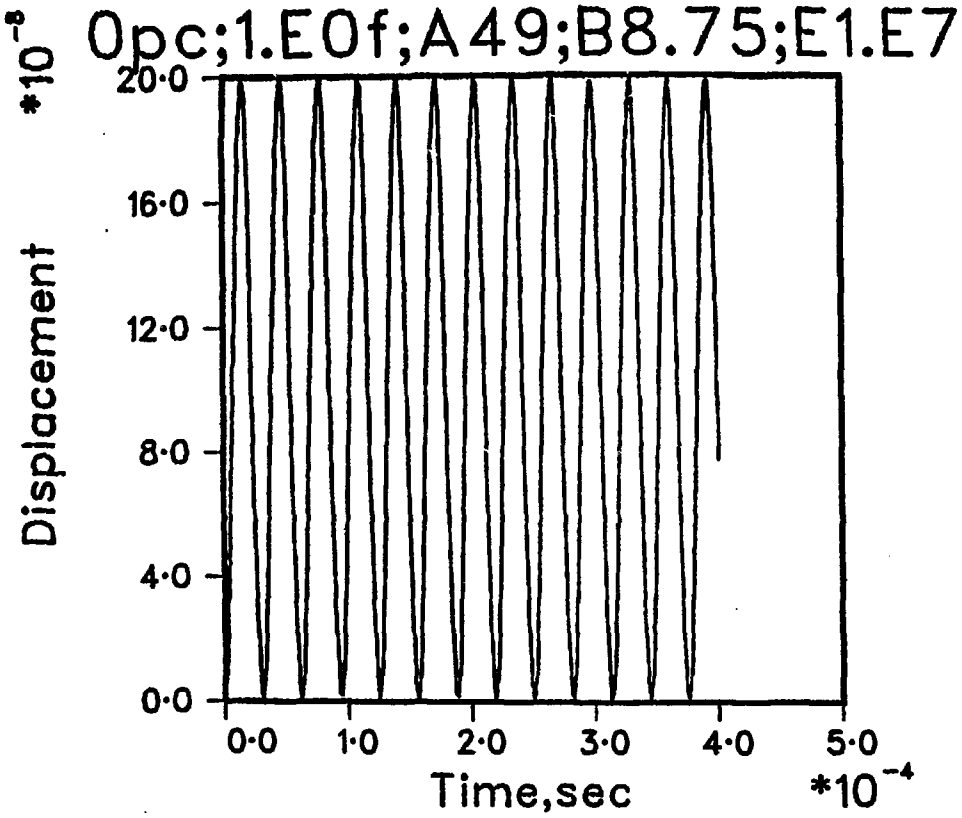


Figure 16

Dynamic responses of a spring-mass system that is subjected to a step loading of 4.448 N. Solid line - endochronic solution; chain-dashed line - elastoplastic solution.

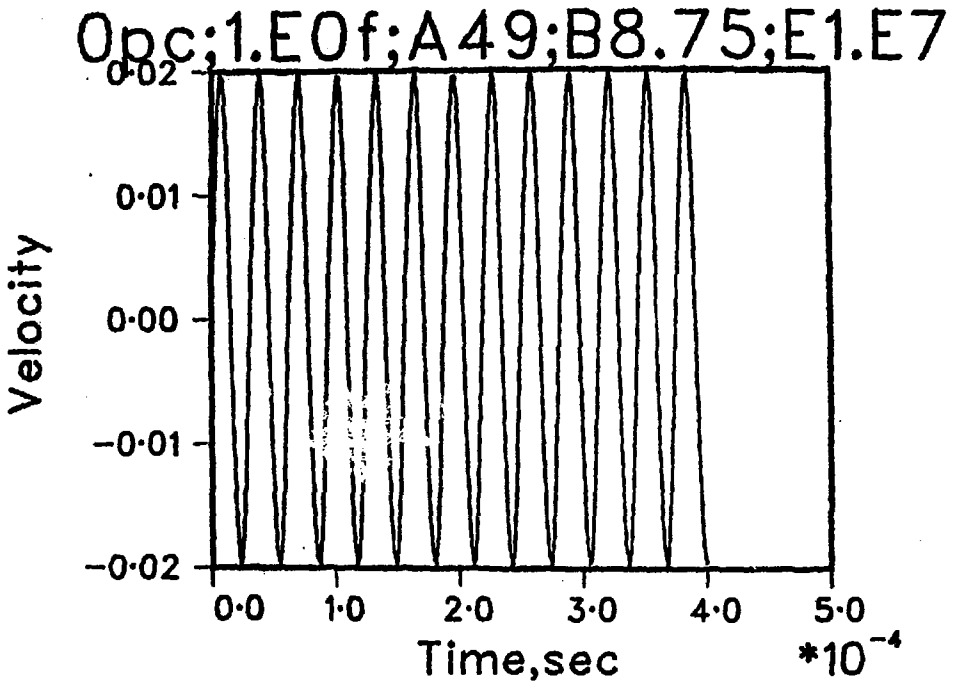


Figure 17

Dynamic responses of a spring-mass system that is subjected to a step loading of 4.448 N. Solid line - endochronic solution; chain-dashed line - elastoplastic solution.

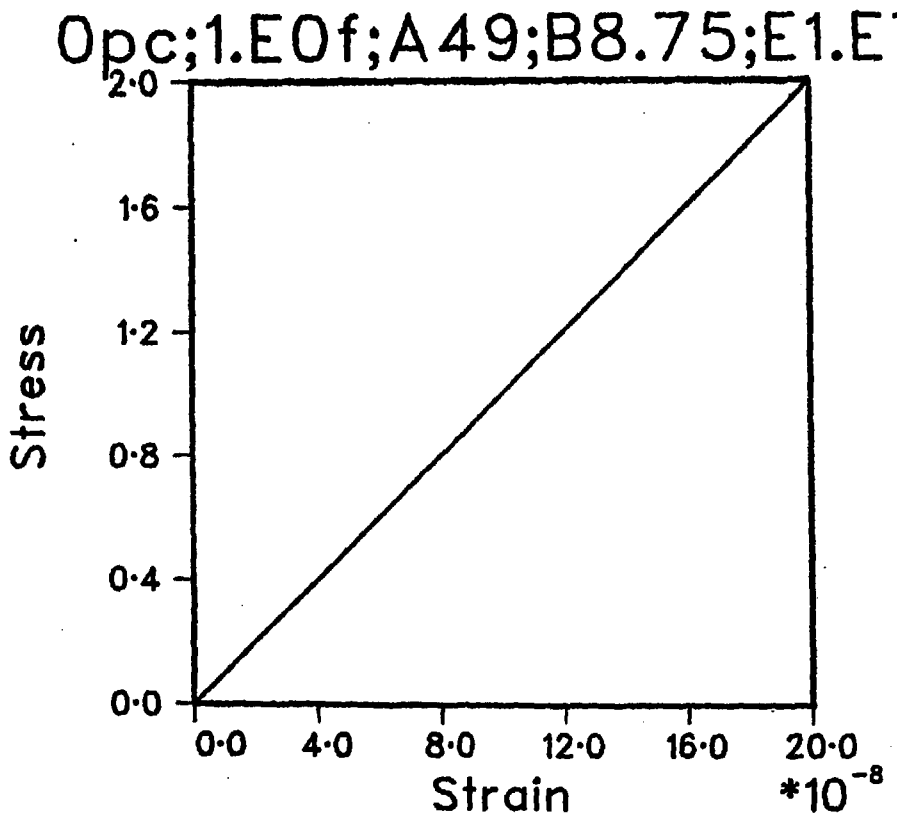


Figure 18

Dynamic responses of a spring-mass system that is subjected to a step loading of 4.448 N. Solid line - endochronic solution; chain-dahsed line - elastoplastic solution.

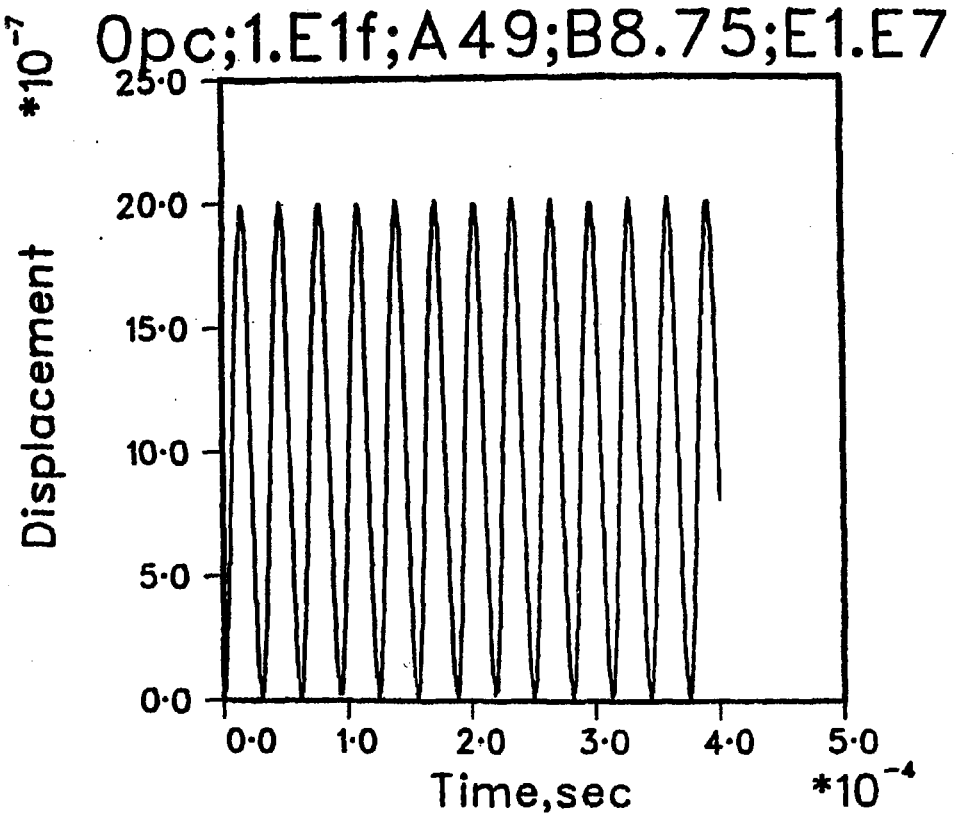


Figure 19

Dynamic responses of a spring-mass system that is subjected to a step loading of 4.448 x 10 N. Solid line - endochronic solution; chain-dashed line - elastoplastic solution.

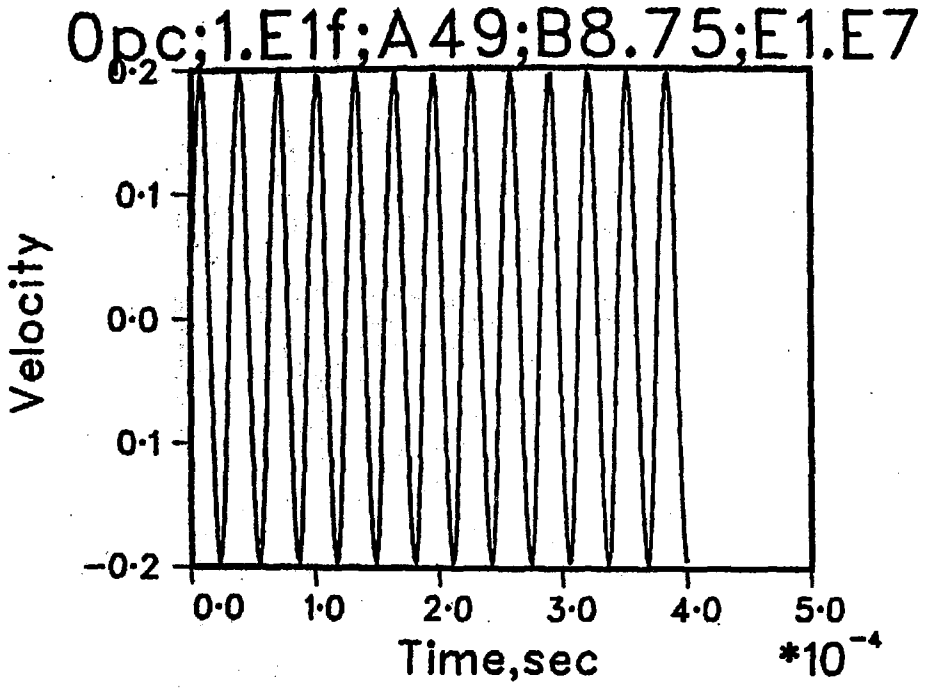


Figure 20

Dynamic responses of a spring-mass system that is subjected to a step loading of 4.448 x 10 N. Solid line - endochronic solution; chain-dashed line - elastoplastic solution.

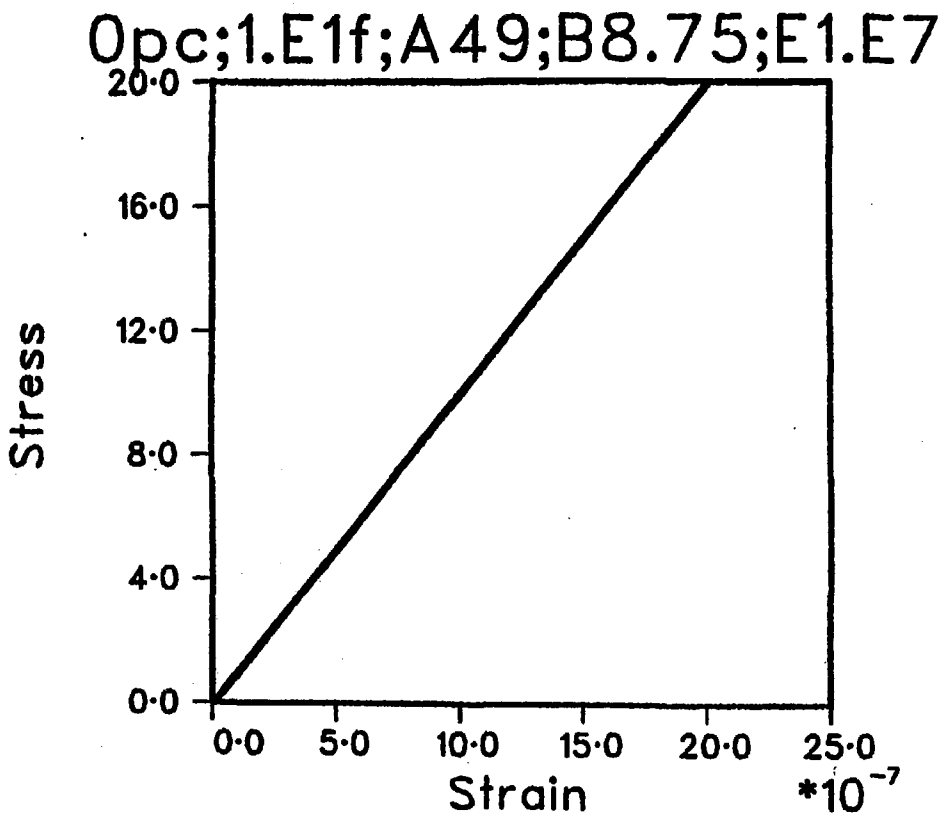


Figure 21

Dynamic responses of a spring-mass system that is subjected to a step loading of 4.448 x 10 N. Solid line - endochronic solution; chain-dashed line - elastoplastic solution.

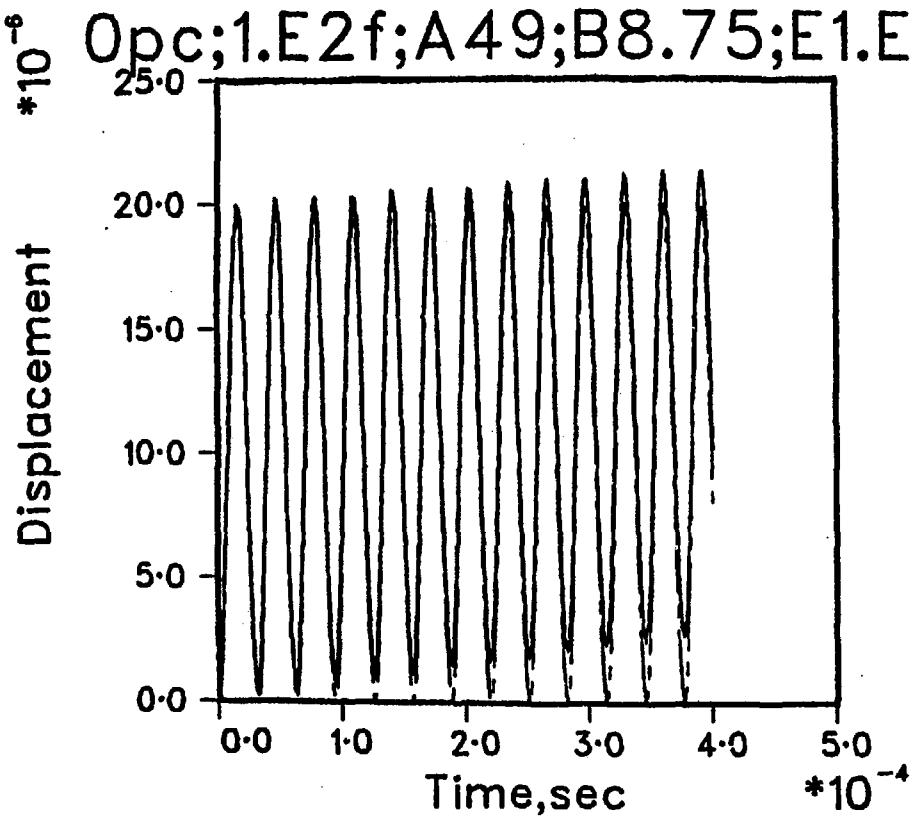


Figure 22

Dynamic responses of a spring-mass system that is subjected to a step loading of $4.448 \times 10^2$ N. Solid line - endochronic solution; chain-dashed line - elastoplastic solution.

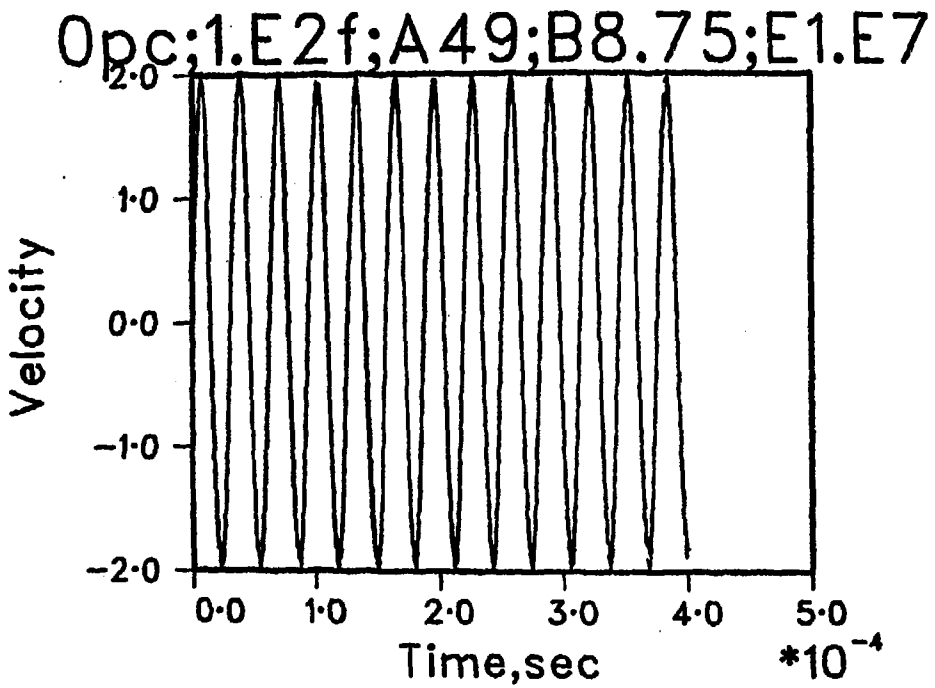


Figure 23

Dynamic responses of a spring-mass system that is subjected to a step loading of $4.448 \times 10^2$ N. Solid line - endochronic solution; chain-dashed line - elastoplastic solution.

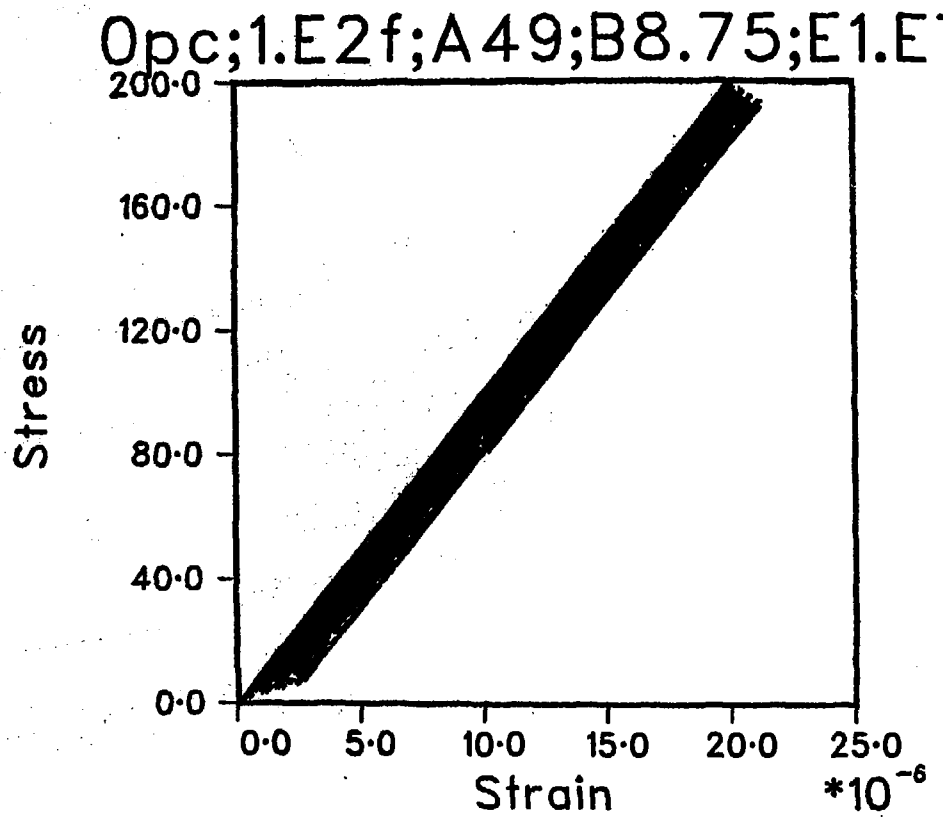


Figure 24

Dynamic responses of a spring-mass system that is subjected to a step loading of $4.448 \times 10^2$ N. Solid line - endochronic solution; chain-dashed line - elastoplastic solution.

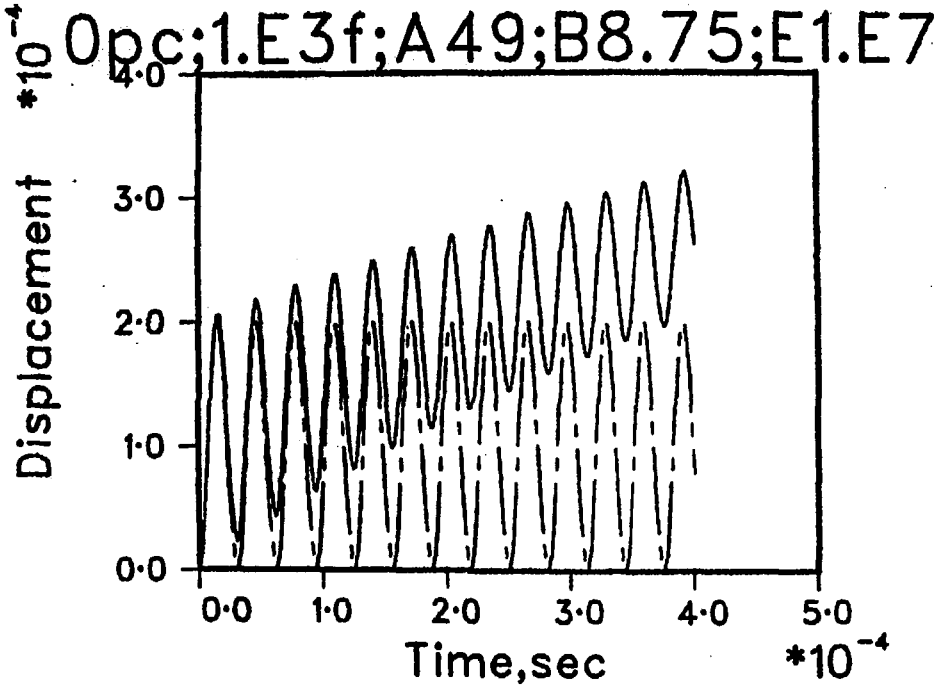


Figure 25

Dynamic responses of a spring-mass system that is subjected to a step loading of $4.448 \times 10^3$ N. Solid line - endochronic solution; chain-dashed line - elastoplastic solution.

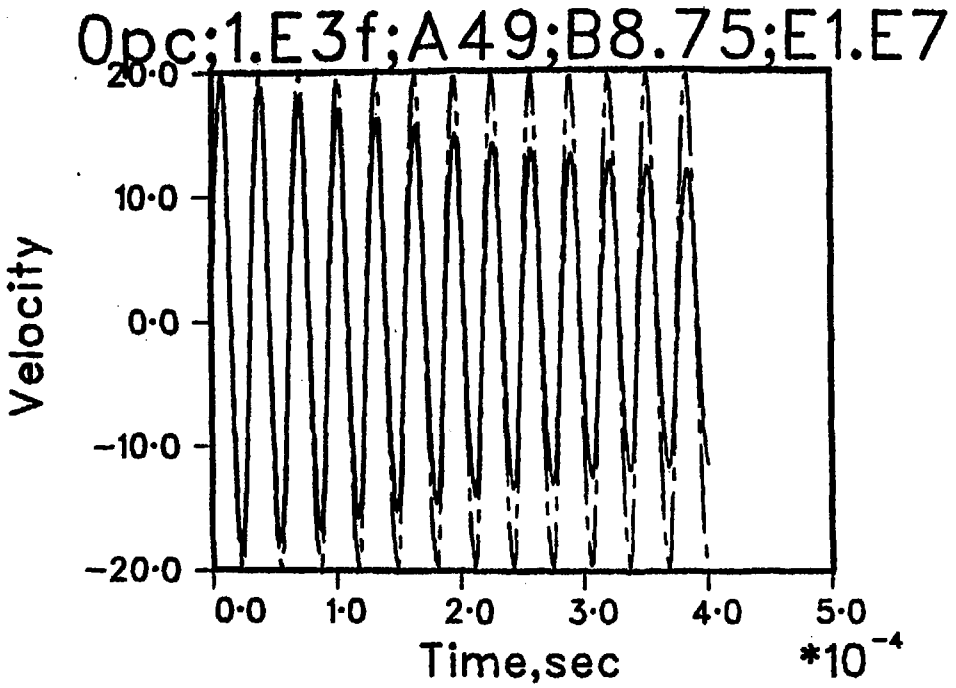


Figure 26

Dynamic responses of a spring-mass system that is subjected to a step loading of $4.448 \times 10^3$ N. Solid line - endochronic solution; chain-dashed line - elastoplastic solution.

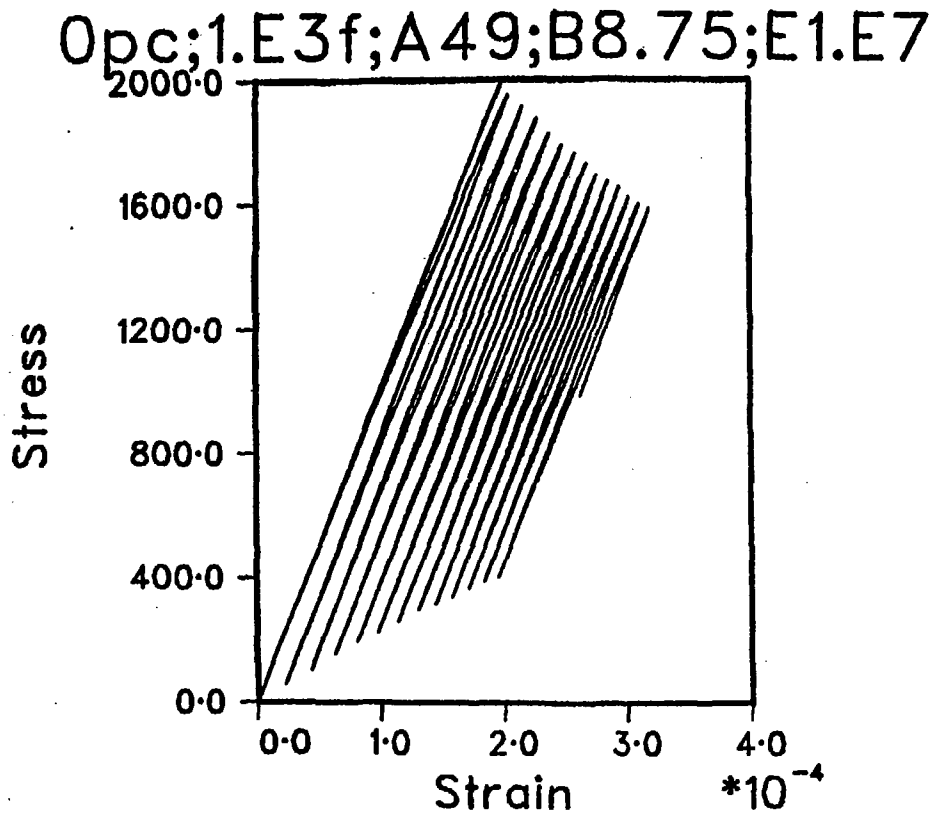


Figure 27

Dynamic responses of a spring-mass system that is subjected to a step loading of $4.448 \times 10^3$ N. Solid line - endochronic solution; chain-dashed line - elastoplastic solution.

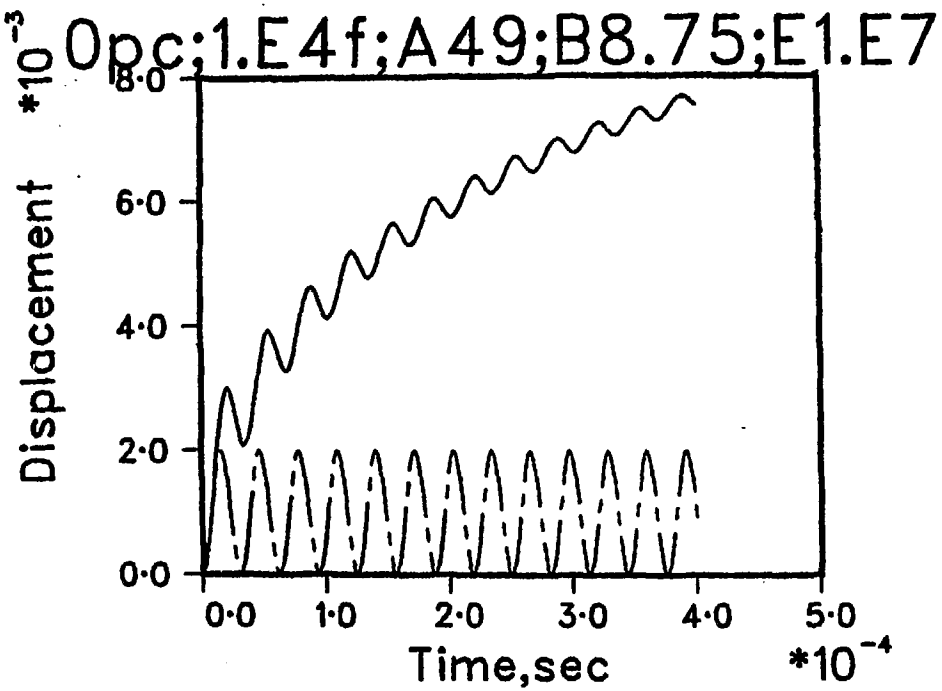


Figure 28

Dynamic responses of a spring-mass system that is subjected to a step loading of $4.448 \times 10^4$ N. Solid line - endochronic solution; chain-dashed line - elastoplastic solution.

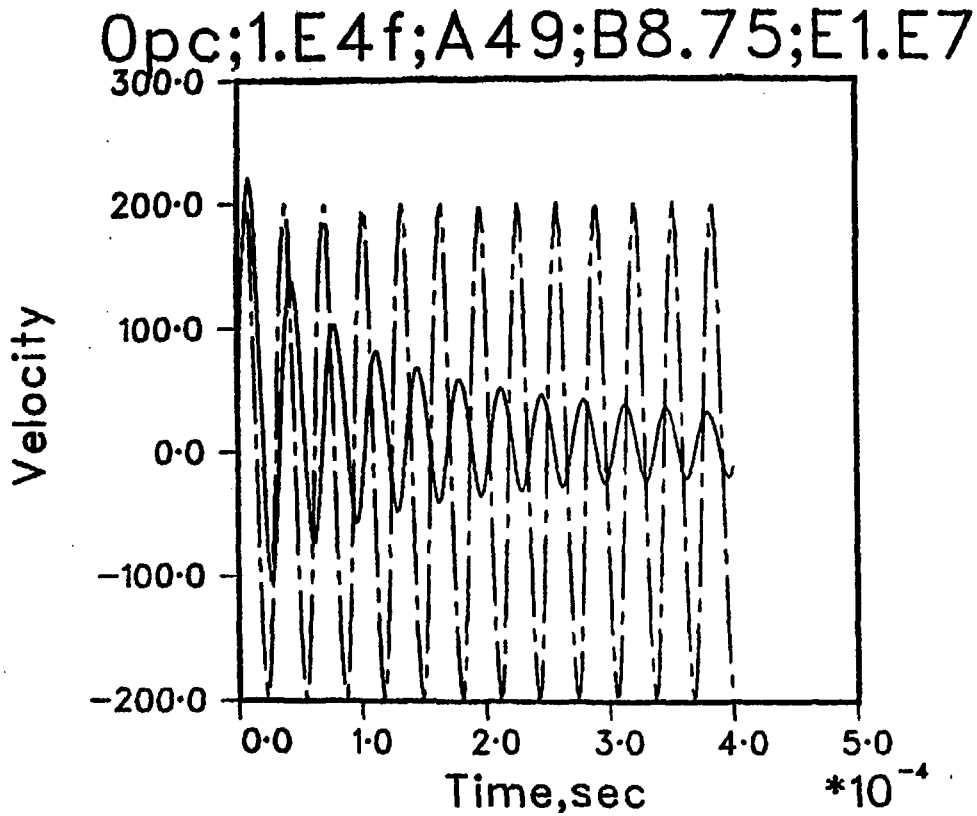


Figure 29

Dynamic responses of a spring-mass system that is subjected to a step loading of $4.448 \times 10^4$ N. Solid line - endochronic solution; chain-dashed line - elastoplastic solution.

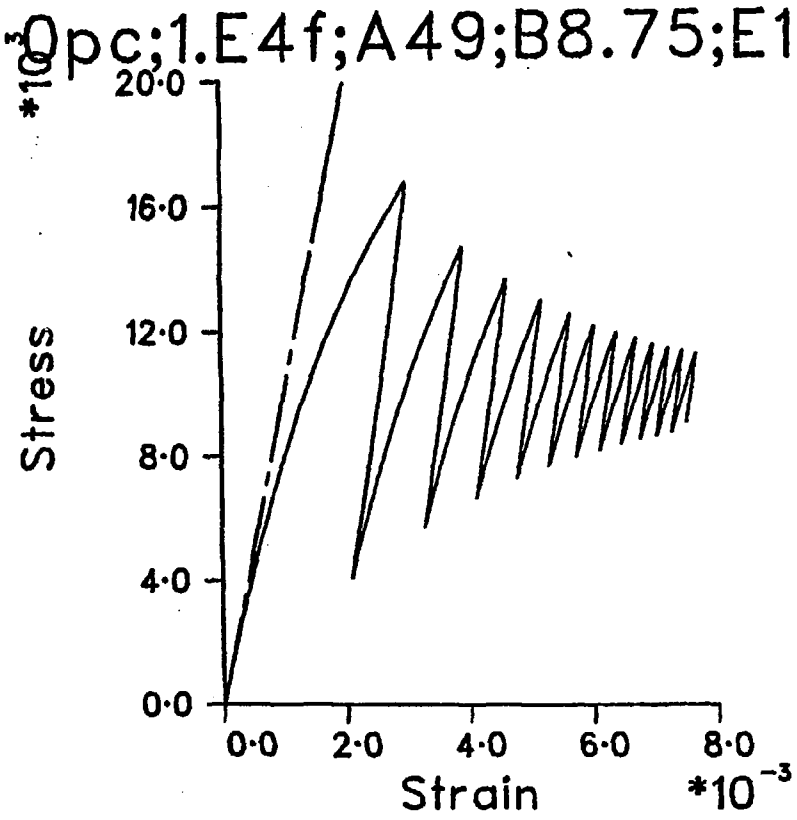


Figure 30

Dynamic responses of a spring-mass system that is subjected to a step loading of $4.448 \times 10^4$ N. Solid line - endochronic solution; chain-dashed line - elastoplastic solution.

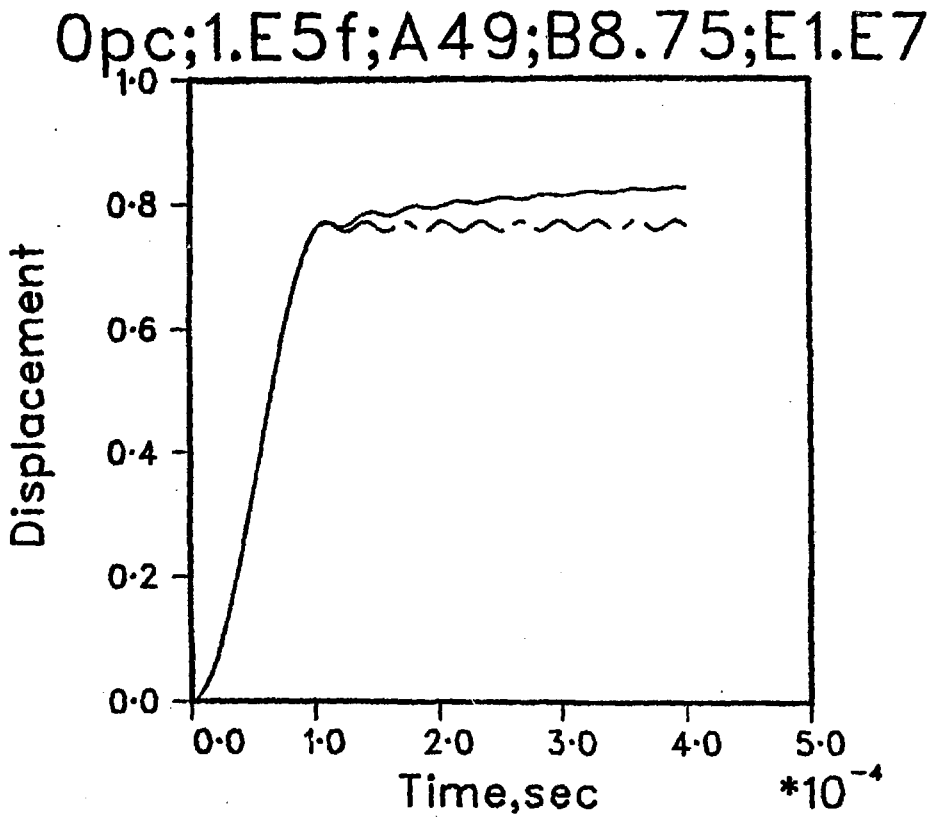


Figure 31

Dynamic responses of a spring-mass system that is subjected to a step loading of $4.448 \times 10^{5}$ N. Solid line - endochronic solution; chain-dashed line - elastoplastic solution.

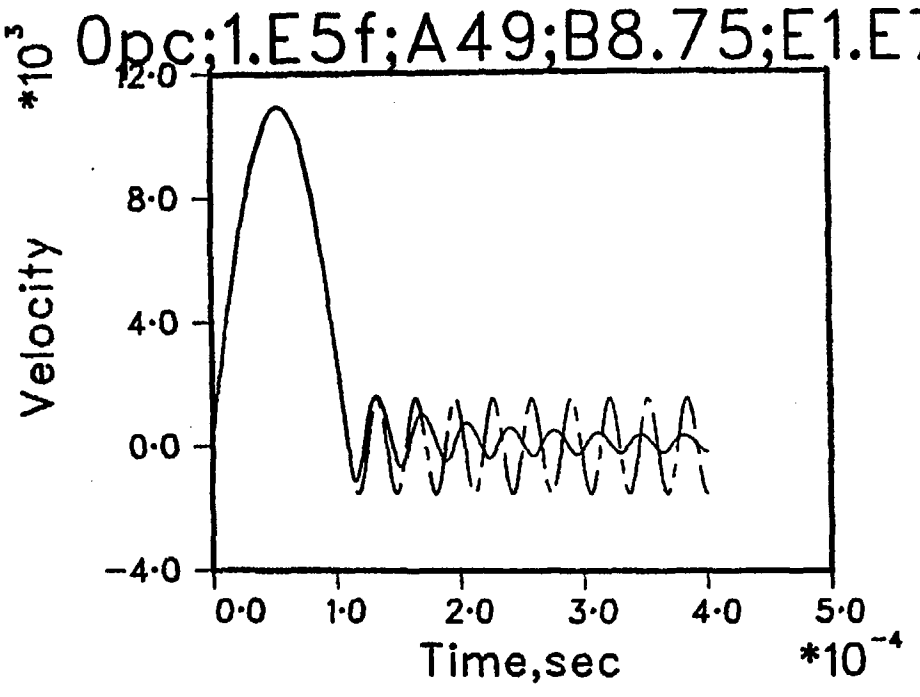


Figure 32

Dynamic responses of a spring-mass system that is subjected to a step loading of $4.448 \times 10^5$ N. Solid line - endochronic solution; chain-dashed line - elastoplastic solution.

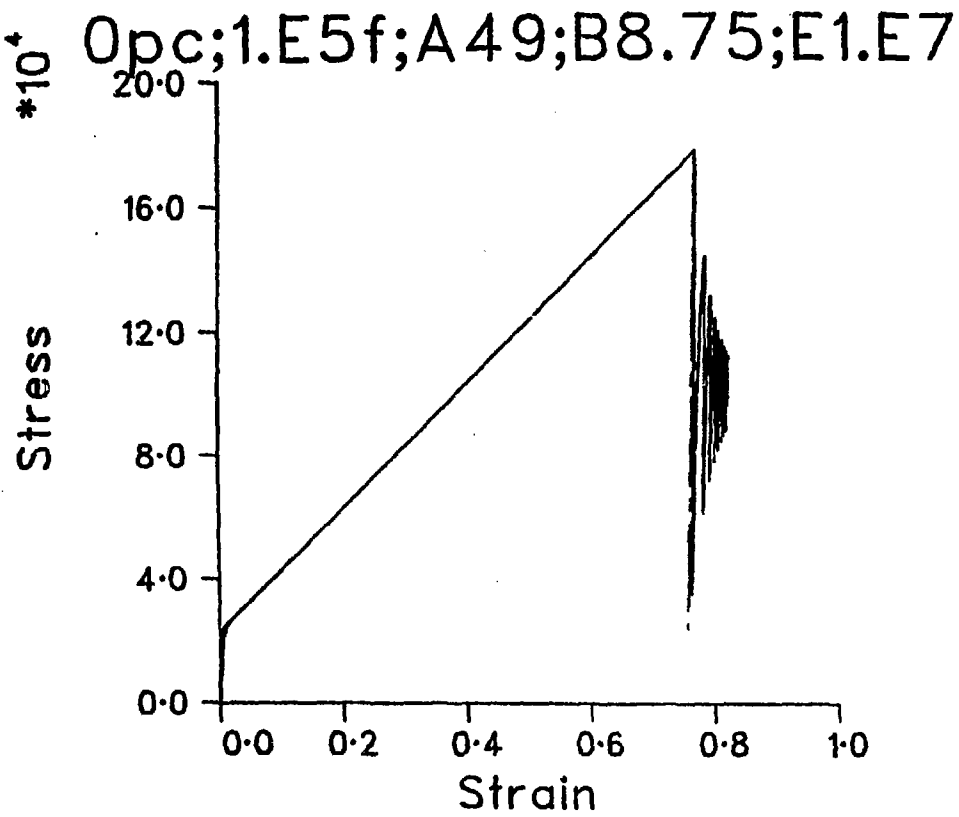


Figure 33

Dynamic responses of a spring-mass system that is subjected to a step loading of $4.448 \times 10^5$ N. Solid line - endochronic solution; chain-dashed line - elastoplastic solution.

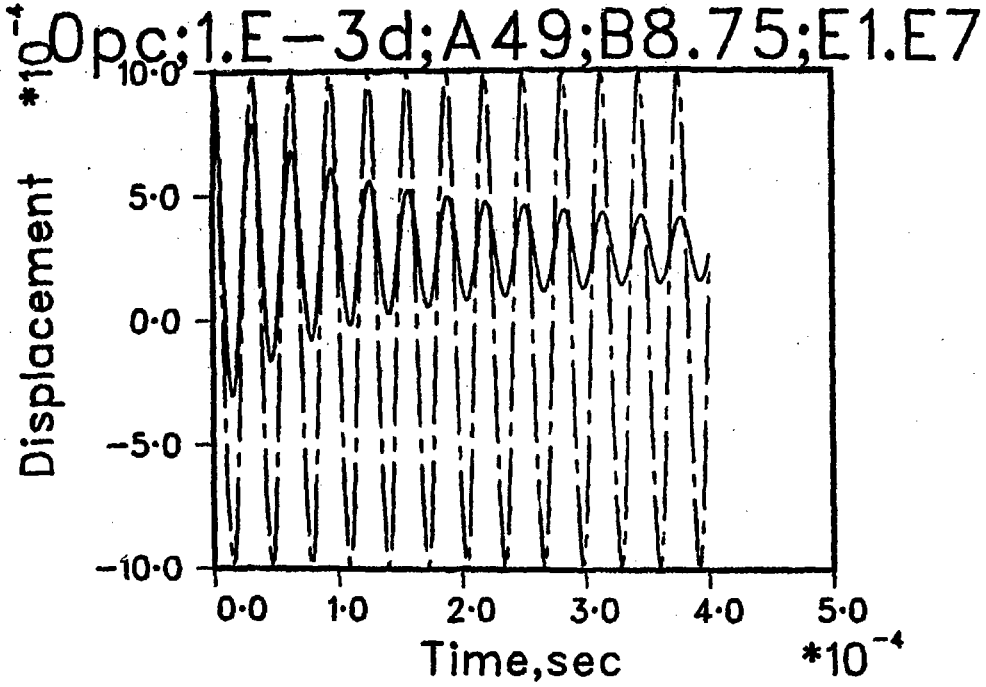


Figure 34

Dynamic responses of a spring-mass system that is subjected to an initial displacement equivalent to 0.1% strain. Solid line - endochronic solution; chain-dashed line - elastoplastic solution.

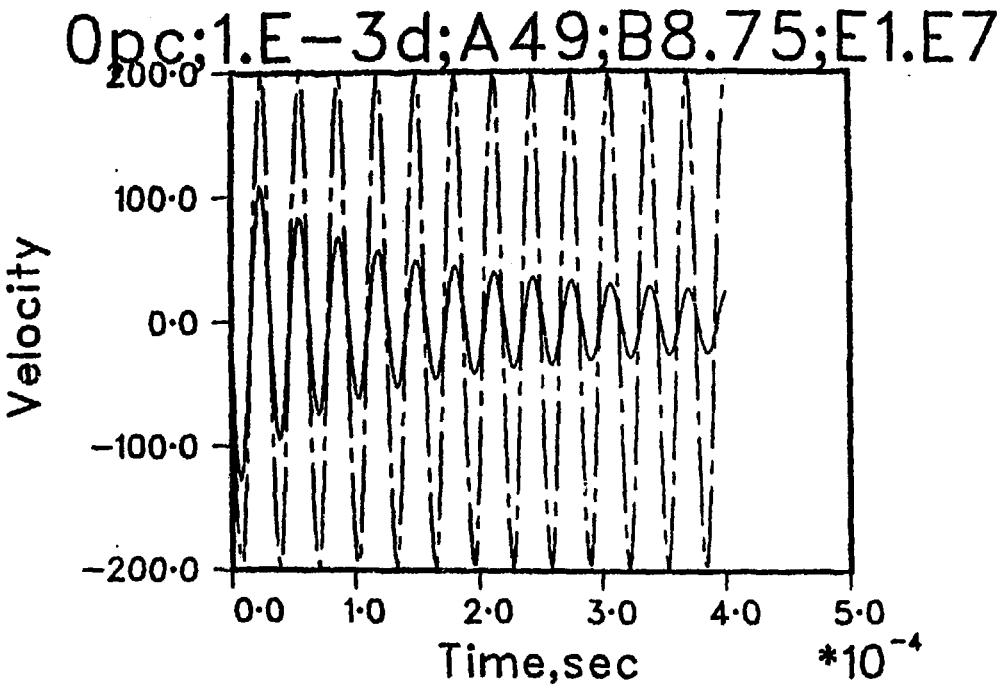


Figure 35

Dynamic responses of a spring-mass system that is subjected to an initial displacement equivalent to 0.1% strain. Solid line - endochronic solution; chain-dashed line - elastoplastic solution.

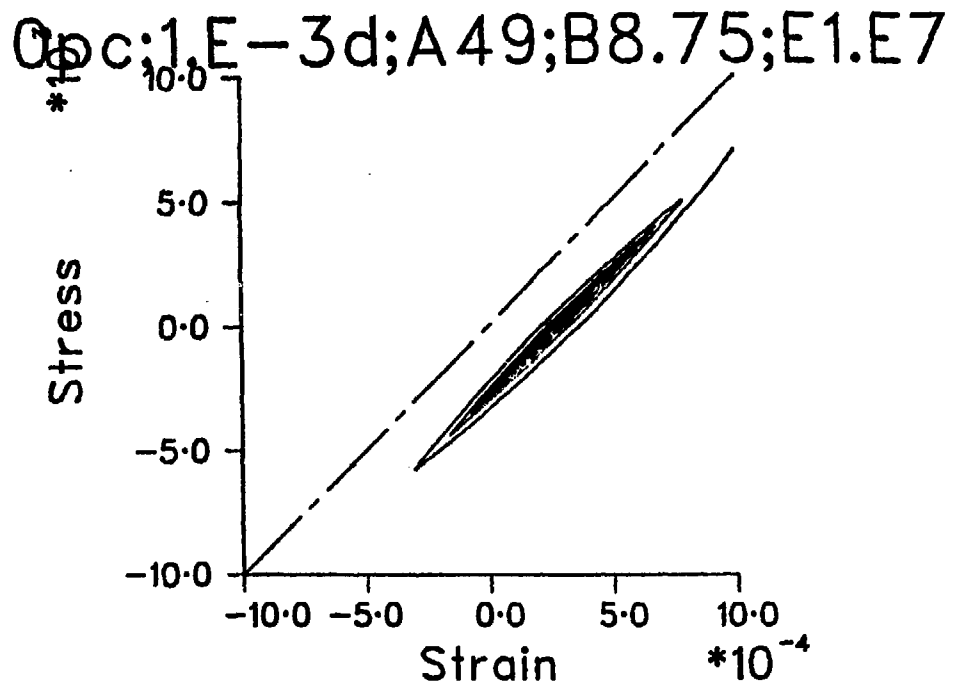


Figure 36

Dynamic responses of a spring-mass system that is subjected to an initial displacement equivalent to 0.1% strain. Solid line - endochronic solution; chain-dashed line - elastoplastic solution.

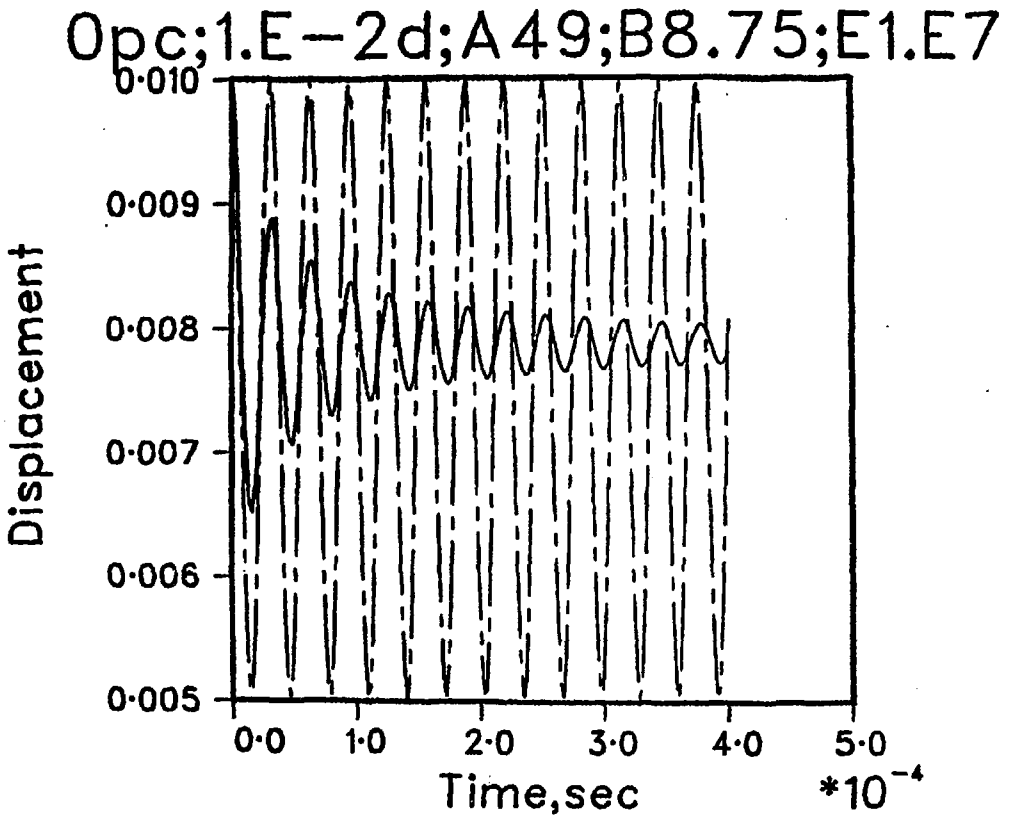


Figure 37

Dynamic responses of a spring-mass system that is subjected to an initial displacement equivalent to 1% strain. Solid line - endochronic solution; chain-dashed line - elastoplastic solution.

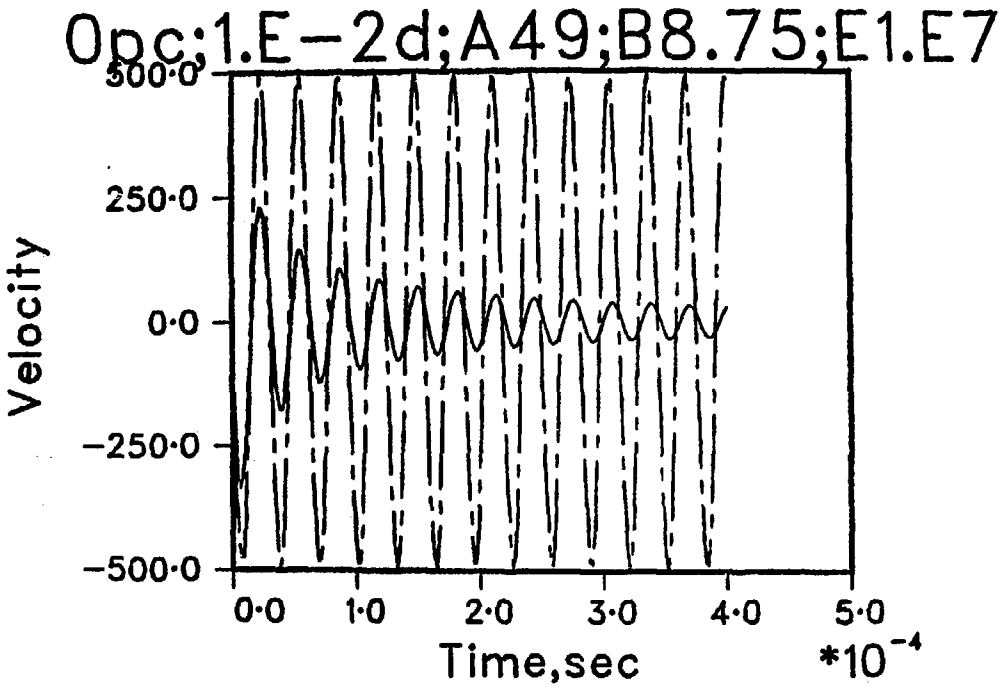


Figure 38

Dynamic responses of a spring-mass system that is subjected to an initial displacement equivalent to 1% strain. Solid line - endochronic solution; chain-dashed line - elastoplastic solution.

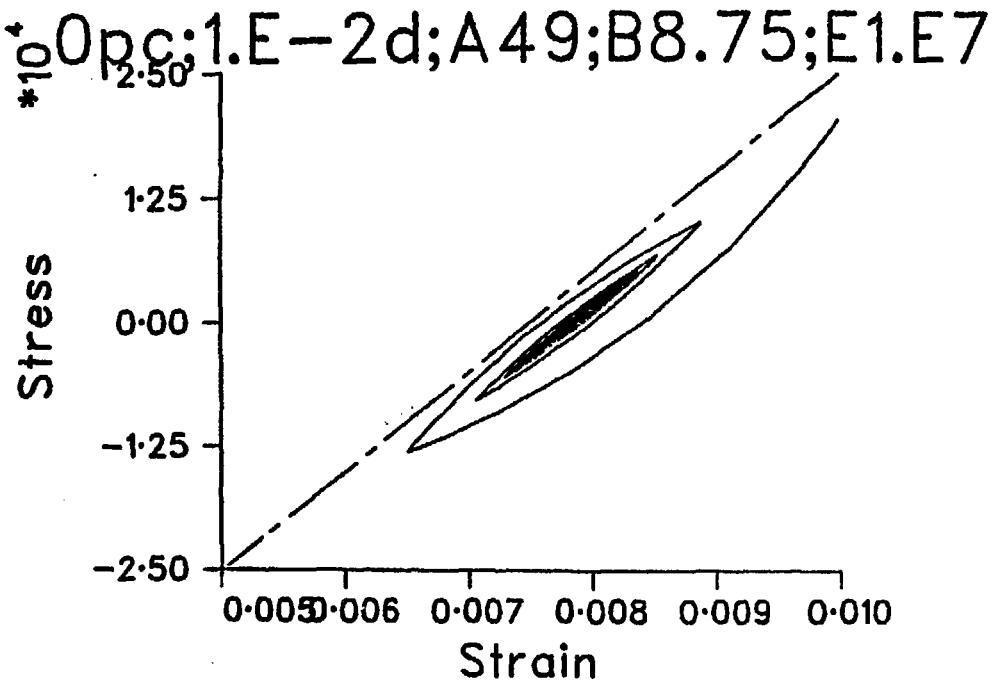


Figure 39

Dynamic responses of a spring-mass system that is subjected to an initial displacement equivalent to 1% strain. Solid line - endochronic solution; chain-dashed line - elastoplastic solution.

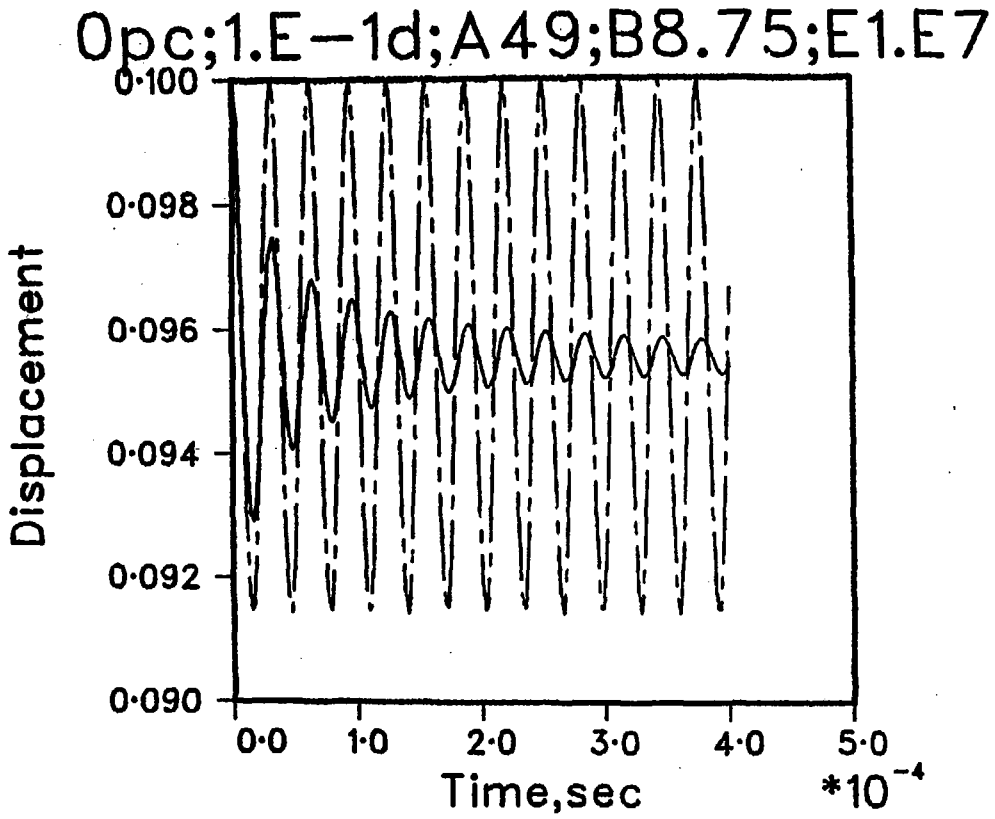


Figure 40

Dynamic responses of a spring-mass system that is subjected to an initial displacement equivalent to 10% strain. Solid line - endochronic solution; chain-dashed line - elastoplastic solution.

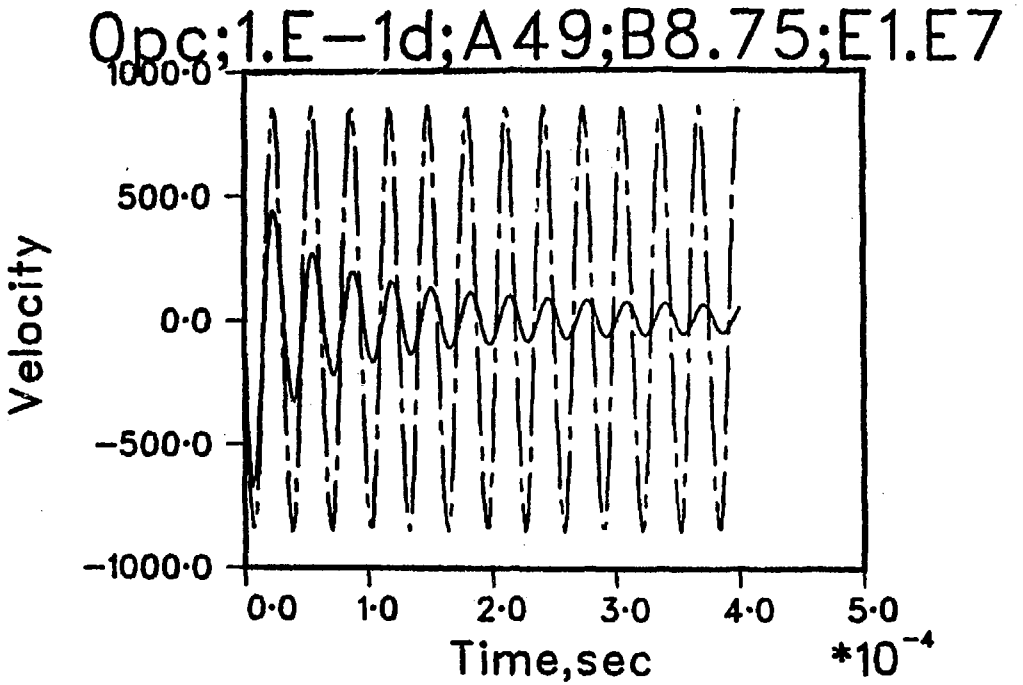


Figure 41

Dynamic responses of a spring-mass system that is subjected to an initial displacement equivalent to 10% strain. Solid line - endochronic solution; chain-dashed line - elastoplastic solution.

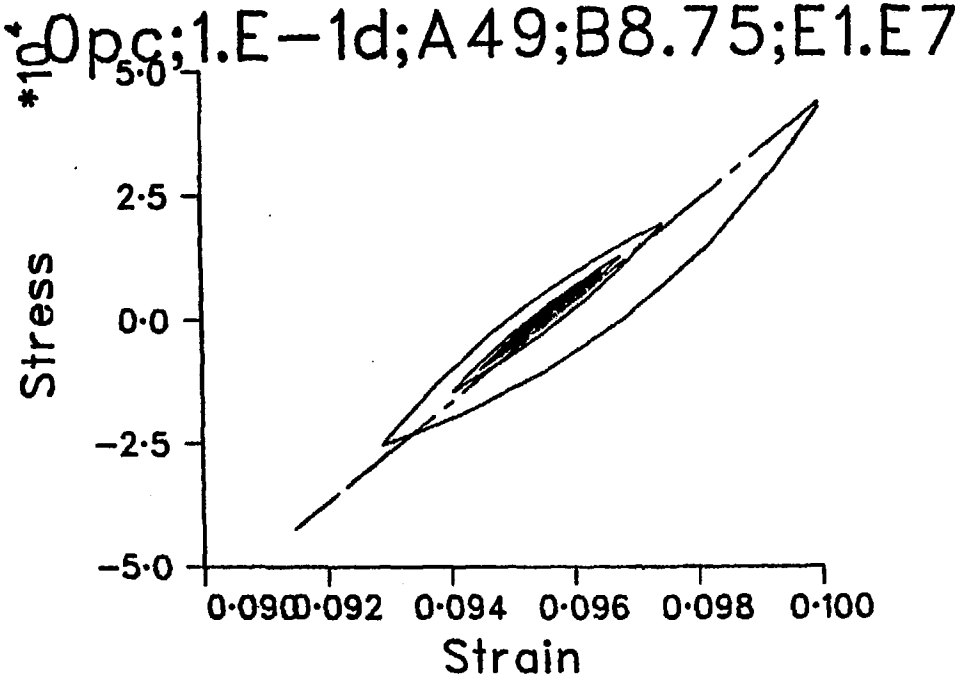


Figure 42

Dynamic responses of a spring-mass system that is subjected to an initial displacement equivalent to 10% strain. Solid line - endochronic solution; chain-dashed line - elastoplastic solution.

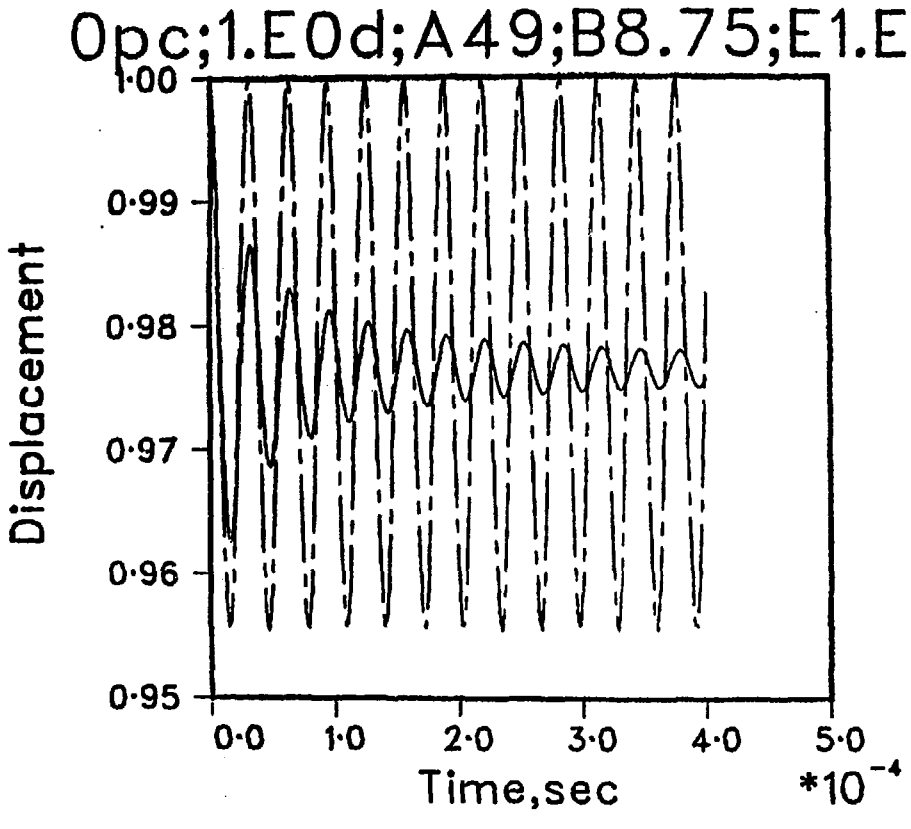


Figure 43

Dynamic responses of a spring-mass system that is subjected to an initial displacement equivalent to 100% strain. Solid line - endochronic solution; chain-dashed line - elastoplastic solution.

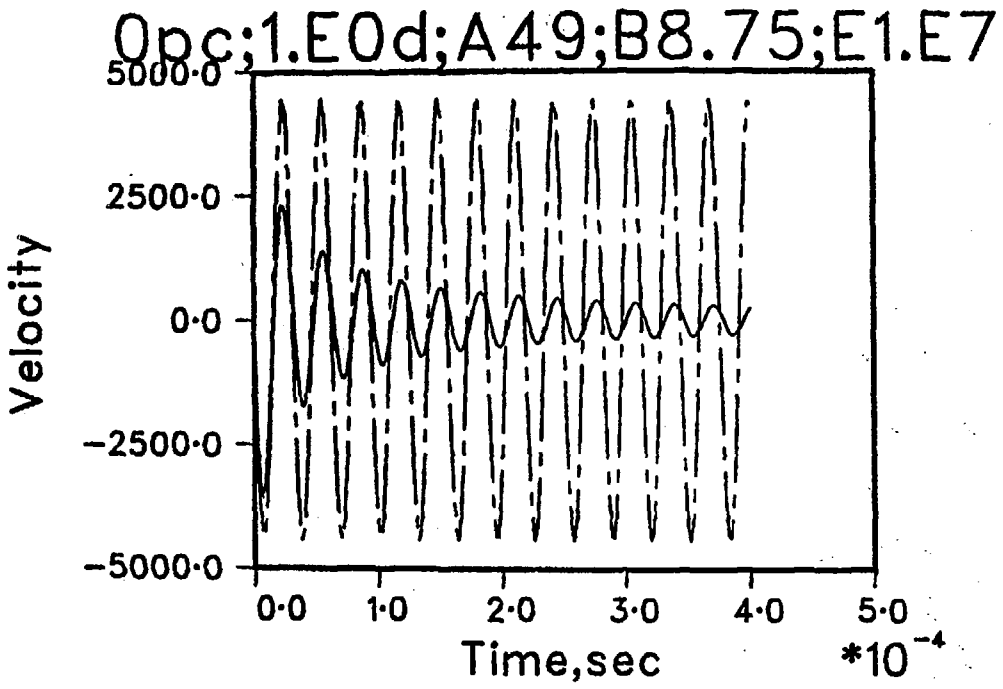


Figure 44

Dynamic responses of a spring-mass system that is subjected to an initial displacement equivalent to 100% strain. Solid line - endochronic solution; chain-dashed line - elastoplastic solution.

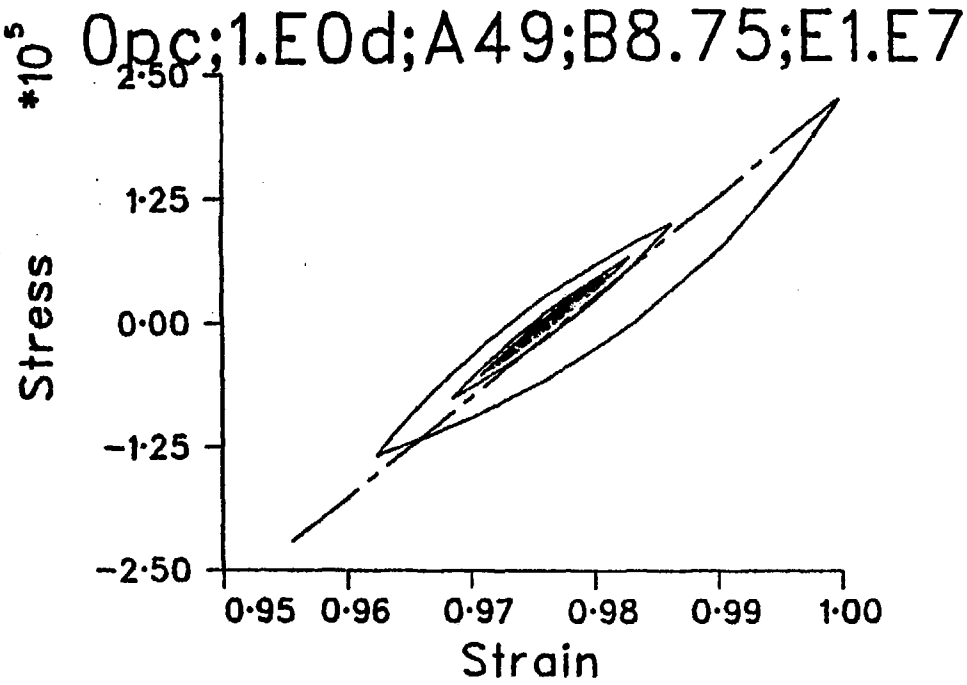


Figure 45

Dynamic responses of a spring-mass system that is subjected to an initial displacement equivalent to 100% strain. Solid line - endochronic solution; chain-dashed line - elastoplastic solution.

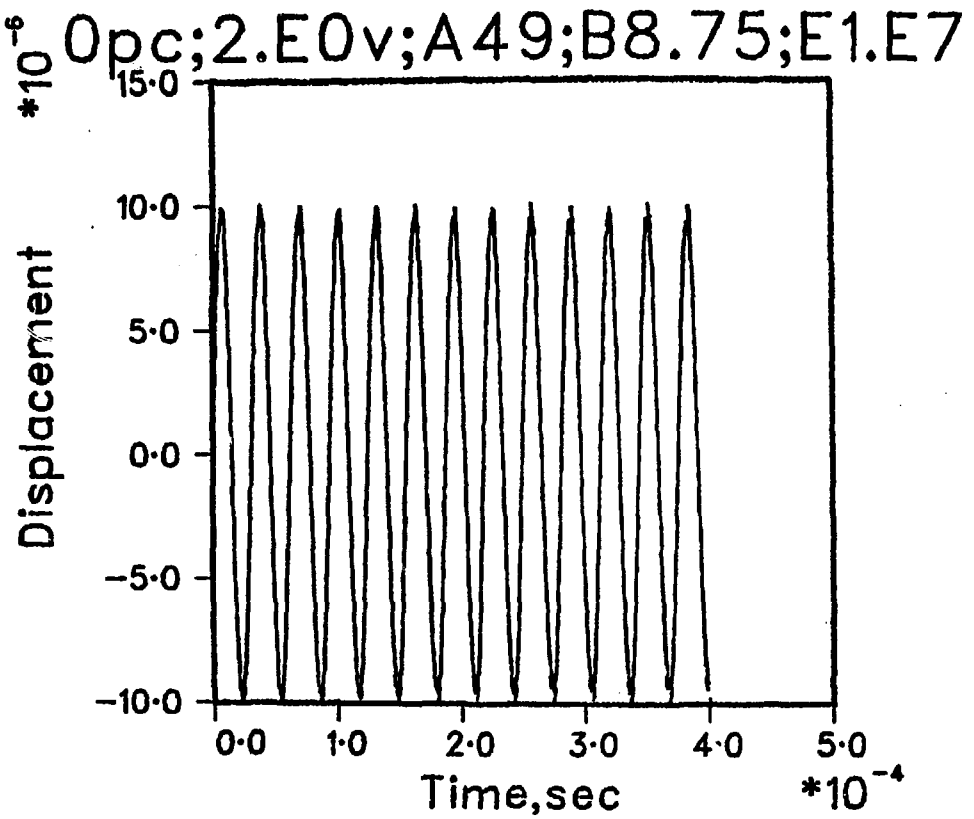


Figure 46

Dynamic responses of a spring-mass system that is subjected to an initial velocity equivalent to 200% strain/second. Solid line - endochronic solution; chain-dashed line - elasto-plastic solution.

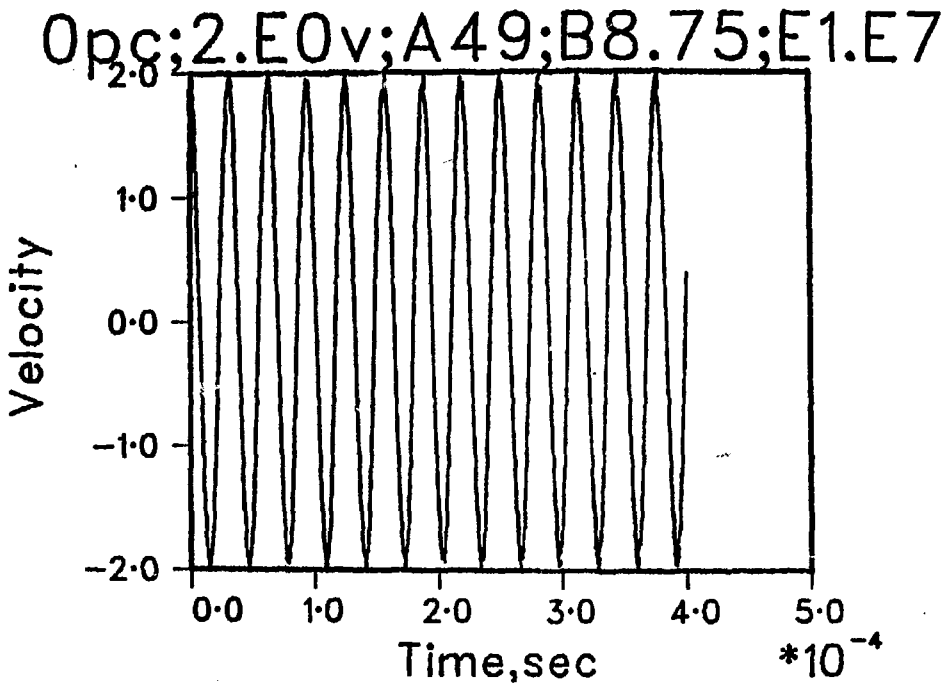


Figure 47

Dynamic responses of a spring-mass system that is subjected to an initial velocity equivalent to 200% strain/second. Solid line - endochronic solution; chain-dashed line - elasto-plastic solution.

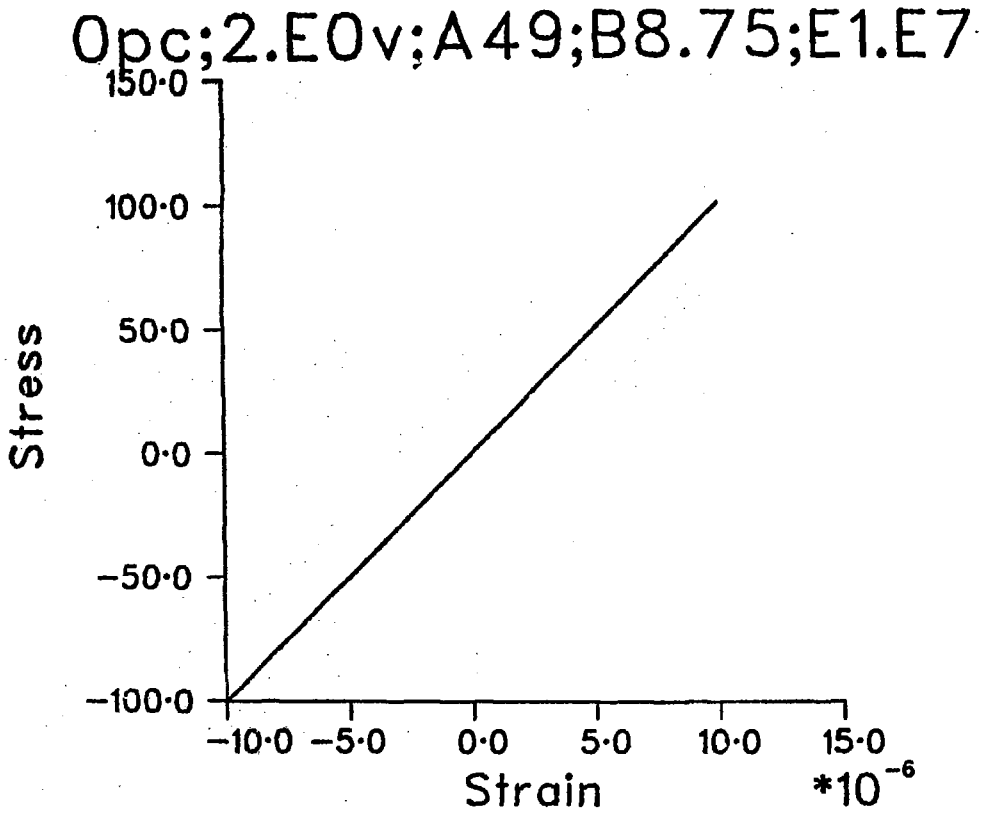


Figure 48

Dynamic responses of a spring-mass system that is subjected to an initial velocity equivalent to 200% strain/second. Solid line - endochronic solution; chain-dashed line - elasto-plastic solution.

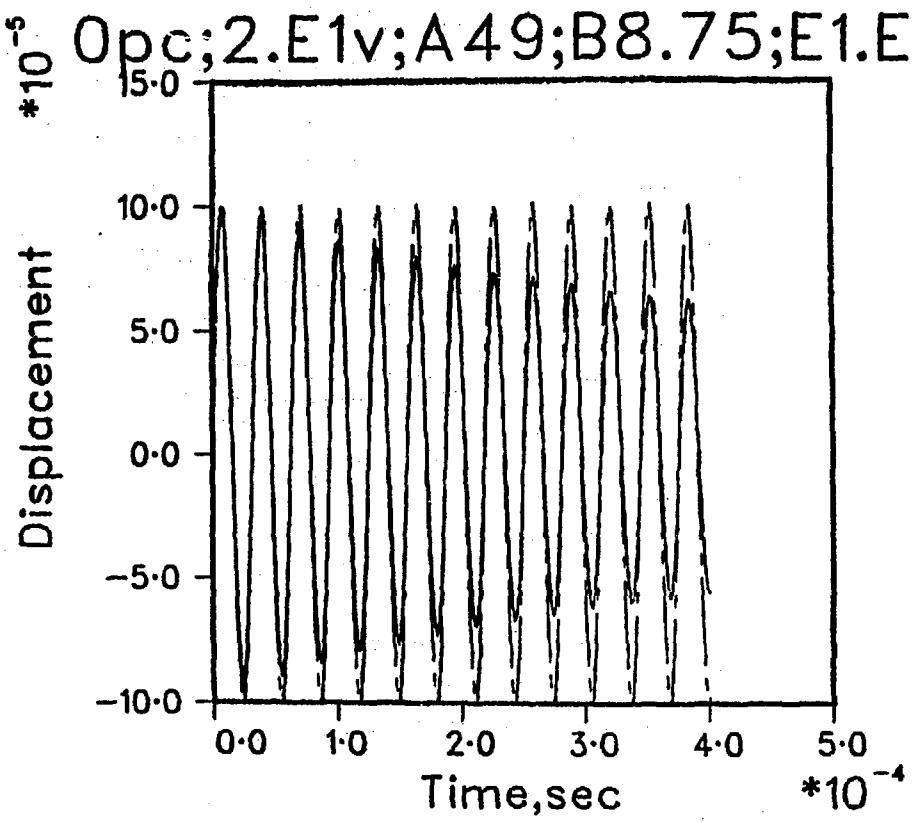


Figure 49

Dynamic responses of a spring-mass system that is subjected to an initial velocity equivalent to 2 x $10^{3}$% strain/second. Solid line - endochronic solution; chain-dashed line - elastoplastic solution.

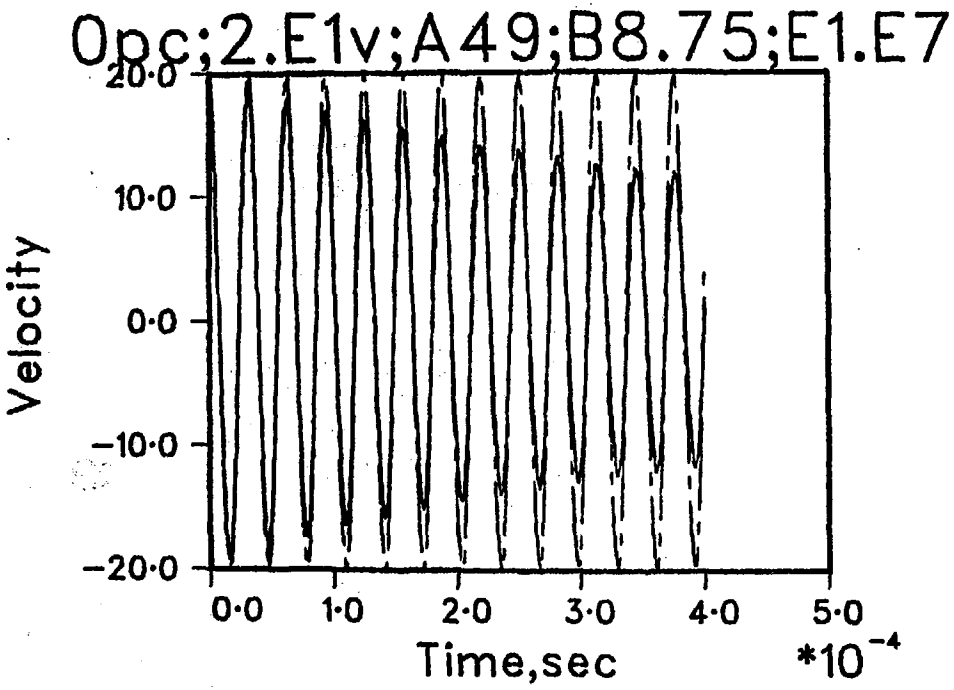


Figure 50

Dynamic responses of a spring-mass system that is subjected to an initial velocity equivalent to 2 x $10^{-3}$% strain/second. Solid line - endochronic solution; chain-dashed line - elastoplastic solution.

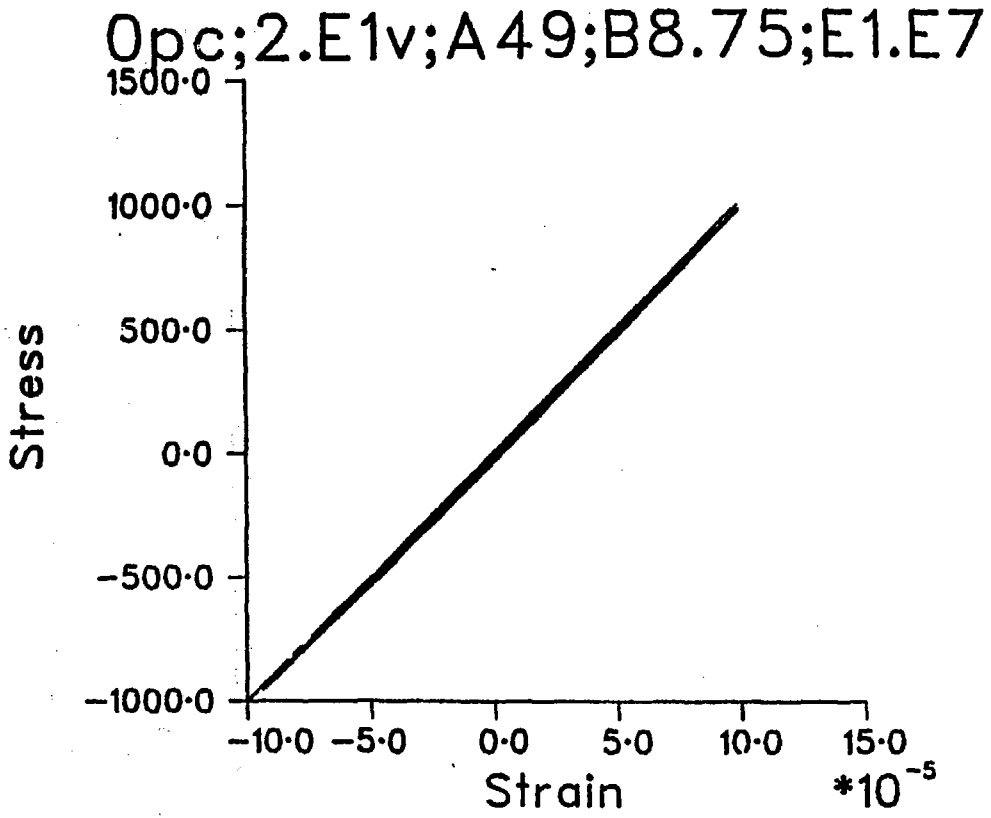


Figure 51

Dynamic responses of a spring-mass system that is subjected to an initial velocity equivalent to 2 x $10^3$% strain/second. Solid line - endochronic solution; chain-dahsed line - elastoplastic solution.

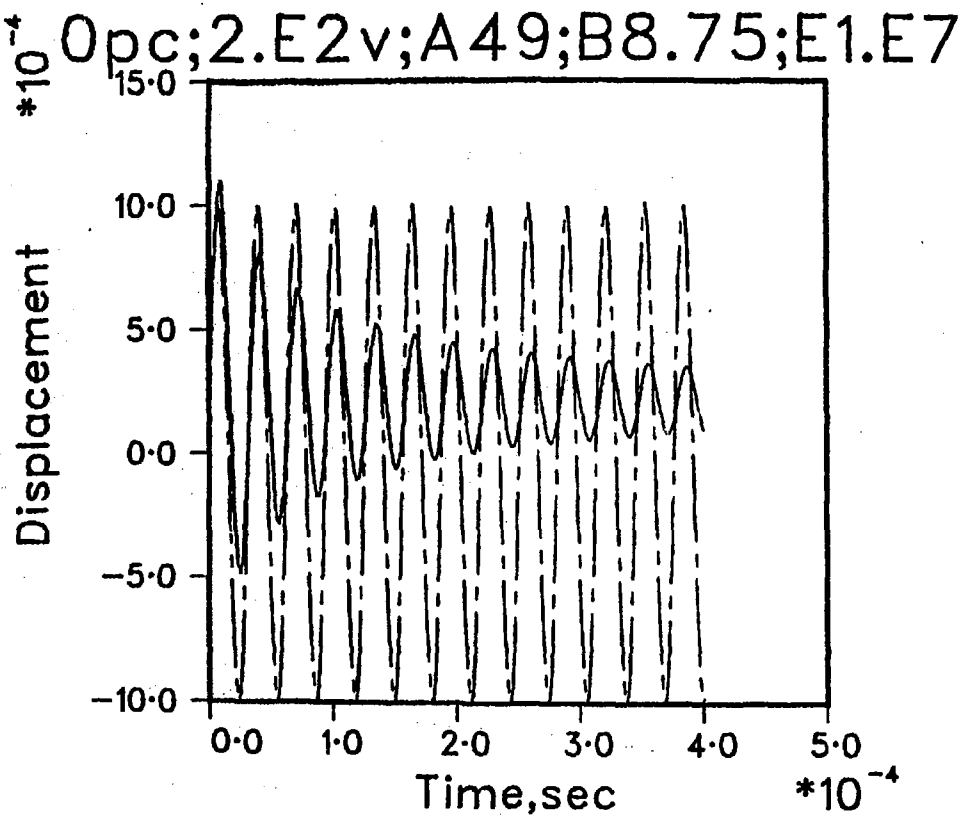


Figure 52

Dynamic responses of a spring-mass system that is subjected to an initial velocity equivalent to 2 x $10^4$% strain/second. Solid line - endochronic solution; chain-dashed line - elastoplastic solution.

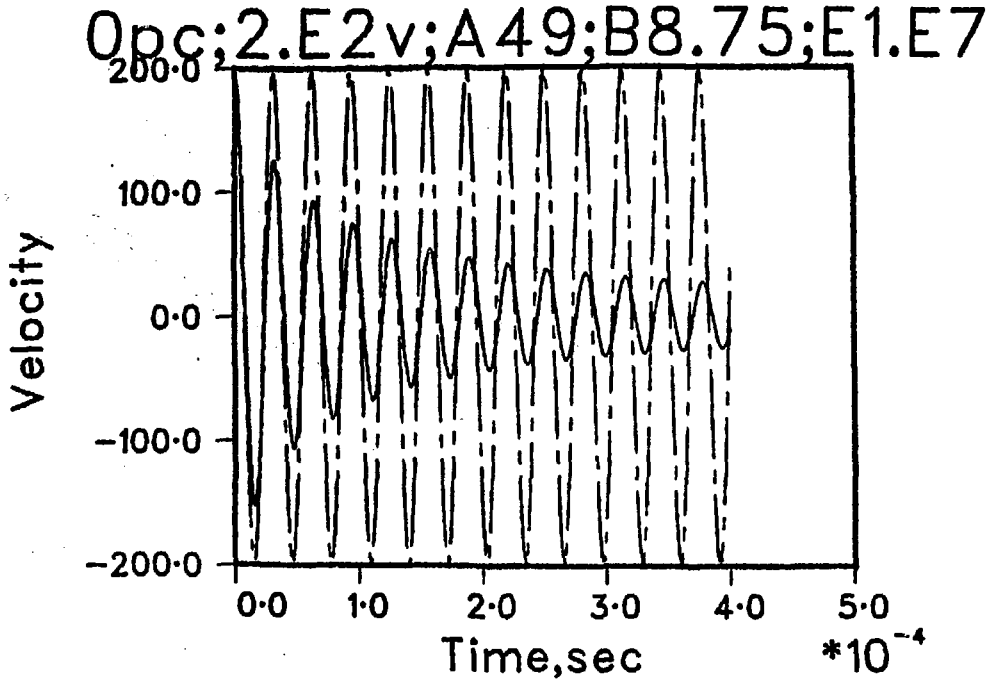


Figure 53

Dynamic responses of a spring-mass system that is subjected to an initial velocity equivalent to 2 x $10^4$% strain/second. Solid line - endochronic solution; chain-dashed line - elastoplastic solution.

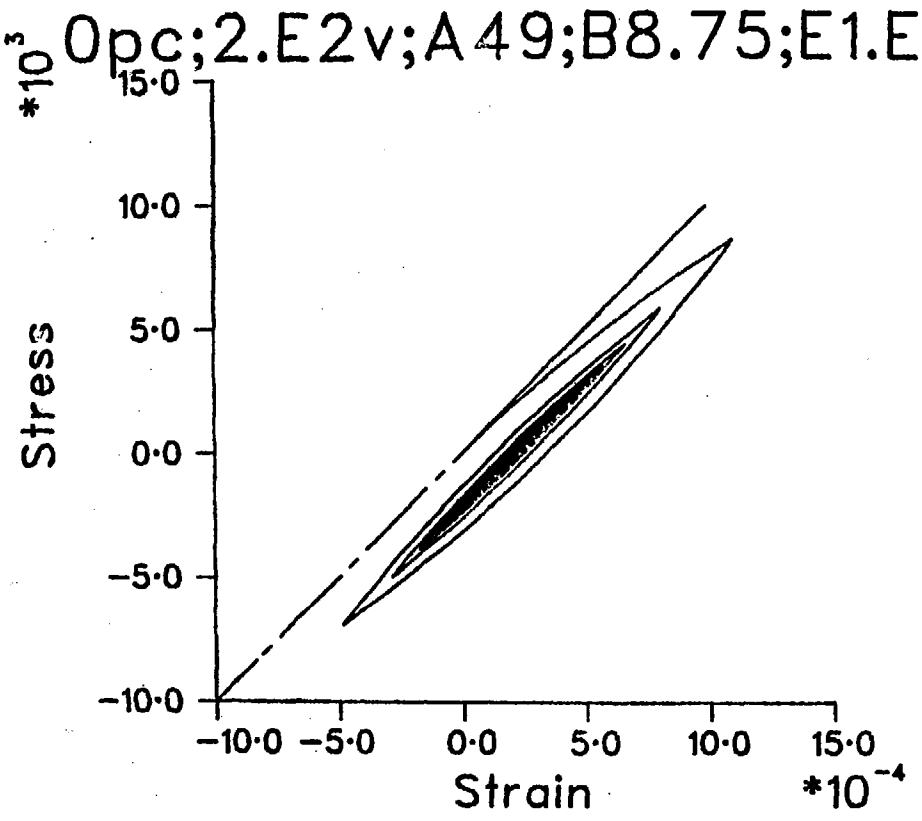


Figure 54

Dynamic responses of a spring-mass system that is subjected to an initial velocity equivalent to 2 x $10^4$% strain/second. Solid line - endochronic solution; chain-dashed line - elastoplastic solution.

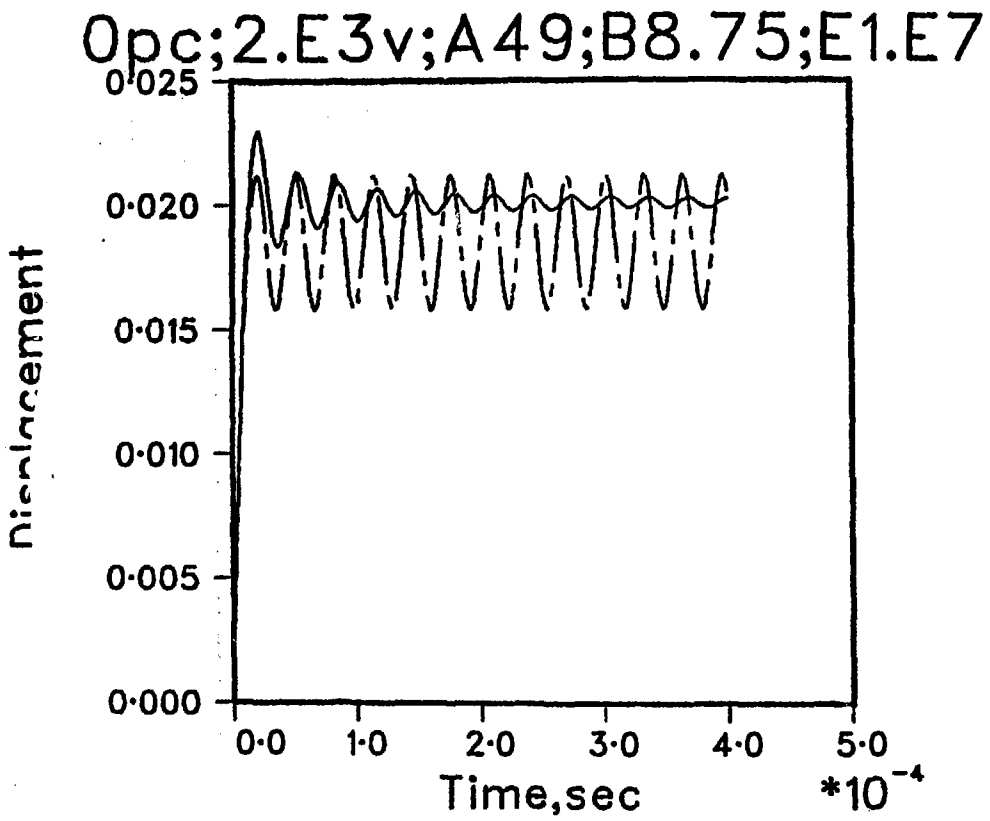


Figure 55

Dynamic responses of a spring-mass system that is subjected to an initial velocity equivalent to 2 x $10^{5}$% strain/second. Solid line - endochronic solution; chain-dashed line - elastoplastic solution.

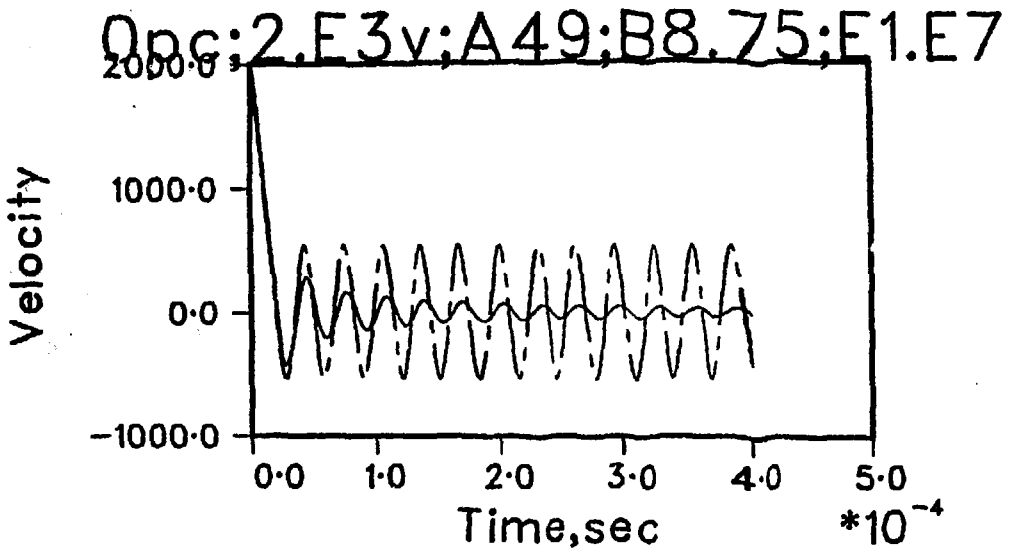


Figure 56

Dynamic responses of a spring-mass system that is subjected to an initial velocity equivalent to 2 x $10^5$% strain/second. Solid line - endochronic solution; chain-dashed line - elastoplastic solution.

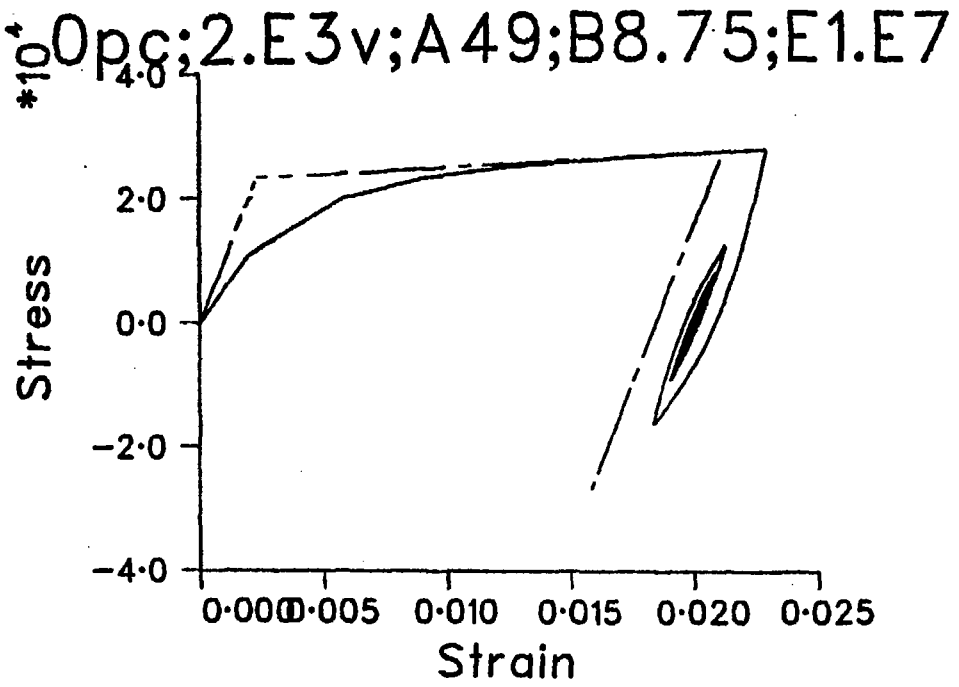


Figure 57

Dynamic responses of a spring-mass system that is subjected to an initial velocity equivalent to 2 x $10^{-5}$% strain/second. Solid line - endochronic solution; chain-dashed line - elastoplastic solution.

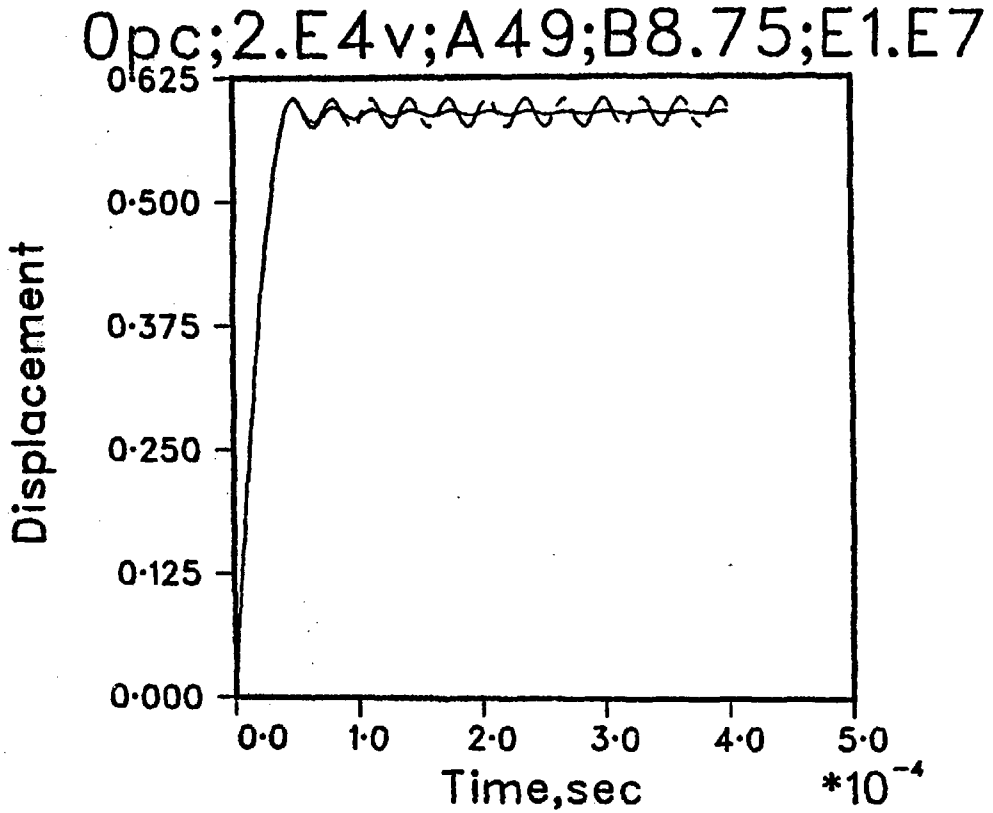


Figure 58

Dynamic responses of a spring-mass system that is subjected to an initial velocity equivalent to 2 x $10^6$% strain/second. Solid line - endochronic solution; chain-dashed line - elastoplastic solution.

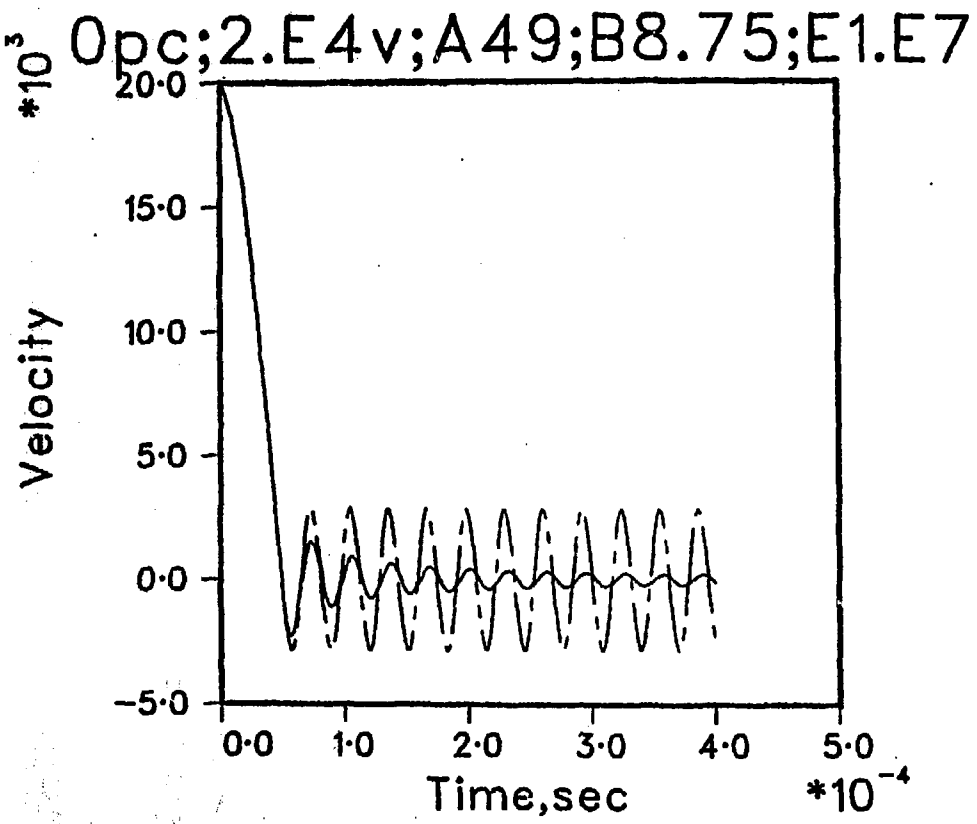


Figure 59

Dynamic responses of a spring-mass system that is subjected to an initial velocity equivalent to 2 x $10^6$% strain/second. Solid line - endochronic solution; chain-dashed line - elastoplastic solution.

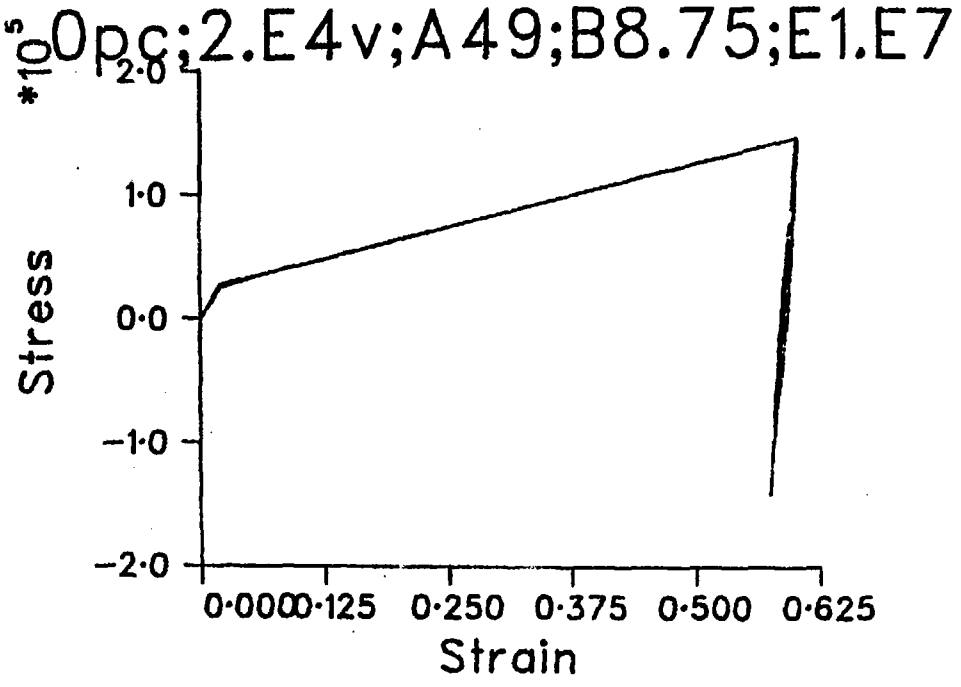


Figure 60

Dynamic responses of a spring-mass system that is subjected to an initial velocity equivalent to 2 x $10^6$% strain/second. Solid line - endochronic solution; chain-dashed line - elastoplastic solution.

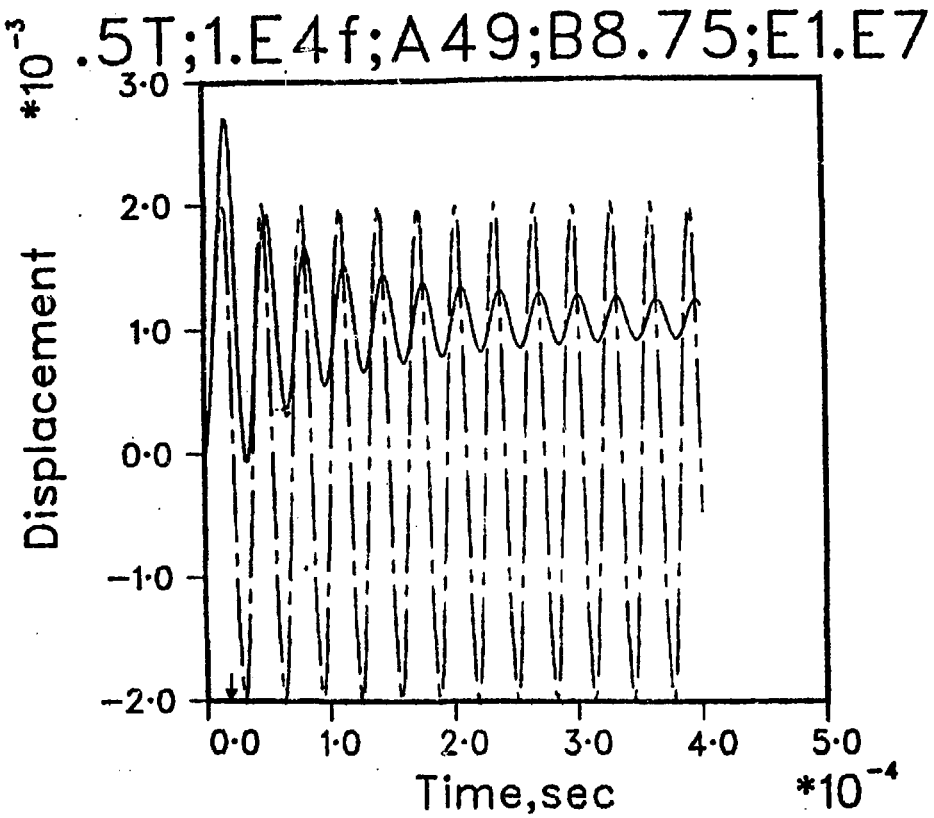


Figure 61

Dynamic responses of a spring-mass system that is subjected to a rectangular pulse whose magnitude is $4.448 \times 10^4$ N and whose duration is 0.5T. Solid line - endochronic solution; chain-dashed line - elastoplastic solution.

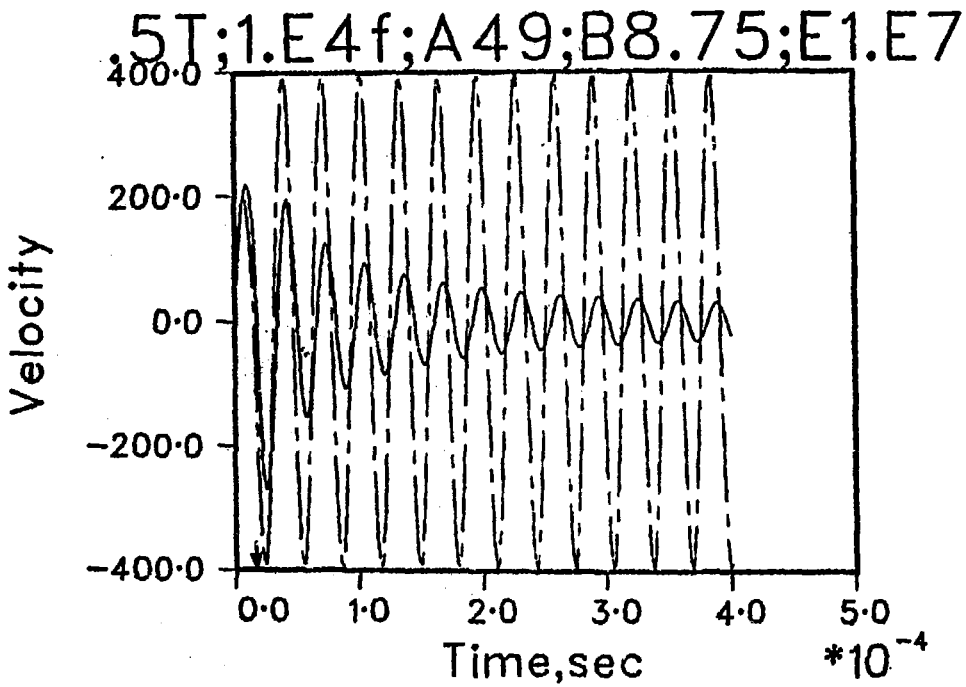


Figure 62

Dynamic responses of a spring-mass system that is subjected to a rectangular pulse whose magnitude is $4.448 \times 10^4$ N and whose duration is 0.5T. Solid line - endochronic solution; chain-dashed line - elastoplastic solution.

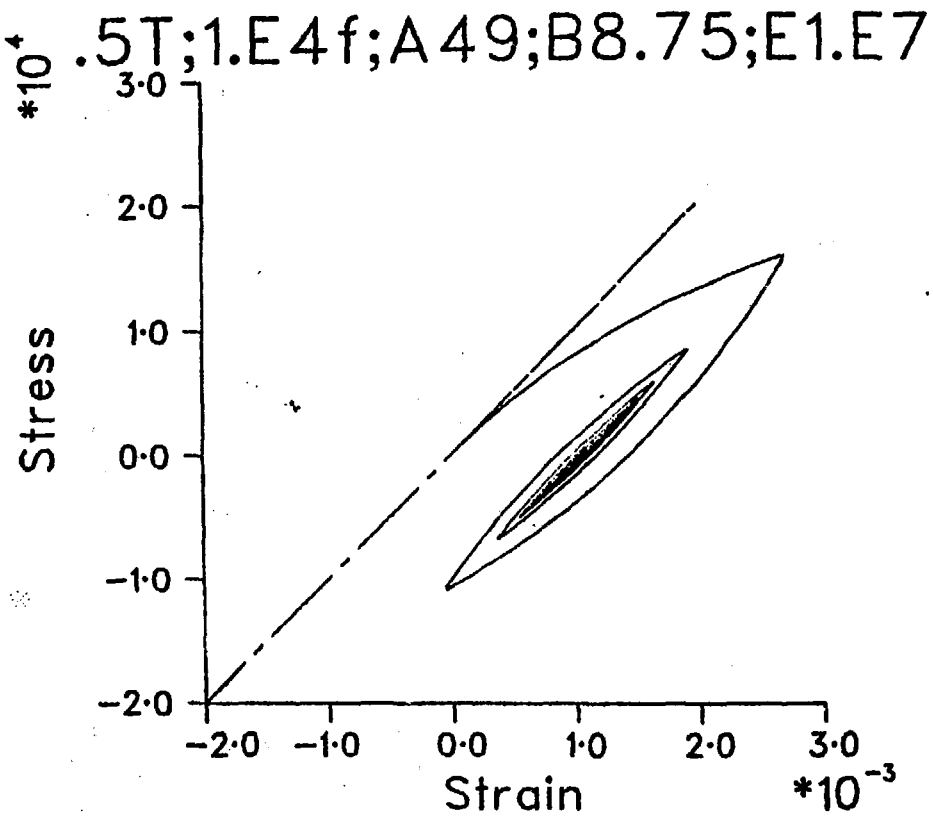


Figure 63

Dynamic responses of a spring-mass system that is subjected to a rectangular pulse whose magnitude is $4.448 \times 10^4$ N and whose duration is 0.5T. Solid line - endochronic solution; chain-dashed line - elastoplastic solution.

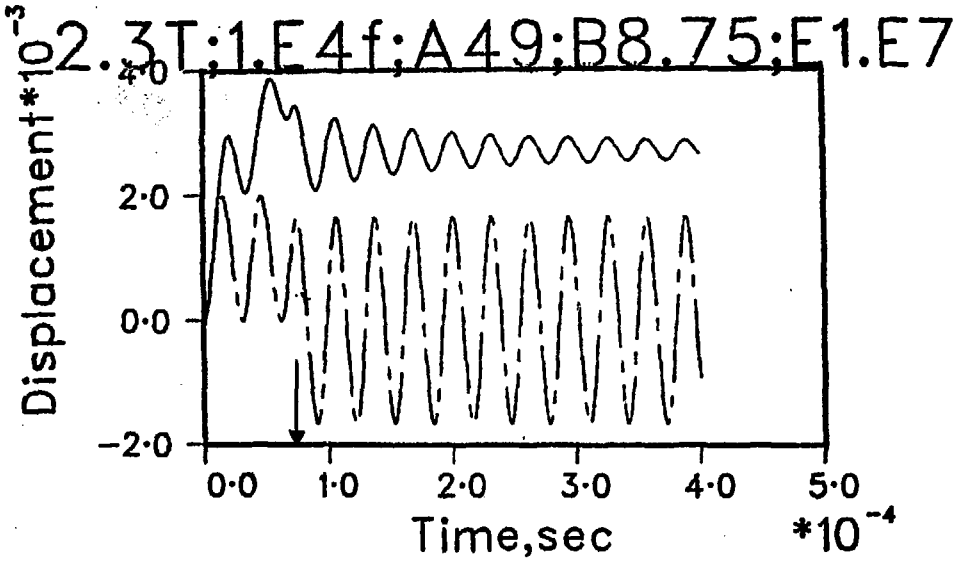


Figure 64

Dynamic responses of a spring-mass system that is subjected to a rectangular pulse whose magnitude is $4.448 \times 10^4$ N and whose duration is 2.3T. Solid line - endochronic solution; chain-dashed line - elastoplastic solution.

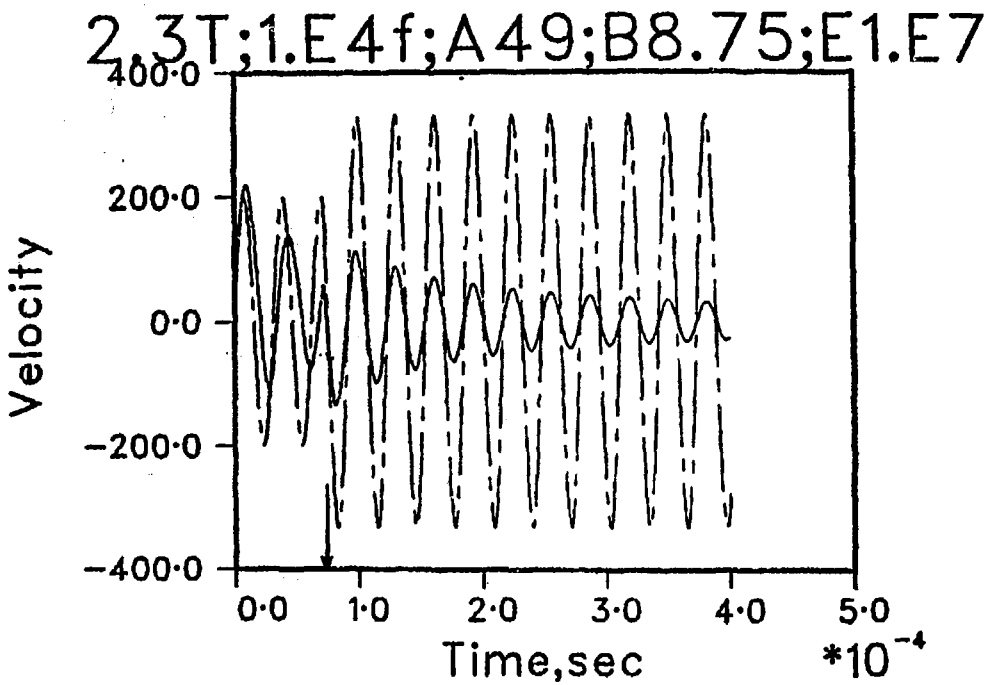


Figure 65

Dynamic responses of a spring-mass system that is subjected to a rectangular pulse whose magnitude id $4.448 \times 10^4$ N and whose duration is 2.3T. Solid line - endochronic solution; chain-dashed line - elastoplastic solution.

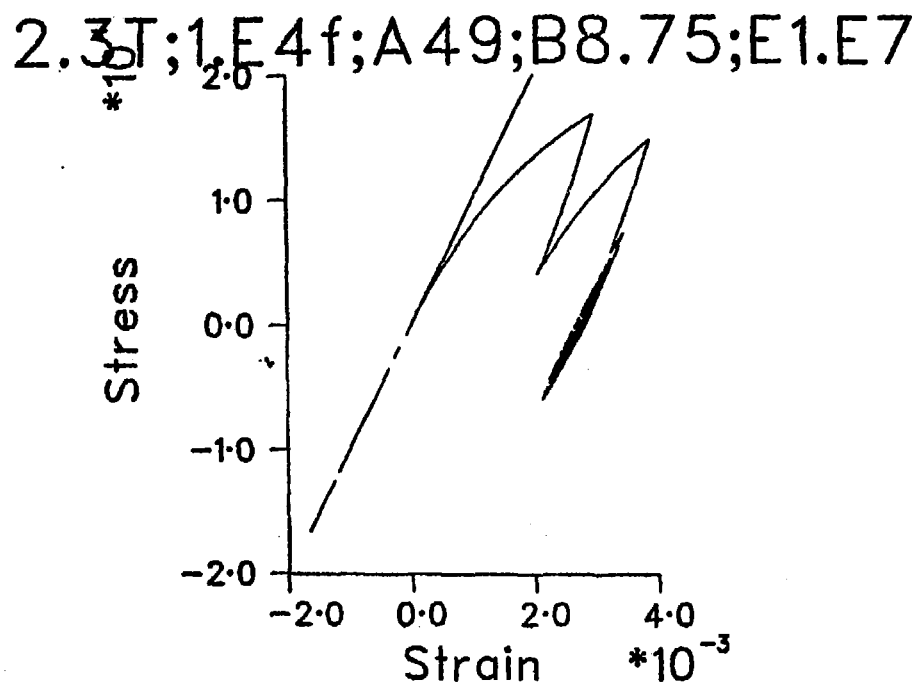


Figure 66

Dynamic responses of a spring-mass system that is subjected to a rectangular pulse whose magnitude is $4.448 \times 10^4$ N and whose duration is 2.3T. Solid line - endochronic solution; chain-dashed line - elastoplastic solution.

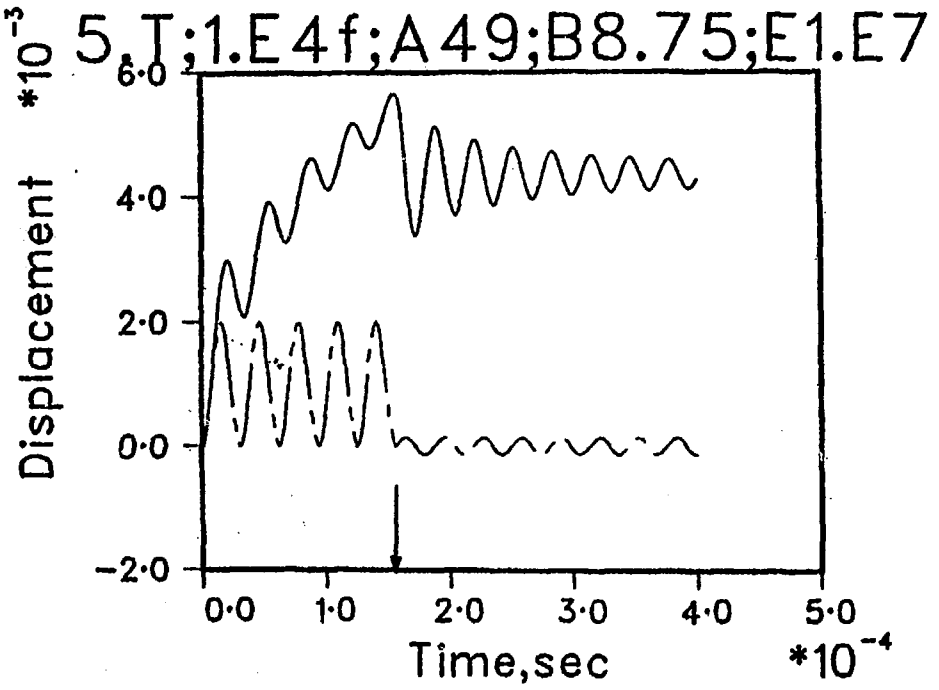


Figure 67

Dynamic responses of a spring-mass system that is subjected to a rectangular pulse whose magnitude is $4.448 \times 10^4$ N and whose duration is 5T. Solid line - endochronic solution; chain-dashed line - elastoplastic solution.

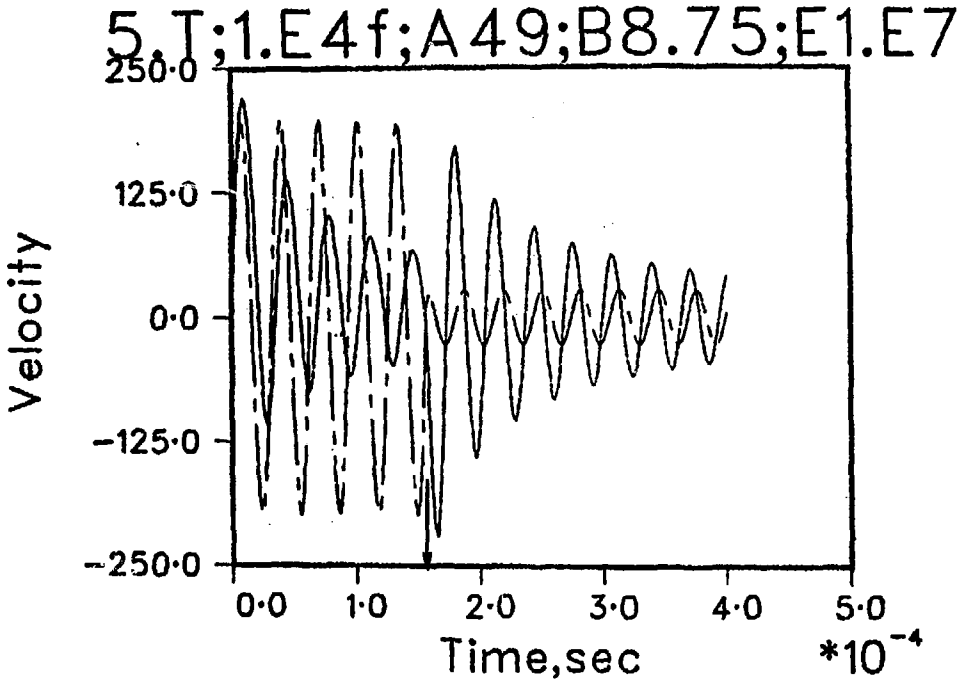


Figure 68

Dynamic responses of a spring-mass system that is subjected to a rectangular pulse whose magnitude is $4.448 \times 10^4$ N and whose duration is 5T. Solid line - endochronic solution; chain-dashed line - elastoplastic solution.

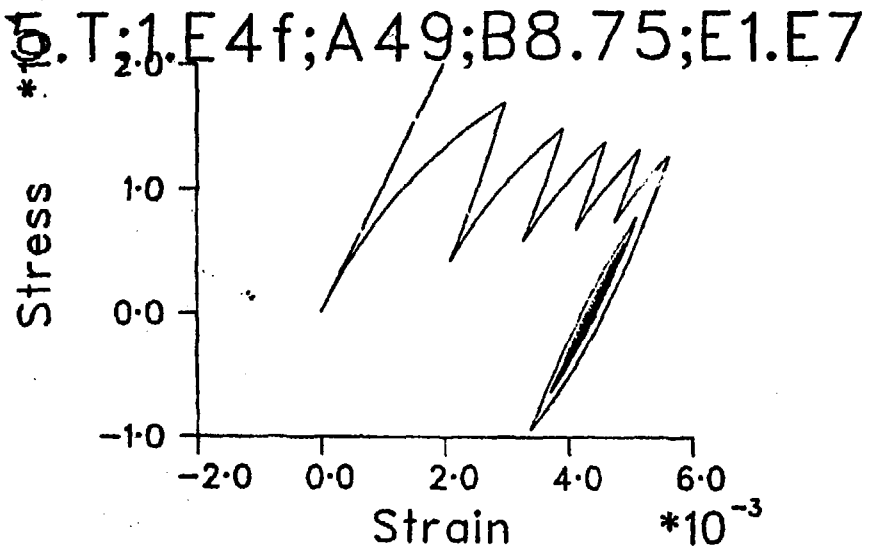


Figure 69

Dynamic responses of a spring-mass system that is subjected to a rectangular pulse whose magnitude is $4.448 \times 10^4$ N and whose duration is 5T. Solid line - endochronic soltuion; chain-dashed line - elastoplastic solution.

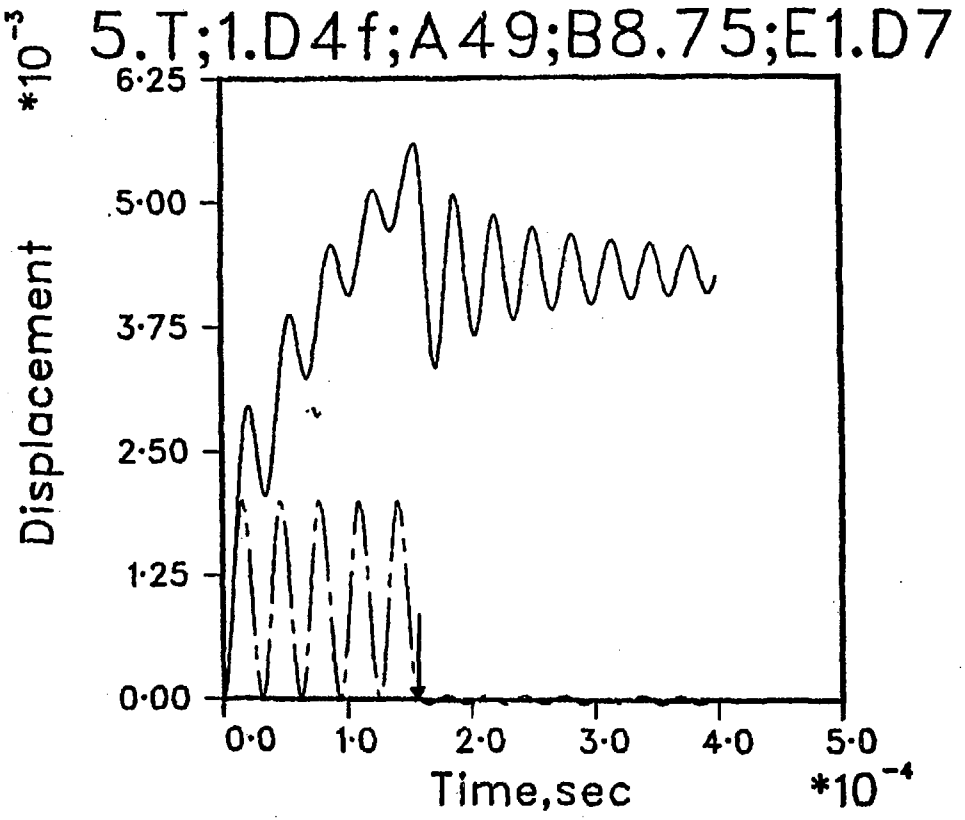


Figure 70

Dynamic responses of a spring-mass system that is subjected to a rectangular pulse whose magnitude is $4.448 \times 10^4$ N and whose duration is 5T. Double precision is used. Time integration step used is an integer fraction of T. Solid line - endochronic solution; chain-dashed line - elastoplastic solution.

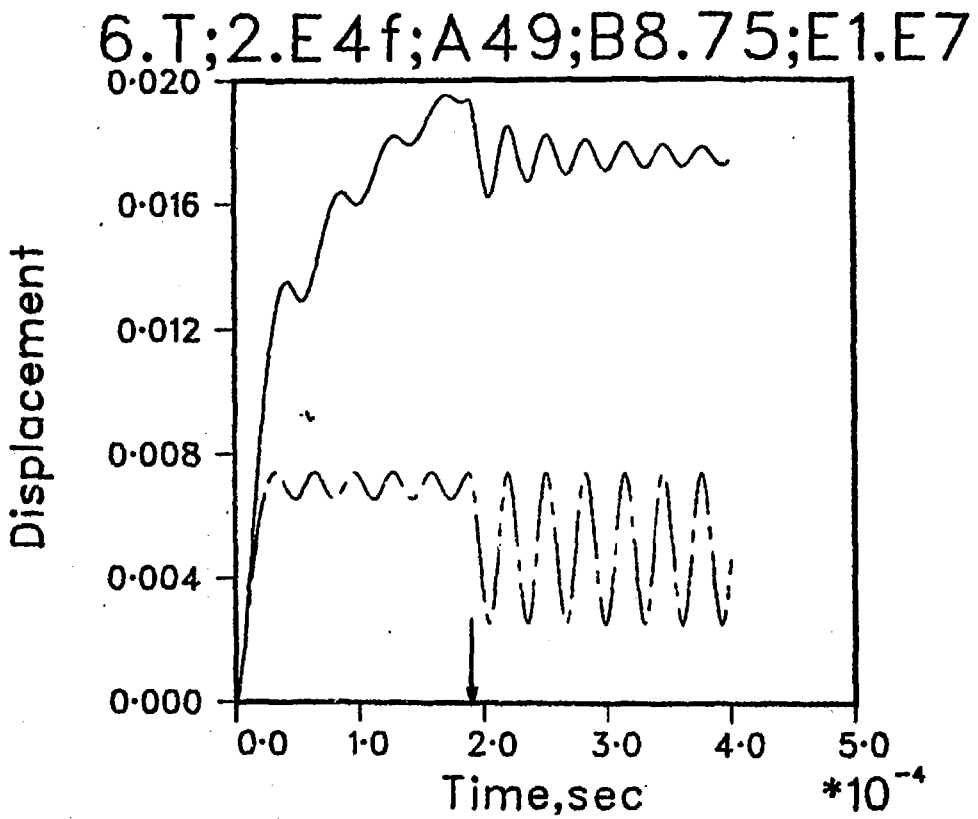


Figure 71

Dynamic responses of a spring-mass system that is subjected to a rectangular pulse whose magnitude is 8.896 x $10^4$ N and whose duration is 6T. Solid line - endochronic solution; chain-dashed line - elastoplastic solution.

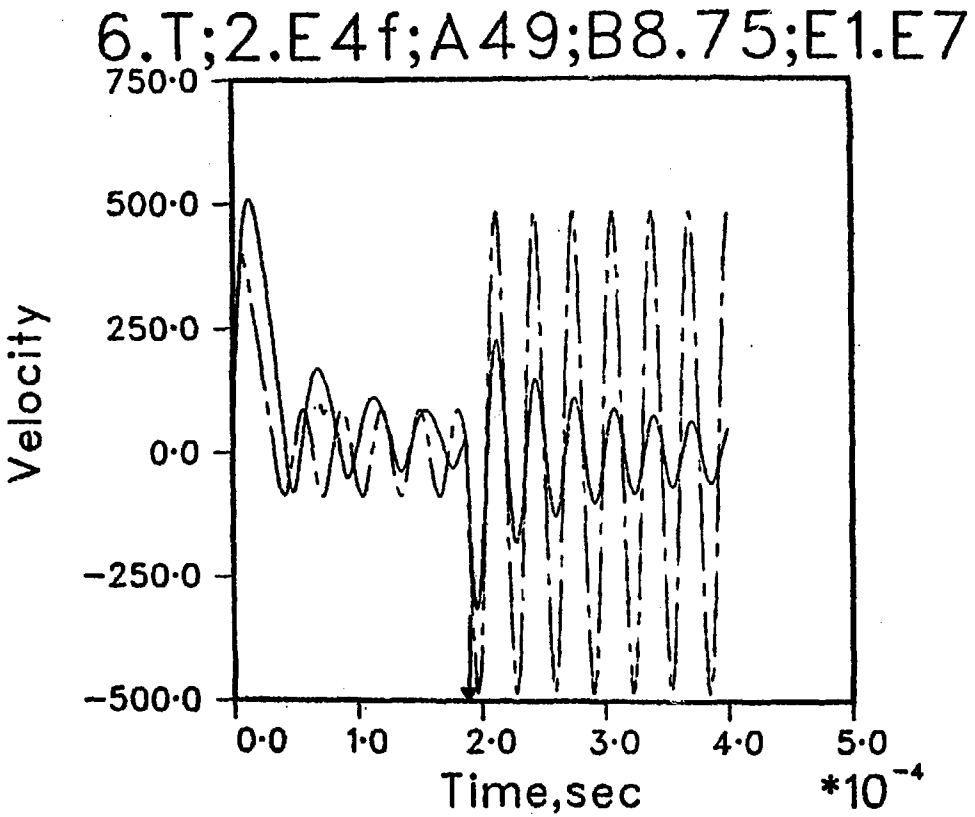


Figure 72

Dynamic responses of a spring-mass system that is subjected to a rectangular pulse whose magnitude is $8.896 \times 10^4$ N and whose duration is 6T. Solid line - endochronic solution; chain-dashed line - elastoplastic solution.

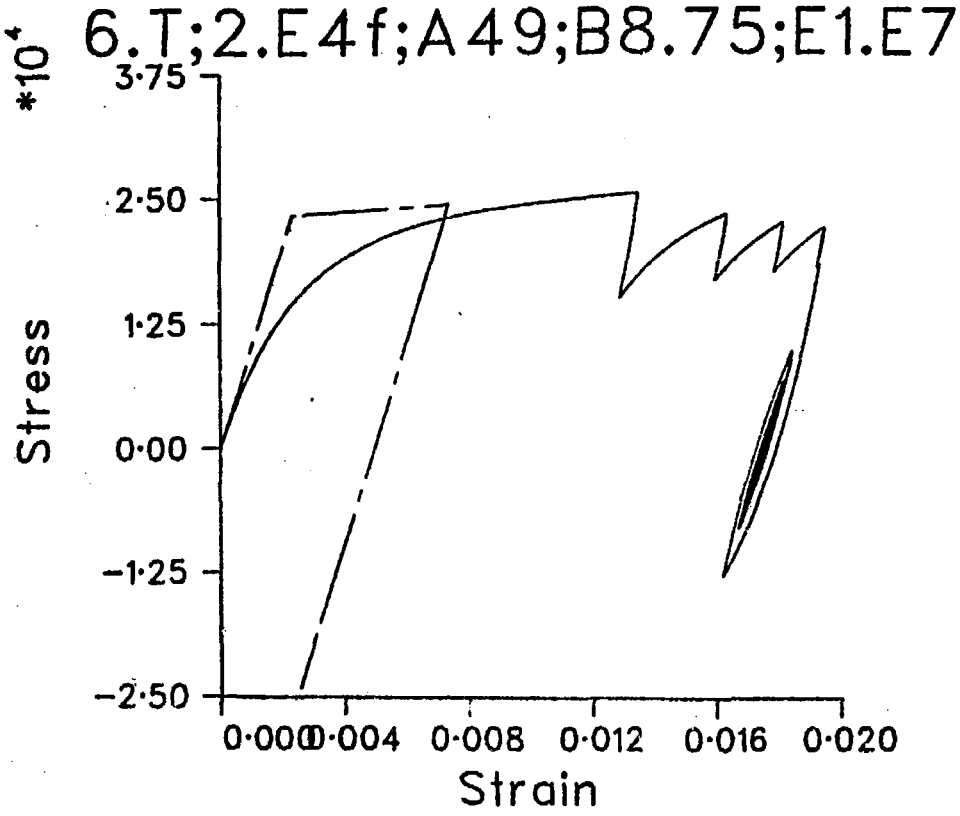


Figure 73

Dynamic responses of a spring-mass system that is subjected to a rectangular pulse whose magnitude is $8.896 \times 10^4$ N and whose duration is 6T. Solid line - endochronic solution; chain-dashed line - elastoplastic solution.

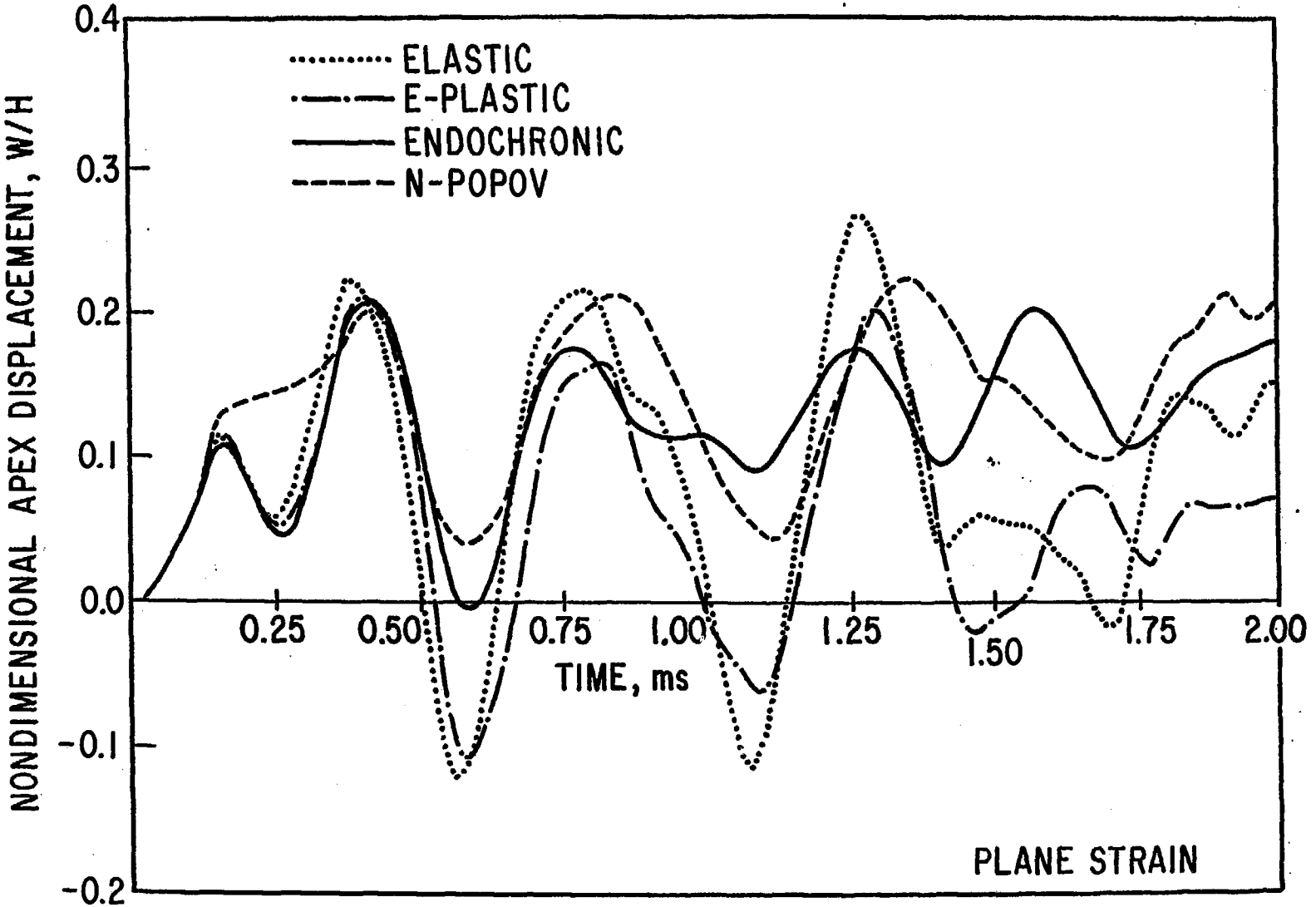


Figure 74

Dynamic apex responses of a clamped spherical cap that is subjected to a uniform step pressure loading of $4{,}137 \times 10^6$ Pa on its convex surface. Plane strain condition is used.

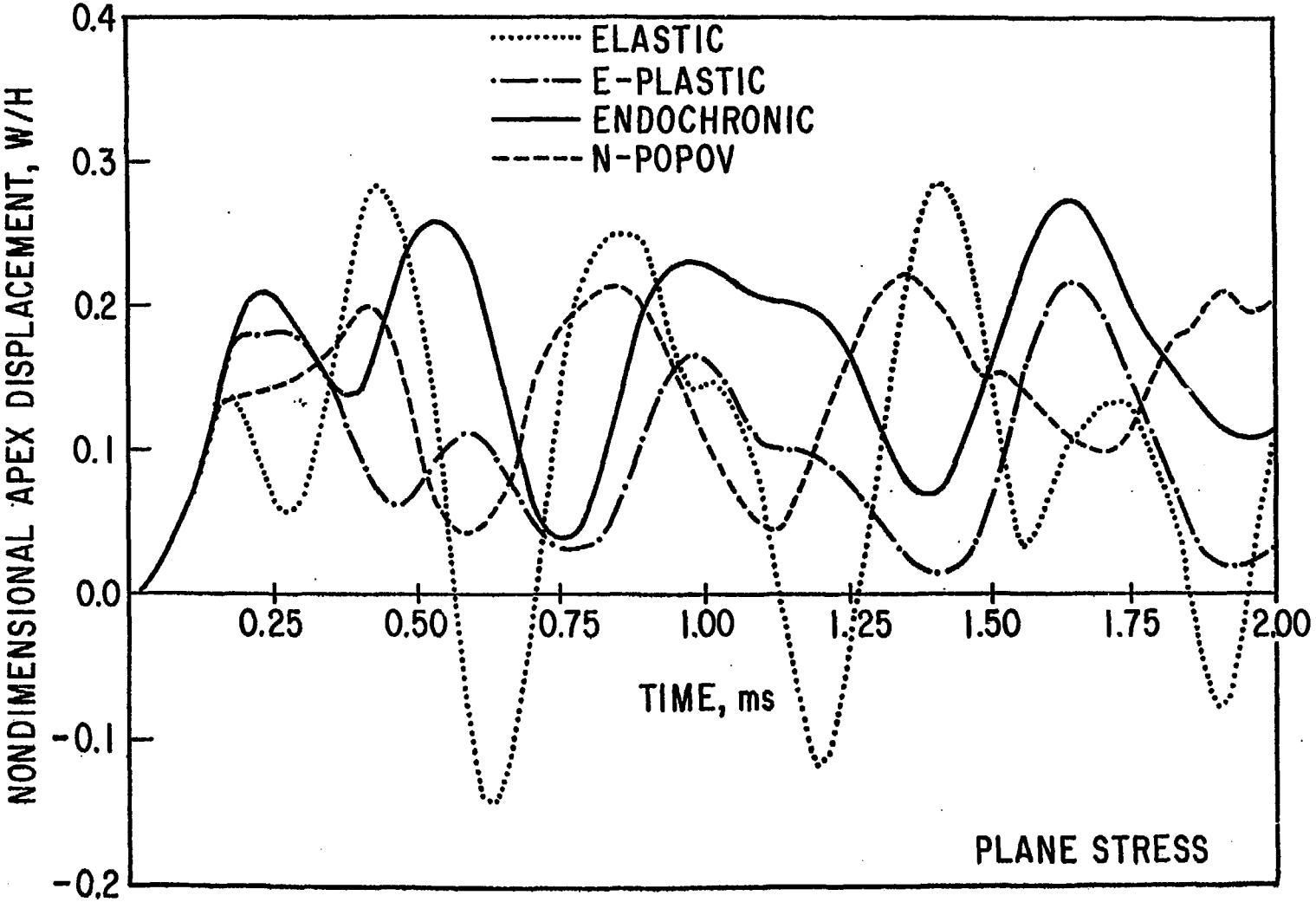


Figure 75

Dynamic apex responses of a clamped spherical cap that is subjected to a uniform step pressure loading of $4.137 \times 10^6$ Pa on its convex surface. Plane stress condition is used.

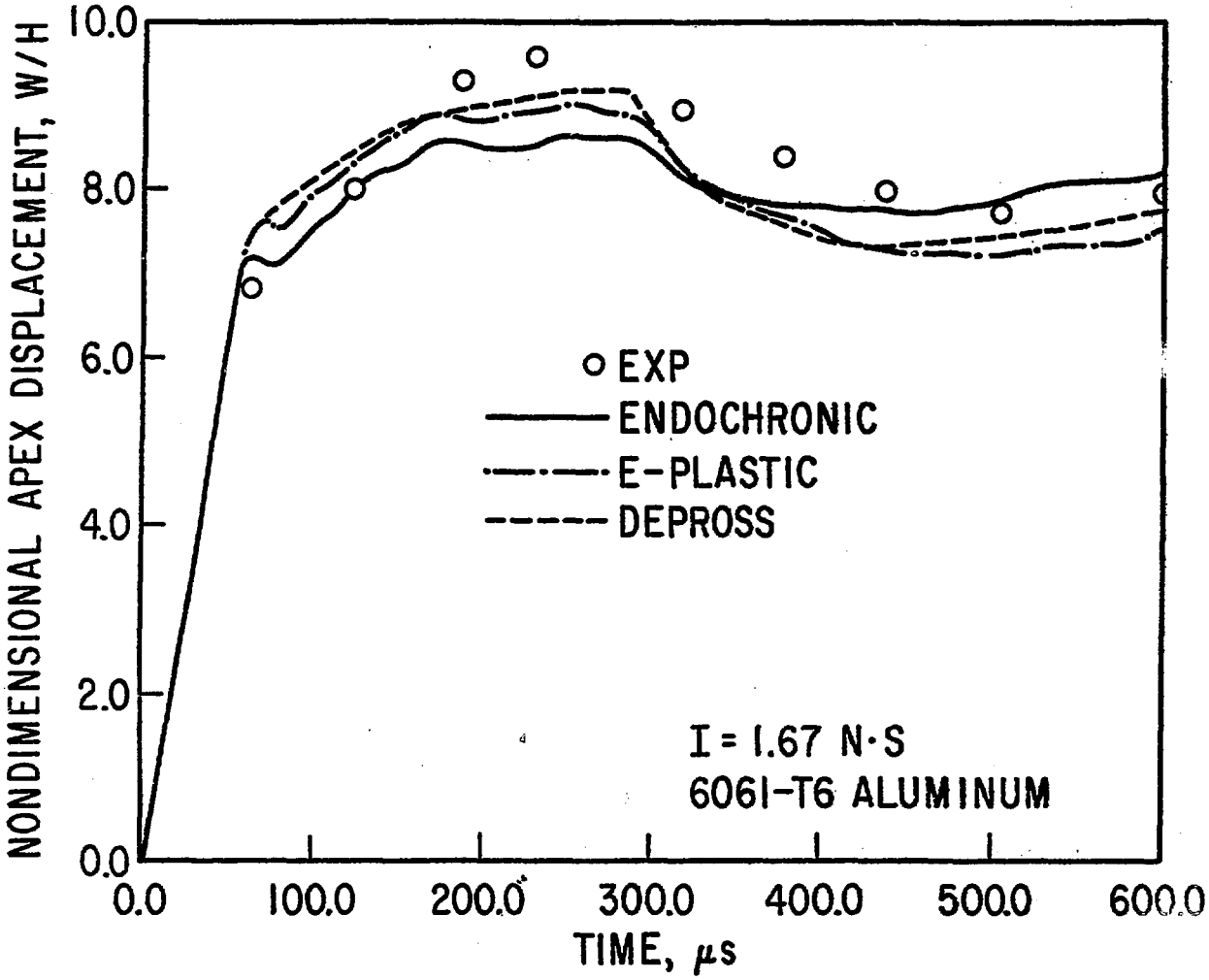


Figure 76

Dynamic central responses of a clamped aluminum plate (thickness = 1/16 inch) that is subjected to sheet explosive applied over a circular central region.

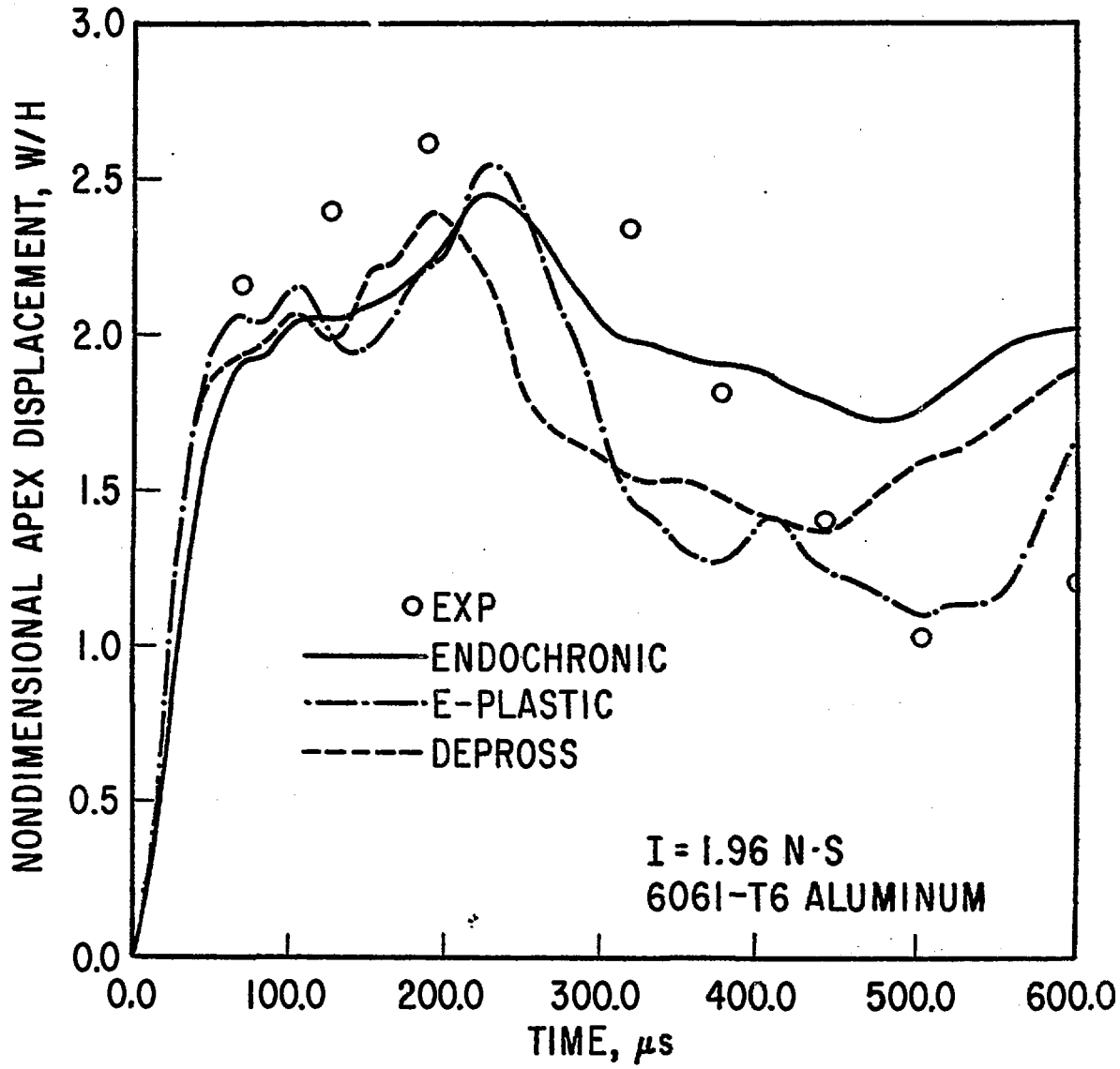


Figure 77

Dynamic central responses of a clamped aluminum plate (thickness = 1/8 inch) that is subjected to sheet explosive applied over a circular central region.

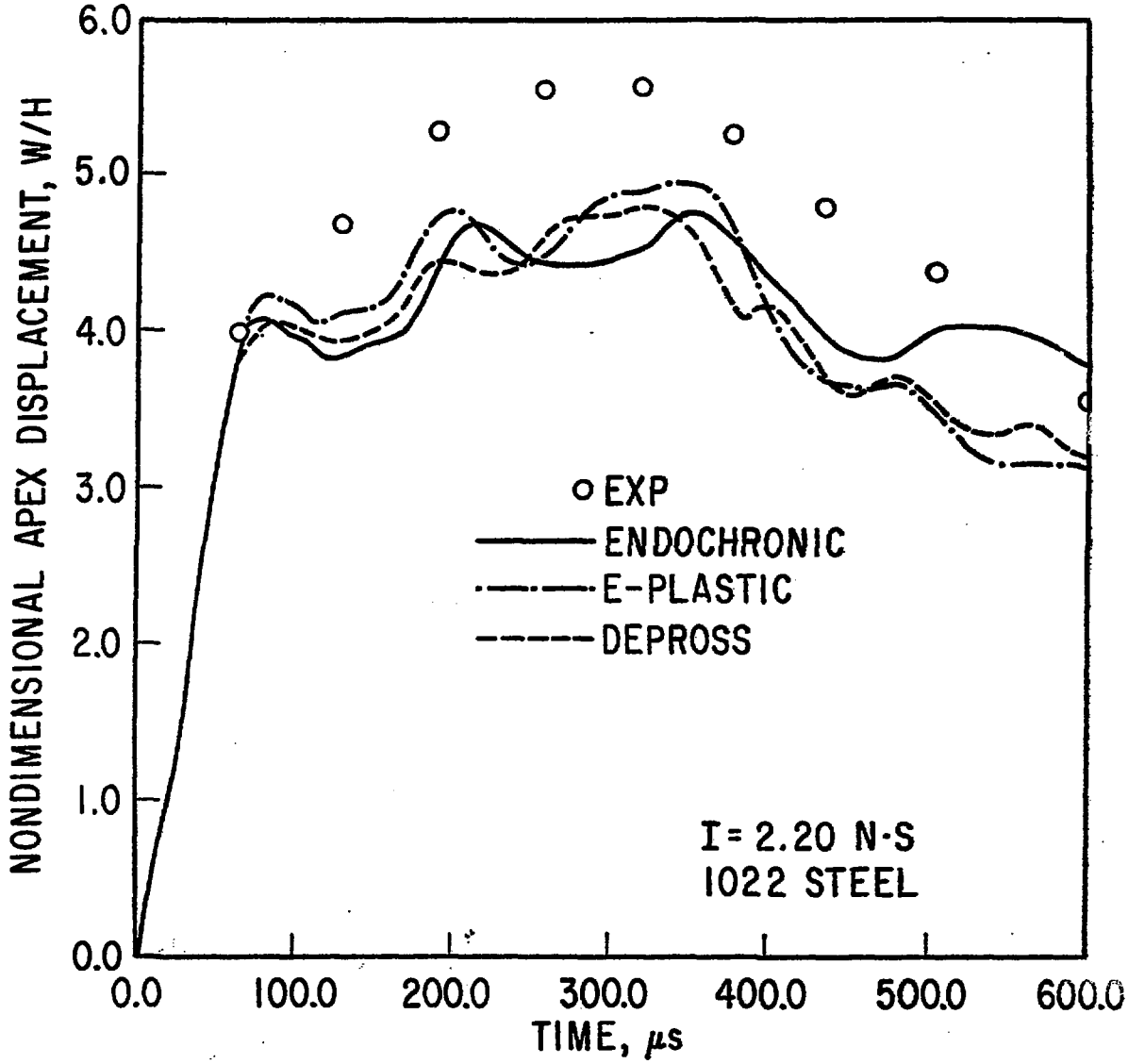


Figure 78

Dynamic central response of a clamped steel plate (thickness = 1/16 inch) that is subjected to sheet explosive applied over a circular central region.

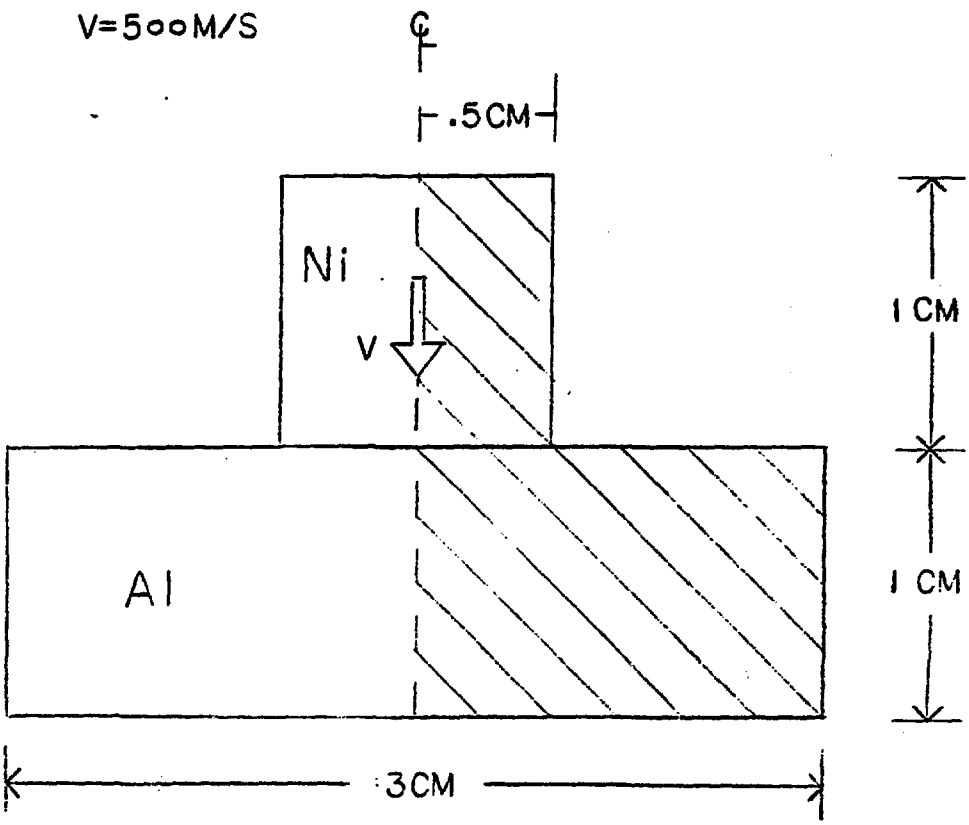


Figure 79

Geometrical configuration of the projectile and the target at the instant of impact.

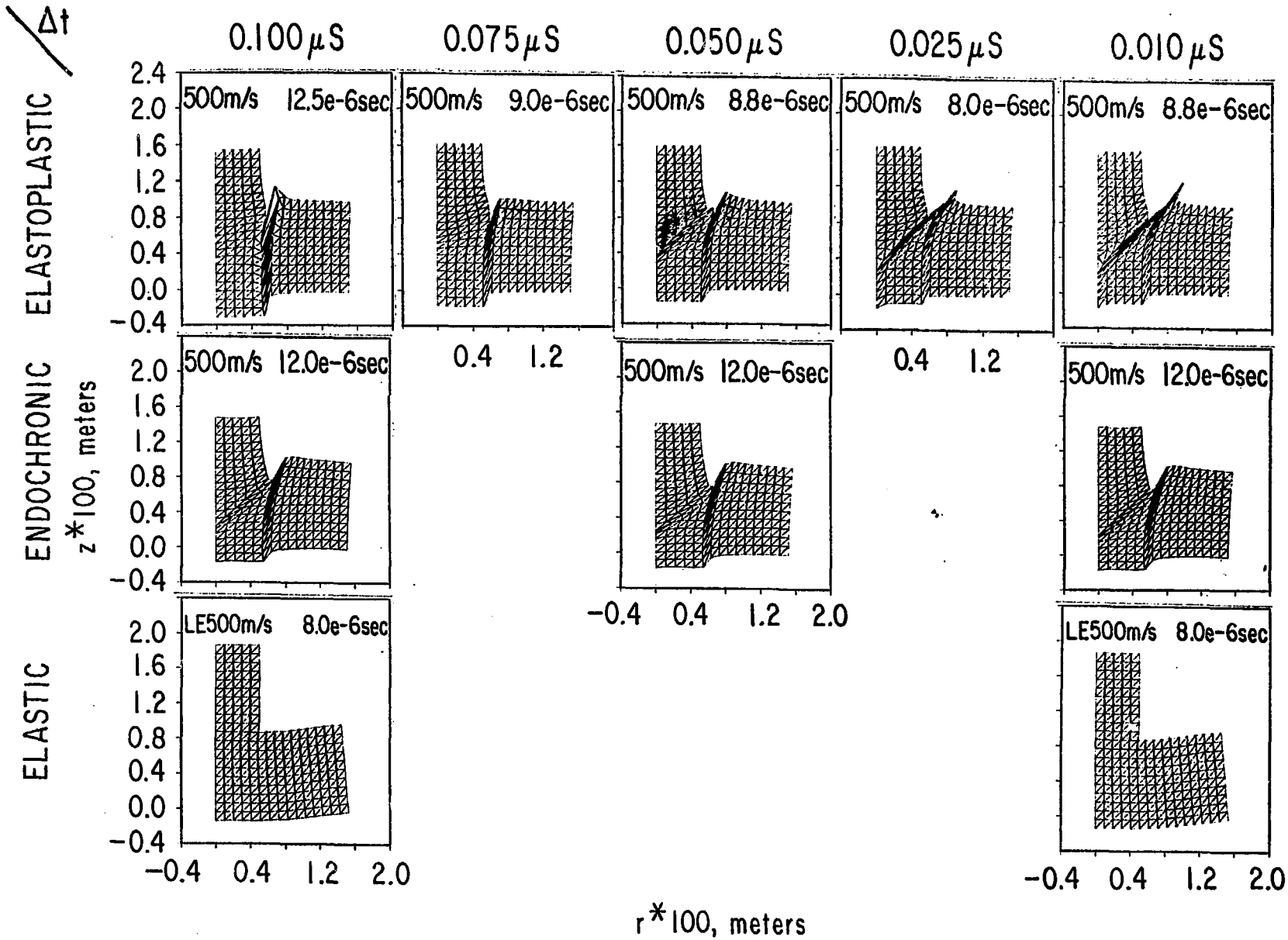


Figure 80

Comparison of deformed configurations of the projectile-target system using various constitutive laws and time steps.

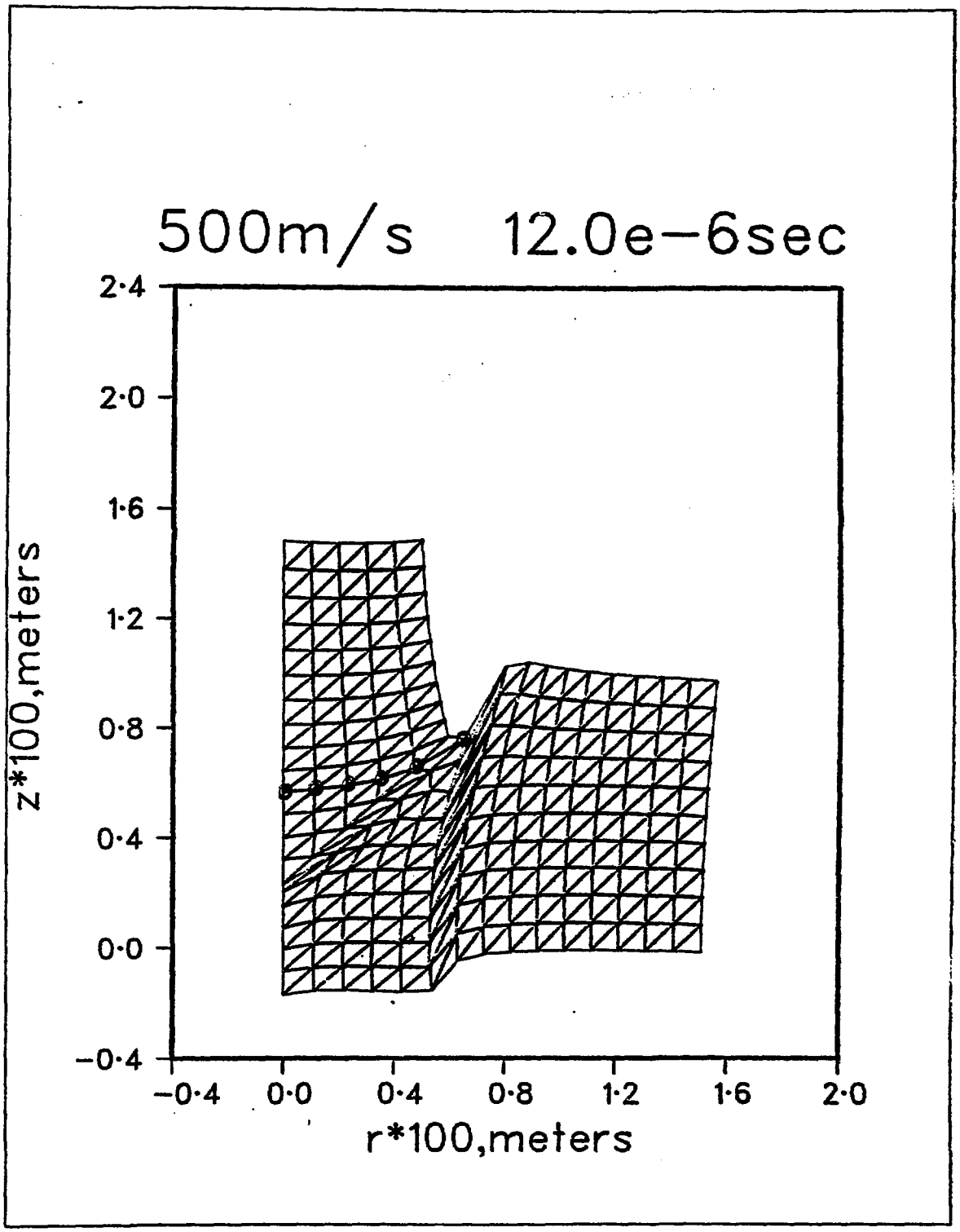


Figure 81

Final configuration of the projectile-target system using one-term endochronic constitutive theory. Circles indicate the interface of projectile and target.